Photogeneration of Charged Species and Subsequent Processes in Polymer Solids

Hideo OHKITA

1997

Photogeneration of Charged Species and Subsequent Processes in Polymer Solids

Hideo OHKITA

1997

Contents

Part II

Part III

Chapter 1

General Introduction

1.1. Historical Backgrounds of This Thesis

The behavior of charged species formed in a condensed phase is of scientific and practical interest as a photophysical and photochemical elementary process. Thus, a great number of studies have been reported in various fields: radiation chemistry and photochemistry. The lifetime of charged species formed in a liquid phase had been too short to be detected directly until laser photolysis or pulse radiolysis was established. Norrish and Porter[1] developed the flash photolysis technique around 1950 before the invention of laser. Their pioneer work brought a new world of research in a microsecond time domain. Furthermore, the advent of laser technique in the 1960s touched off the extension of the observation time domain from microsecond to picosecond. Nowadays, one can discuss ultrafast phenomena with a resolution of ten femtoseconds; time scale reduction reached of about eight order of magnitudes from the establishment of the flash photolysis technique. Furthermore, even ambitious challenge to a few hundred attoseconds is reported.[2] On the other hand, pulse radiolysis was for the first time introduced to the field of radiation chemistry at the end of the 1950s. Recently, the picosecond pulse radiolysis technique has been established and a preliminary examination starts aiming at femtosecond pulse radiolysis.

Although the dynamic measurement is a powerful tool for observing transient species directly, it is occasionally confronted with technical problems such as the limitation of time resolution, difficult identification of transient species because of overlapping of the absorption spectra or the broad absorption, and analytical problems in the complex decay kinetics. Therefore, the steady state measurement is also widely used as an alternative method for obtaining information on the transient species. There are two typical techniques of steady state measurements.

One is the scavenging method providing dynamic information of transient charged species indirectly. Hummel pointed out that the survival probability of ionic pairs in the absence of scavenger can be obtained from the Laplace inverse transformation of scavenging probability.[3] Although the survival probability and the scavenging probability are defined as a different function of time and of concentration respectively, both of them have the same information because they are connected with each other through the Laplace transformation. At a low concentration of scavenger, the scavenging yield is proportional to the square root of the concentration: the square-root law. On the other hand, the scavenging probability is close to unity at higher concentrations. Schuler *et al.* proposed an empirical equation satisfied with these conditions: the WAS equation.[4] These equations have been widely used for the theoretical analysis. Nowadays, the charge recombination in solution is rather discussed on the basis of the strict solution for time-dependent Smoluchowski equation settled by Hong and Noolandi.[5]

Another is the rigid solvent technique at a low temperature, which is simple and convenient enough to investigate radiation- and photoinduced radicals, ionic species and chemical reactions at a low temperature by spectroscopy. The usefulness of this technique in studying the photochemistry was brought out in the pioneer work of Lewis and his co-workers.[6-9] Later, the rigid solvent technique has been also developed to examine the structure and nature of short-lived unstable species such as free radicals and reaction intermediates.[10,11] Owing to the usefulness of this method, the spectroscopic identification of the trapped electron was for the first time achieved for an irradiated rigid solution; Linschitzs, Berry, and Schweitzer[12] found that an irradiated amine glass mixed with lithium shows an absorption peak at 600 nm with a broad background absorption extending throughout the visible and near-IR region. They assigned the former absorption to solvated electrons and the latter to incompletely solvated electrons. On the other hand, the first spectroscopic measurements of hydrated electrons by pulse radiolysis were done by Hart and Boag in 1962[13] after 8 years from the Linschitzs' work. These works gave rise to a jump for the study of trapped electrons, solvated electrons, and hydrated electrons.

In this thesis, the behavior of charged species and charge transfer complex formed in polymer solids is examined by the rigid matrix technique at cryogenic temperatures and by the transient absorption measurement using nanosecond laser photolysis. In the following sections, short surveys of some topics for this thesis are introduced.

1.1.1. Two-Photon Ionization in Condensed Media[14,15]

The investigation on photoionization in condensed phases began with celebrated works of Lewis and his collaborators.[7,8] The absorption spectrum of a photoirradiated EPA glass doped with *N,N,N',N'*-tetramethyl-*p*-phenylenediamine (TMPD) is identical with that of a chemically oxidized TMPD (Wurster's blue), indicating that TMPD is photoionized and changes into TMPD radical cation ($TMPD^{\bullet+}$). Although they failed to detect photoejected electrons, later the trapped electrons was also identified by absorption spectroscopy.[12,16,17]

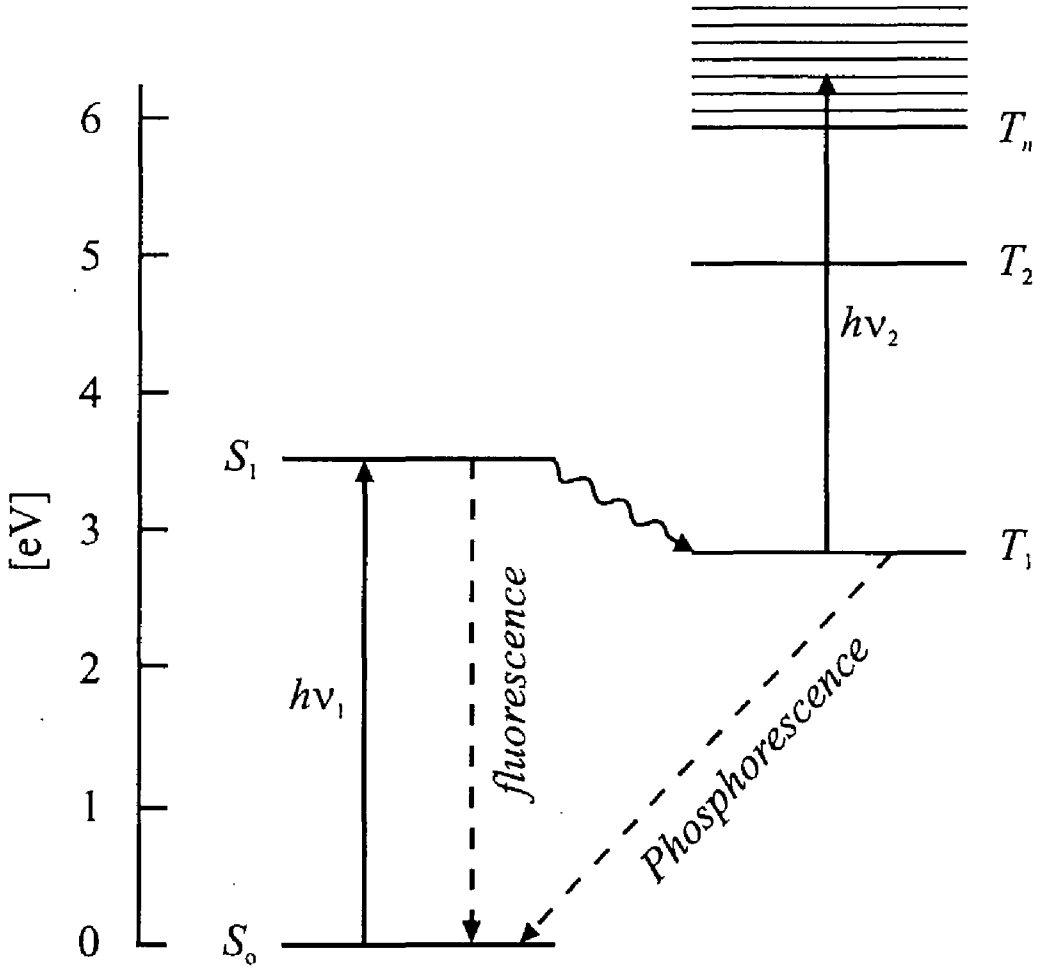

Figure 1–1. Energy diagram for stepwise two-photon ionization of TMPD in a condensed phase.

Lewis and Kasha[9] had already suggested the possibility of two-photon process as early as 1944. They proposed that the triplet state is a possible candidate for the metastable intermediate. Almost twenty years later in the 1960s, experimental evidences indicating two-photon process have been reported.[18-23] Cadogan and Albrecht showed that the photoionization of TMPD in a 3-methylpentane rigid glass at 77 K is two-photon process *via* the triplet state.[24,25] Furthermore, they examined the charge recombination of

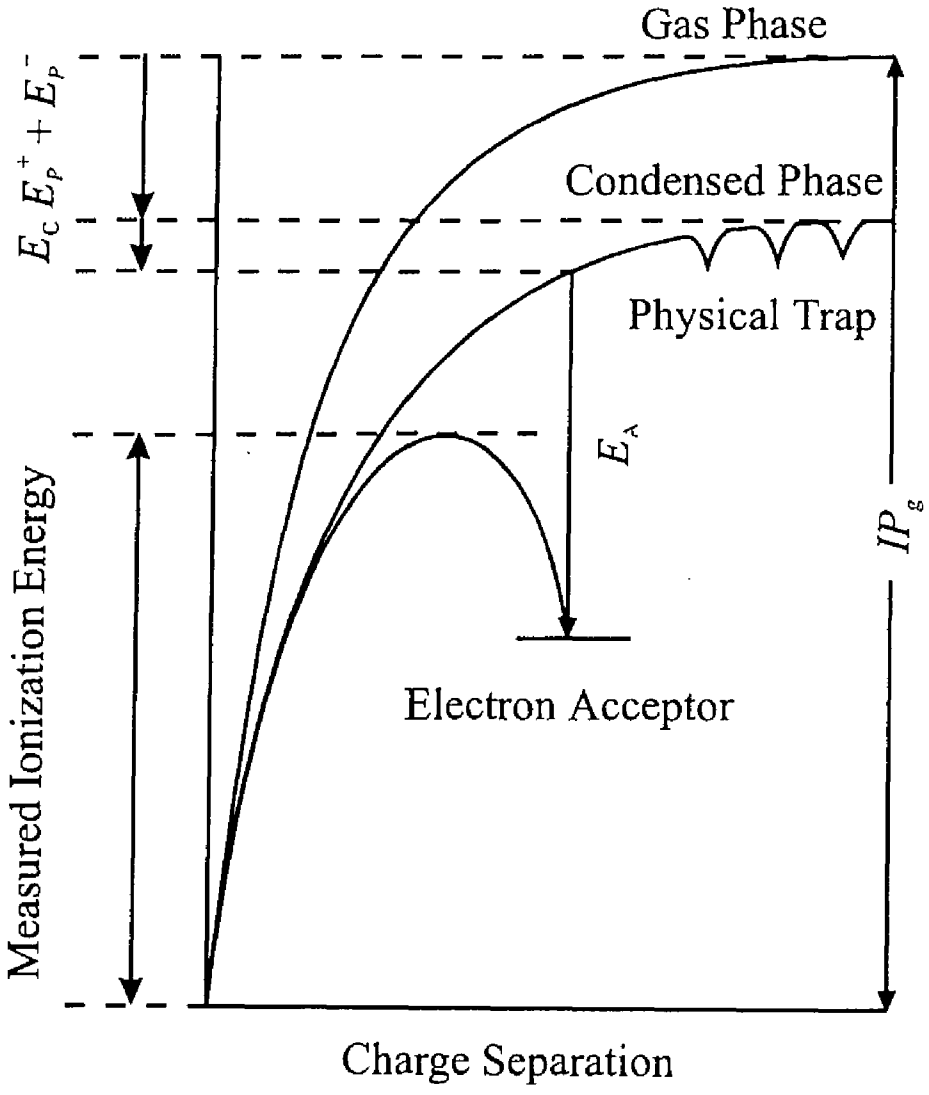

Figure 1–2. The reduction in the ionization energy of an aromatic molecule in condensed media. The denotations in the figure are as follows: the ionization potential in the gas phase IP_g, the sum of the solvent polarization energy $E_P^+ + E_P^-$, the trap electron affinity E_A, and the Coulomb energy E_C between the ionic species

an ejected electron with the parent $TMPD^{\bullet+}$ in detal:[26] photoconductivity and external electric field effect on the isothermal luminescence (electrophotoluminescence).

Although most aromatic compounds have ionization potentials between 6 and 9 eV in a gas phase,[27] the photoionization in condensed media requires only 3 – 5 eV which is a few electron volts lower than that in a gas phase. In general, the reduction in the ionization energy of an aromatic molecule in condensed media, ΔIP can be expressed by eq 1–1: the sum of the solvent polarization energy E_P^+ and E_P^-, the trap electron affinity E_A, and the Coulomb energy E_C between the ionic species.

$$\Delta IP = E_P^+ + E_P^- + E_A + E_C \qquad (1-1)$$

According to eq 1–1, the reduction energy ΔIP depends on kinds of matrix: ΔIP = 0.9 eV for TMPD in a 3-methylpentane glass; $\Delta IP \approx$ 1.7 eV for most organic crystals;[28] ΔIP = 1.9 eV for TMPD in methanol at 77 K.

Although numerous efforts have been, as mentioned above, devoted to the study of two-photon ionization in liquids and rigid glasses, surprisingly few studies have so far been reported on two-photon ionization in polymer solids. Most polymer solids have glass transition temperatures much higher than rigid glass solvents. For example, the glass transition temperature of 2-methyltetrahydrofuran is 88 K[29] while conventional polymers such as PMMA and PSt have higher glass transition temperatures far above room temperature: PMMA (378 K), PSt (373 K).[30] Thus, ionic species formed in polymer solids are stable enough to exist even at room temperature. The photoexcitation of TMPD doped in a PMMA solid develops Wurster's blue just as Lewis *et al.* reported. The $TMPD^{\bullet+}$ formed in a PMMA solid is so stable that it can be recognized even after a one-year storage at room temperature.[31–34]

As described above, a dopant chromophore in a condensed phase can be ionized with lower energy than the ionization potential in a gas phase. Furthermore, two-photon ionization requires only half energy of the ionization potential, corresponding to a photon energy for near-UV light. The two-photon process enables one to ionize a dopant chromophore selectively without a direct excitation of the matrix polymer. For example, PMMA has no absorption band at wavelengths longer than 300 nm whereas the absorption tail of TMPD extends to 370 nm. Thus, a 351-nm light pulse from a XeF excimer laser is one of the most suitable light sources for the selective excitation of TMPD.

Two-photon processes can be classified into two categories. One is stepwise two-

photon absorption *via* a real intermediate state just as Albrecht *et al.* reported. In the case where the excitation light source has a low photon density or the intermediate excited state has a short lifetime, the dopant chromophore cannot obtain another photon within its lifetime. An intense pulse from an excimer laser consists of numerous photons within tens of a few nanoseconds; the laser pulse can provide one molecule with about eighty photons under appropriate conditions. The other mechanism is simultaneous two-photon absorption *via* a virtual intermediate state. Since the transition probability for the latter process is far lower than that for the former, simultaneous two-photon absorption was impossible until the advent of intense laser light source.

Finally, a short survey of two-photon ionization of a dopant chromophore in polymer solids is described from the viewpoint of practical application. A colorless PMMA film is colored by two-photon ionization of dopant aromatic chromophores; this phenomenon is expected to be a new kind of photochromism. The photoionization has a threshold for input photon energy. Therefore, one can distinguish a writing process and a reading process according to the input photon intensity. The access time for writing or reading process is extremely fast corresponding to electronic transition time ($\approx 10^{-15}$ s). Then, once written information (coloration) is steadily stored at room temperature. On the other hand, stored information can be easily erased with heating, application of electric field, and photobleaching. Furthermore, a combination of these photochromic properties and two-photon process can be expected to be applied to three-dimensional optical storage memory.[35,36]

1.1.2. Charge Recombination in Condensed Media

High energy radiation, such as γ-ray, X-ray, electron beam, and deep UV-light, produces ejected electrons in condensed media. Then, ejected electrons are captured in a shallow trap whose energy level is higher than an electronic excited state of a luminescence center. Most of the captured electrons stay in trap sites at a low temperature but some of them recombine with holes even at a low temperature, and the charge recombination is promoted with increasing temperature. Thus, the emission caused by the charge recombination is observed at a fixed temperature as well as with increasing temperature. The former emission is called isothermal luminescence (ITL) or preglow. The latter emission is called thermoluminescence (TL) or glow.[37]

The striking feature of ITL is an extremely long lifetime. The decay kinetics of ITL cannot be explained in terms of the first order kinetics or the second order kinetics. The ITL intensity is proportional to the inverse of time t^{-1},[38-41] which is called the t^{-m} law with $m \approx 1$ or the Debye-Edwards law.[42] This luminescence has been believed to be due to the charge recombination of trapped electrons with the parent cation produced by the irradiation. Historically, Debye and Edwards[39] were the first to apply a diffusion mechanism to the ion-recombination reaction considering a spatial distribution of trapped electrons. However, in their model, the total amount of produced ionic species diverges into infinity owing to neglect of the normalization of the distribution function. Later, Abell and Mozumder[43] avoided the divergence using a normalized distribution function; however, their model was able to reproduce the t^{-1} decay only at an intermediate time scale. In other words, the ITL decay kinetics, the t^{-m} law, cannot be explained in terms of a simple diffusion mechanism on the basis of a random walk of trapped electrons. In a simple diffusion model, the number of trapped electrons is proportional to the square root of the inverse of time $t^{-1/2}$ in the long time region, the square-root law, and thus the intensity of the charge-recombination luminescence is proportional to $t^{-3/2}$.

Hamill and Funabashi[44] proposed that the t^{-m} decay kinetics of the recombination luminescence can be explained in terms of a non-Gaussian diffusion process whose hopping time distribution is an asymptotic type derived by Scher and Montroll. Scher and Montroll[45] applied the continuous-time random walk (CTRW) model[46] to the long tail of the transient photocurrent in amorphous solids. They insisted that the hopping time distribution $\varphi(t)$ for localized electrons in disordered systems should be expressed as an asymptotic type ($\varphi(t) \sim t^{-(1+\alpha)}$, $0 < \alpha < 1$), not an exponential type ($\varphi(t) = \lambda e^{-\lambda t}$, $\lambda = const.$) resulting in the familiar Gaussian diffusion. The hopping time distribution of the asymptotic type reflects that trap sites have a distribution for space and/or energetic depth. If trap depth has a wide distribution, the rate of electron transfer from a trap to another one will depend strongly upon temperature.

The dependence of the ITL decay kinetics on temperature was examined by Kieffer, Meyer, and Rigaut.[47,48] They showed that the ITL decay kinetics in an irradiated rigid solution of methylcyclohexane remains the same at temperatures from 4 to 77 K. This finding indicates that trapped electrons recombine with the parent cation without thermal activation. Thus, many authors have explained the charge recombination at a low

temperature in terms of long-range electron transfer by electron tunneling.[49-53]

On the other hand, the first observation of TL was already reported by Boyle as early as 1663.[37] However, the first theoretical explanation for the phenomenon was offered about 300 years later, in the 1940s. The pioneer work of Randall and Wilkins brought a big step in the theoretical analysis of the TL.[54] The TL is nowadays assumed to result from the charge recombination of electron-cation pairs. This method is sensitive to the charge release process more than other spectroscopic methods, *e.g.*, ESR or UV-visible absorption. Thus, it has been established as a sensitive technique for examining defects and impurities in insulators and semiconductors; radiation dosimetry is therefore a major application.[55]

Nikolski and Buben were the first to study the TL of irradiated polymer solids. They found the TL glow curve reflects polymer chain motions sensitively.[56] Since then, the TL technique has been demonstrated to be a powerful tool for detecting the characteristic molecular motions and structural transitions in polymers.[57-61] However, there remain still unknown problems on the mechanism of luminescence owing to lack of information on the nature of electron traps. In other words, elucidation of the behavior of charged species will enable one to obtain more detailed information on polymer motions from the TL method.

1.1.3. Initial Distribution Function of Ejected Electrons

The ionization and the following charge recombination have been studied as one of the most elementary and important primary processes of radiation chemistry and photochemistry. In particular, the initial distribution of ejected electrons is essential for the discussion on the following charge recombination.

Historically, Mozumder and Magee discussed thermalization of ejected electrons in a Coulomb potential using the prescribed diffusion model of ejected electrons. They used a Gaussian distribution as an approximated thermalization distance.[62,63] This approximation corresponds to considering electron thermalization as a diffusion of classical particles. On the other hand, Abell and Funabashi insisted that the thermalization should be rather considered to be scattering of electron as a quantum wave because of a thermal de Broglie length as long as 50 Å at 300 K.[64] From a simple consideration, they proposed an initial spatial distribution function expressed as an exponential function, and showed that

the exponential distribution is in good agreement with the electron scavenging experiments of Warman and Rzad.[65] Thus, there have been numerous reports discussing correspondence of several initial distribution functions with experimental results.[66–69]

Yoshida *et al.* considered the initial distribution function for geminate charge recombination in nonpolar solvents by pulse radiolysis; the solute ionic species were observed instead of an ejected electron and the parent cation pairs. They showed that the initial spatial distribution of ionic species is Exponential type in low mobile liquids such as *n*-hexane, *trans*-decalin, *cis*-decalin, isooctane, and methylcyclohexane while Gaussian type in the high mobile liquids such as neopentane and tetramethylsilane.[70–72]

On the other hand, the initial distribution function of geminate recombination in solids was theoretically considered by Tachiya and Mozumder.[52] They explained the t^{-m} behavior of ITL in γ-irradiated rigid glasses in terms of geminate charge recombination by electron tunneling assuming the initial distribution function of Exponential type of Abell and Funabashi. Hama and his co-workers also discussed the ITL decay in terms of long-range electron transfer by electron tunneling; the rate constant $k(r)$ was assumed to be expressed as a function of the distance r between an ejected electron and the parent cation by

$$k(r) = \nu \exp(-\beta r). \tag{1–2}$$

They showed that the Laplace inverse transformation of an empirical ITL decay function,

$$I(t) = \frac{I_0}{(1+\alpha t)^m}, \tag{1–3}$$

leads to the initial distribution function $n(r,0)$ of the distance between a trapped electron and the parent cation just after the irradiation:[73,74]

$$\begin{aligned} n(r,0) &= \frac{\beta}{\lambda}\mathcal{L}^{-1}\left[I(t)\right] \\ &= \frac{\beta I_0}{\lambda \alpha^m \Gamma(m)} \nu^{m-1} \exp\left[-(m-1)\beta r - \frac{\nu}{\alpha}\exp(-\beta r)\right]. \end{aligned} \tag{1–4}$$

1.1.4. Photoinduced Chemical Reaction in Polymer Solids

There have been a great number of studies on the effects of high energy radiation on polymers.[75–78] Radiation of polymers causes changes in the molecular structure and in physical properties. Polymer degradation leads to a decrease in molecular weight, generation of fragment gases, and coloration due to the formation of double bonds.

Crosslinking of chains results in an increase in molecular weight and gelation, leading to improvement of thermal stability and insolubility.

The radiation effects on polymers can be classified into main-chain scission and crosslinking, although both of them occur generally at the same time. Polymers having quaternary carbon atom in the main chain such as PMMA are classified as main-chain scission type to radiation.[79-82] On the other hand, polymers containing a hydrogen atom adjacent to the chain such as PSt are classified as crosslinking type to high energy radiation with minor chain scission.[83] It is noteworthy that PSt is twenty times more stable to

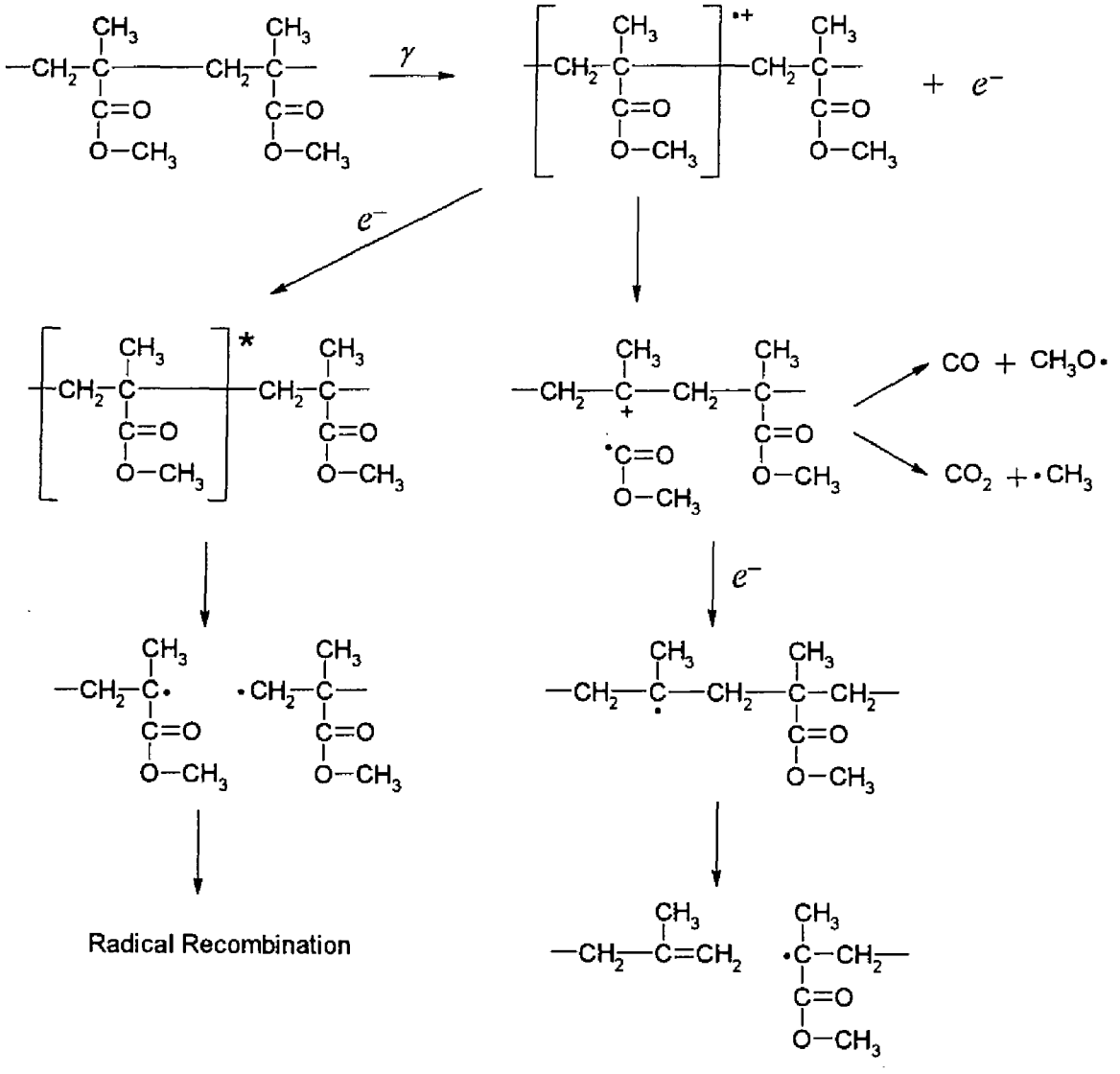

Figure 1–3a. Degradation mechanism of main-chain scission in γ-irradiated PMMA proposed by Geuskens and his co-workers on the basis of the analysis of radiation products and the effect of added ethylmercaptan.[78,80-82]

radiation than PMMA.[84] This reduction of sensitivity to radiation is the nature common to polymers containing aromatic components in their structure.

There have been investigated radical intermediates formed in γ-irradiated PMMA by ESR and/or absorption measurements. In particular, the ESR method is a powerful tool for elucidating the mechanism of radical reactions. Thus, one of the most detailed mechanism of main-chain scission in γ-irradiated PMMA has been proposed by Geuskens and his co-workers on the basis of the analysis of radiation products and the effect of added ethylmercaptan.[78,80-82] However, the degradation mechanism in PMMA is not yet

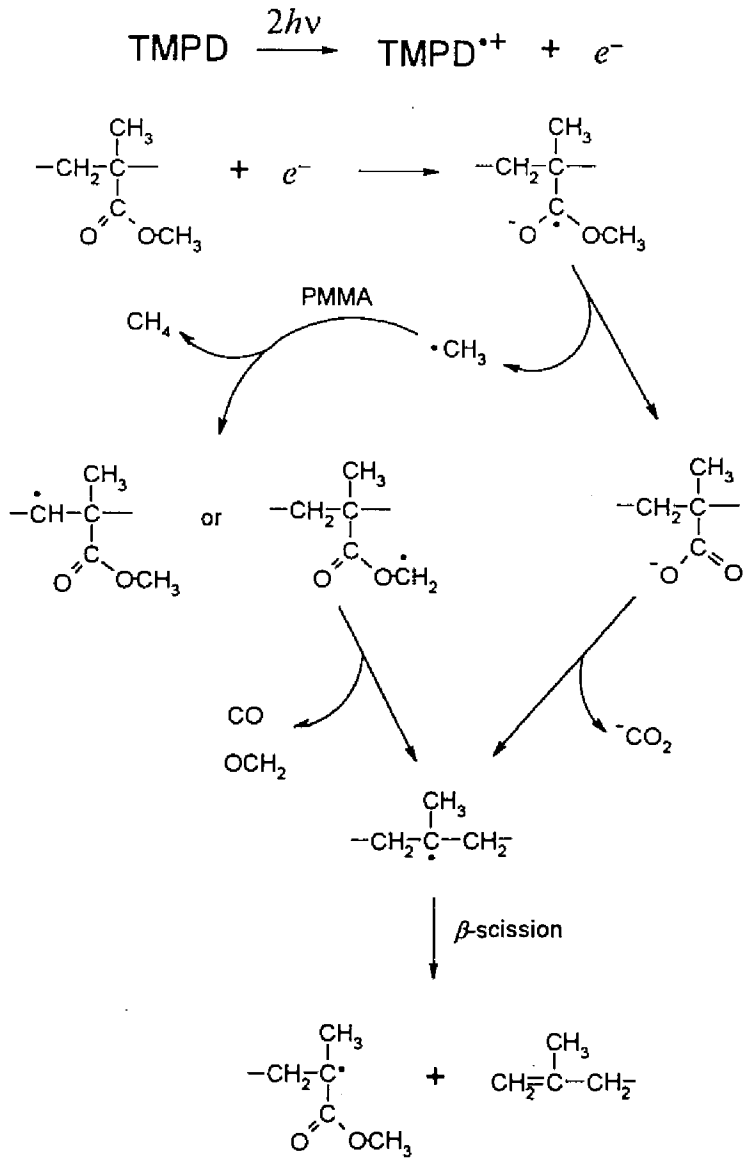

Figure 1–3b. Degradation mechanism of main-chain scission in a photoirradiated PMMA film doped with TMPD proposed by Sakai and his co-workers on the basis of the ESR measurements.[88,89]

understood in detail because of the coexistence of several radical species resulting in overlapped ESR spectra. Ichikawa and his co-workers studied the role of radical species in the degradation of γ-irradiated PMMA using the ESR and ESE (Electron Spin Echo) techniques complementarily.[85-87] They proposed a mechanism different from that reported by Geuskens *et al.* Recently, Sakai *et al.* reported the main-chain scission of PMMA induced by two-photon ionization of dopant aromatic molecules, which is initiated through the formation of ester radical anions.[88,89]

Owing to the degradable nature, PMMA was for the first time used as a positive resist for electron beam. On the other hand, PSt derivatives work as the negative resist because of the crosslinking nature. It is needless to say that this practical technology is based on the basic research of the behavior of intermediate radicals or ionic species as mentioned above. Recently, photosensitive polyimides have received considerable attention as a photoresist owing to their excellent material properties such as high thermal stability, mechanical toughness, low dielectric constant, and high chemical resistance. In recent years, concern has been raised about photochemical properties of photosensitive polyimides.[90]

1.1.5. Stabilization of Radical Cation by Charge Resonance in Polymer Solids

One of the most important factors dominating photophysical processes in polymer systems is the interaction between neighboring chromophoric groups, which strongly depends on main chain motions, configuration of chromophoric groups, and tacticity.[91] Even in an isolated polymer chain, a chromophoric group easily interacts with neighboring groups because the high concentration of chromophoric groups results from a linkage with the main chain. For example, the emission spectrum of a dilute poly(*N*-vinylcarbazole) (PVCz) solution consists of major excimer emission and minor monomeric emission owing to the efficient energy migration. These interactions should be favorable to polymer solid systems and predominate its photophysical properties. Here, as an example, a short survey of photophysical processes from photoexcitation to carrier generation in PVCz is introduced.

Poly(*N*-vinylcarbazole) is one of the most representative polymers, which has been actually utilized, as the first commercial photoconductive polymer, in photocopying machines.[92] Thus, its photophysical and photoconductive properties have been intensively

studied from the viewpoint of 1) excited energy relaxation and carrier generation processes; what photophysical processes are involved from an initial photoexcitation to a final carrier generation, and 2) carrier relaxation process including photoconductive mechanism and the nature of carrier trap sites.

The former process can be observed directly by spectroscopic measurements such as absorption,[93] fluorescence,[94,95] phosphorescence,[96,97] excimer emission,[94,95] and exciplex emission.[98] Therefore, the energy relaxation processes, *e.g.*, energy migration, excimer formation, have been elucidated in a shorter time domain with progress in the laser photolysis technique.[99,100] Since these excited energy relaxation processes are closely related to the light harvesting mechanism in photosynthetic systems, numerous studies have been reported in this field.

To the latter carrier relaxation process, radical cations play important roles. Although transient absorption measurements for a PVCz film should provide dynamic information on the behavior of radical cations, the transient absorbance is usually too small to be detected owing to its short optical path length and the efficient deactivation process. Thus, most researches have been reported on steady-state luminescence and time-of-flight photoconductivity for PVCz films. There have been only a few reports on the dynamics of hole transport in PVCz films by transient absorption spectroscopy.[101-103]

On the other hand, the dynamics of ionic species formed in a dilute solution of PVCz has been elucidated in detail by transient absorption measurements. Masuhara *et al.* measured the transient absorption spectra of radical cations of polymers having carbazolyl (Cz) chromophores[104] and of ionic dicarbazolyl compounds in solution.[105] Tsujii *et al.* measured the charge-resonance (CR) band of Cz dimer radical cations by nanosecond laser photolysis, indicating that the positive charge of a Cz radical cation formed in its dimer compounds is delocalized over the other Cz chromophore.[106,107] Recently, Tsuchida *et al.* showed the existence of charge resonance among more than two Cz chromophores in Cz oligomers using the radical transfer method and CR band measurements.[108]

As mentioned above, there have been various studies on the stabilization of Cz radical cations in solution. On the contrary, little is known about the stabilization of Cz radical cations in solids, although it is closely related to photoconduction.

1.2. Outline of This Thesis

The aim of this thesis is to elucidate the behavior of charged species and charge transfer complex formed by photoirradiation of polymer solids. In this thesis, spectroscopic measurements were mainly used: absorption measurement of ionic species at

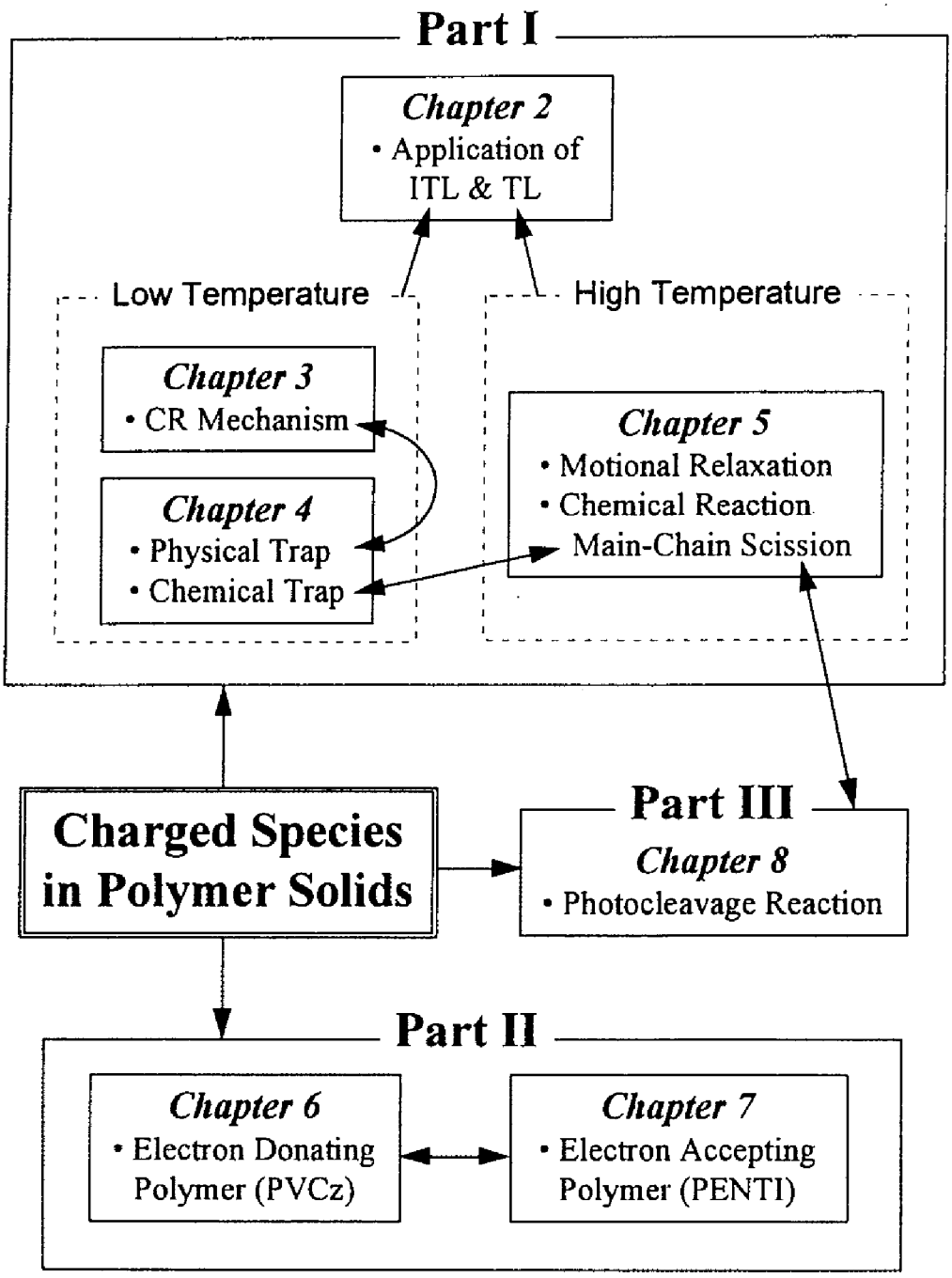

Scheme 1–1. Relationship among each chapter in this thesis.

temperatures from 20 to 300 K; emission measurements of charge recombination luminescence, *i.e.*, isothermal luminescence (ITL) and thermoluminescence (TL); transient absorption measurement by laser photolysis.

In Chapter 1, historical backgrounds of this thesis are described. Each chapter is related as shown in Scheme 1–1.

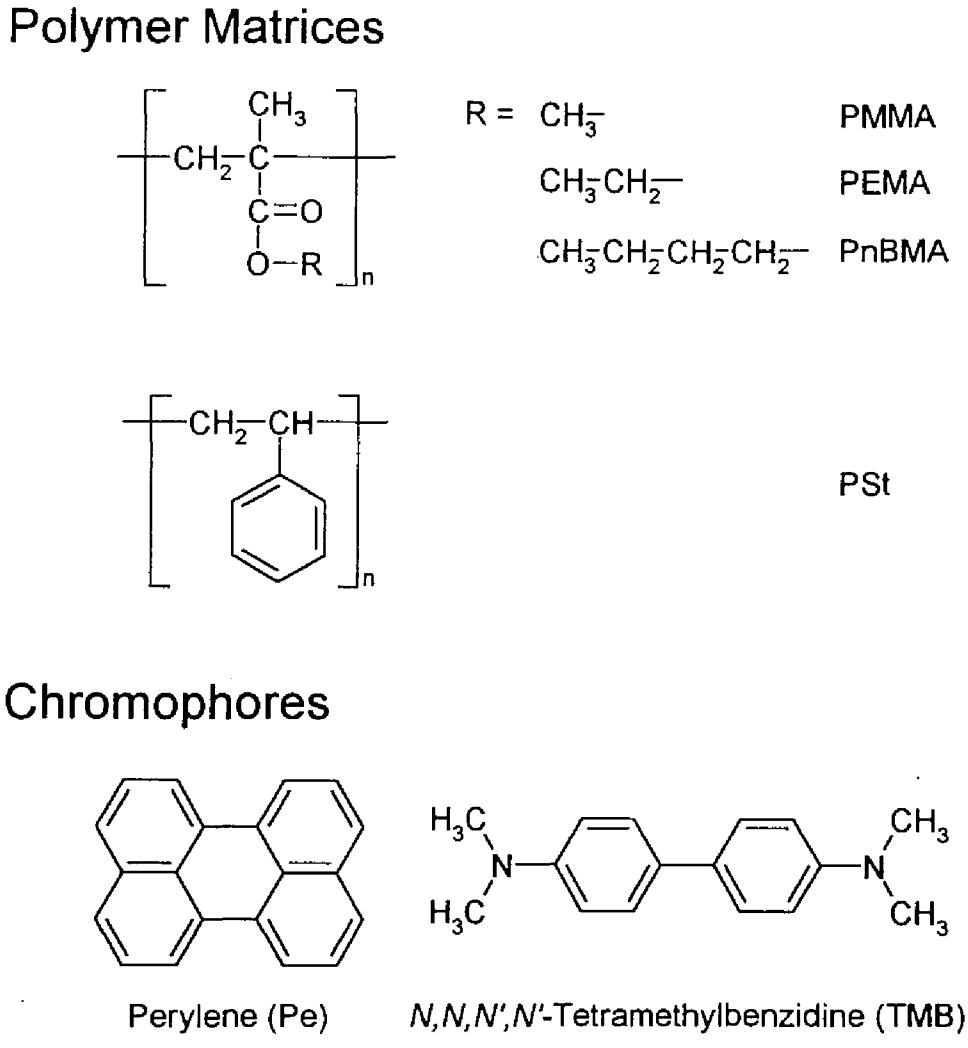

Figure 1–4. Chemical structures of the polymers and dopant chromophores used in Part I.

In Part I, the behavior of ionic species formed through two-photon ionization of dopant chromophores is examined for poly(alkyl methacrylate)s classified as scission type polymers to radiation and for polystyrene higher resistant to radiation. In Chapter 2, the photochromism induced by two-photon ionization is demonstrated for polymer films doped

with aromatic chromophores. The backward charge recombination is also observed through ITL and TL. Some applications of ITL and TL as well as the photochromism are presented. In Chapter 3, the ITL mechanism at low temperatures is examined in terms of long-range electron transfer by electron tunneling. In the following Chapter 4, on the basis of electron tunneling examined in Chapter 3, the ITL decay is quantitatively compared with the absorbance decay of the radical cation at 20 K for poly(alkyl methacrylate)s and polystyrene. In Chapter 5, the charge recombination of a photoejected electron with the parent cation formed through two-photon ionization of a dopant chromophore in polymer solids is observed through ITL at a fixed temperature of 20 K and TL at temperatures from 20 to 300 K. The behavior of a photoejected electron formed in polymer solids is examined from the viewpoint of the difference in motional relaxation between poly(alkyl methacrylate)s and in photoinduced chemical reactivity of polymers between poly(alkyl methacrylate)s and polystyrene. Furthermore, the trap depth at higher temperatures is estimated from the TL spectral change.

In Part II, polymers having functional groups in the side chain or the main chain are

a) VCz(*x*)/MMA

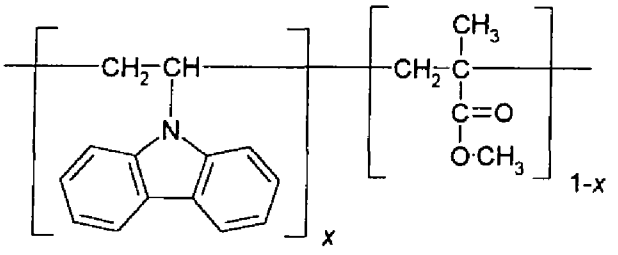

x = 0.015, 0.25, 0.48

b) PENTI

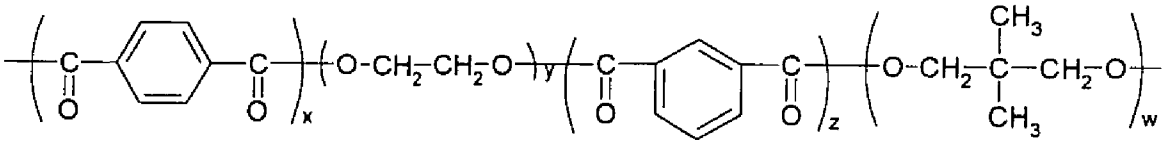

Figure 1–5. Chemical structures of the copolymers used in Part II: a) copolymer of *N*-vinylcarbazole (VCz) with methyl methacrylate (MMA), VCz(*x*)/MMA, in Chapter 6; b) poly[(ethylene glycol ; neopentyl glycol)-*alt*-(terephthalic acid ; isophthalic acid)], PENTI, in Chapter 7.

studied. In Chapter 6, the stability of cationic species in the copolymer solids containing electron-donating Cz groups in the side chain is evaluated by CR band measurements. In Chapter 7, anionic as well as cationic species formed through photoionization of dopant chromophores in a polyester film having a weak electron-accepting group, phthaloyl group, are observed at 20 K by absorption measurement.

In Part III (Chapter 8), the photocleavage reaction mechanism of photosensitive

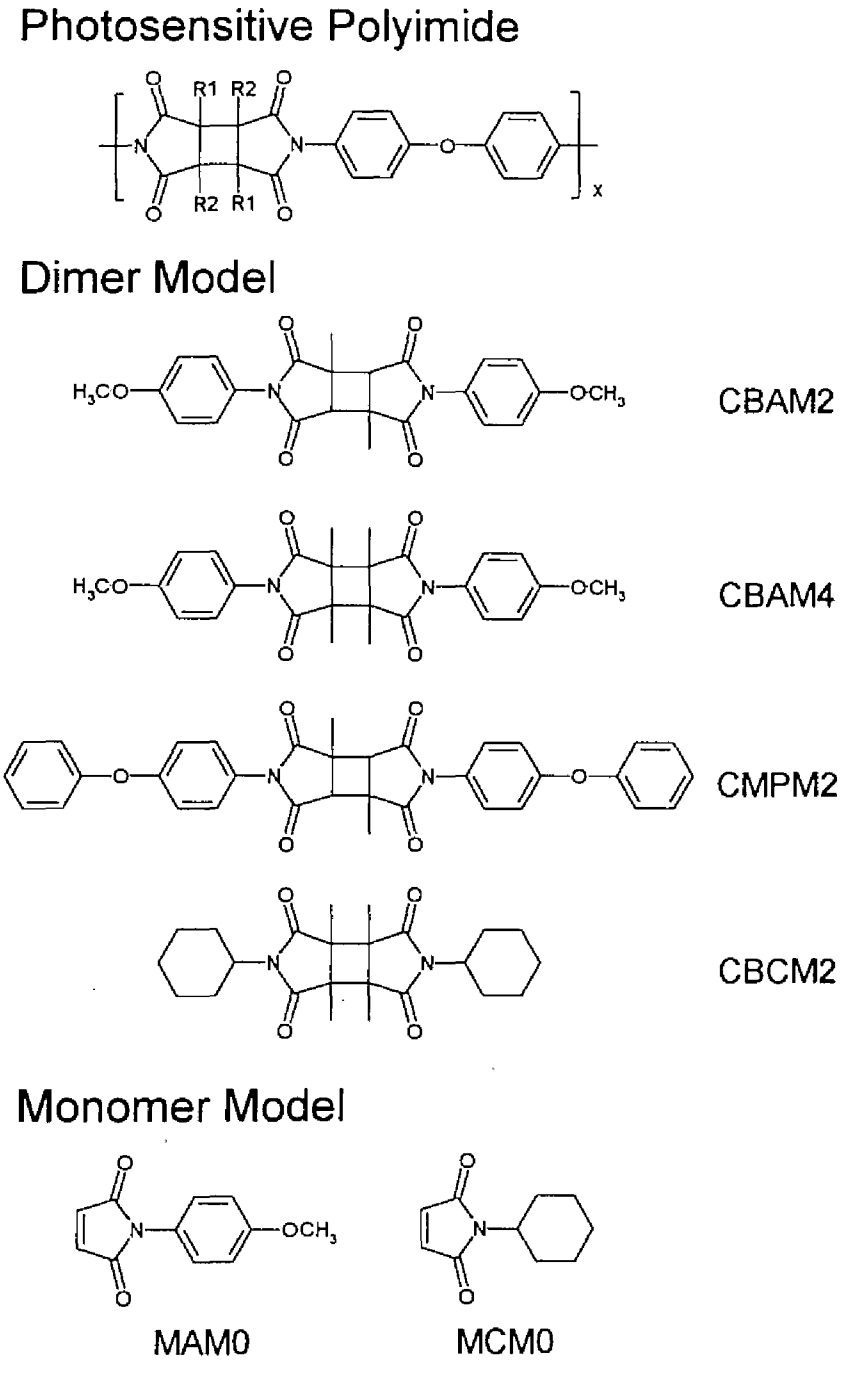

Figure 1–6. Chemical structures of photosensitive polyimides and its model compounds studied in Part III (Chapter 8).

polyimides having cyclobutane rings in the main chain is studied using their dimer model compounds in terms of the cleavage quantum yield, solvent polarity effects on the cleavage quantum yield, and the quenching of excited triplet state by transient absorption measurement.

References

1) G. Porter, in *"Techniques of Organic Chemistry"*, Vol. VIII, Part II, ed. A. Weissberger, Wiley Interscience (1963), p. 1055.
2) R. F. Service, *Science*, **269**, 634 (1995).
3) A. Hummel, *J. Chem. Phys.*, **49**, 4840 (1968).
4) J. M. Warman, K. -D. Asmus, and R. H. Schuler, *J. Phys. Chem.*, **73**, 931 (1969).
5) K. H. Hong and J. Noolandi, *J. Chem. Phys.*, **68**, 5163 (1978).
6) G. N. Lewis, D. Lipkin, and T. T. Magel, *J. Am. Chem. Soc.*, **63**, 3005 (1941).
7) G. N. Lewis and D. Lipkin, *J. Am. Chem. Soc.*, **64**, 2801 (1942).
8) G. N. Lewis and J. Bigeleisen, *J. Am. Chem. Soc.*, **65**, 520 (1943).
9) G. N. Lewis and M. Kasha, *J. Am. Chem. Soc.*, **66**, 2100 (1944).
10) E. Whittle, D. A. Dows, and G. C. Pimentel, *J. Chem. Phys.*, **22**, 1943 (1954).
11) I. Norman and G. Porter, *Nature*, **174**, 508 (1954).
12) H. Linschitz, M. G. Berry, and D. Schweitzer, *J. Am. Chem. Soc.*, **76**, 5833 (1954).
13) J. W. Boag and E. J. Hart, *J. Am. Chem. Soc.*, **84**, 4090 (1962).
14) R. Lesclaux and J. J-. Dubien, in *"Organic Molecular Photophysics"*, Vol. 1, ed. J. B. Birks, Wiley Interscience, New York (1973), p. 460.
15) C. A. Parker, *"Photoluminescence of Solutions"*, Elsevier, Amsterdam (1968), Chap. 1, p. 48.
16) J. Jortner and B. Sharf, *J. Chem. Phys.*, **37**, 2506 (1962).
17) M. Ottolenghi, *J. Am. Chem. Soc.*, **85**, 3557 (1963).
18) K. S. Bagdasar'yan, V. I. Muromtsev, and Z. A. Sinitsyna, *Dokl. Akad. Nauk SSSR*, **152**, 349 (1963).
19) V. J. Kholmogorov, E. V. Baranov, and A. N. Terenin, *Dokl. Akad. Nauk SSSR*, **152**, 399 (1963).
20) J. J-. Dubien and R. Lesclaux, *J. Chim. Phys.*, **61**, 1631 (1964).
21) P. Douzou and M. Ptak, *J. Chim. Phys.*, **61**, 1681 (1964).
22) H. S. Pilloff and A. C. Albrecht, *Nature*, **212**, 499 (1966).
23) H. S. Pilloff and A. C. Albrecht, *J. Chem. Phys.*, **49**, 4891 (1968).
24) K. D. Cadogan and A. C. Albrecht, *J. Phys. Chem.*, **72**, 929 (1968).
25) K. D. Cadogan and A. C. Albrecht, *J. Chem. Phys.*, **51**, 2710 (1969).

26) A. C. Albrecht, *Acc. Chem. Res.*, **3**, 238 (1970).

27) K. Kimura, S. Katsumata, Y. Achiba, T. Tamazaki, and S. Iwata, *"Handbook of HeI Photoelectron Spectra of Fundamental Organic Molecules"*, Japan Scientific Societies Press (1981).

28) N. Sato, K. Seki, and H. Inokuchi, *J. Chem. Soc., Faraday Trans. 2*, 77, 1621 (1981).

29) K. K. Ho and L. Kevan, *J. Phys. Chem.*, **81**, 1865 (1977).

30) P. Peyser, in *"Polymer Handbook"*, 3rd ed., eds. J. Brandrup and E. H. Immergut, John Wiley & Son, New York (1989).

31) A. Tsuchida, M. Nakano, M. Yoshida, M. Yamamoto, and Y. Wada, *Polym. Bull.*, **20**, 297 (1988).

32) M. Yamamoto, A. Tsuchida, and M. Nakano, *MRS Int. Meeting Adv. Mater.*, **12**, 243 (1989).

33) A. Tsuchida, W. Sakai, M. Nakano, M. Yoshida, and M. Yamamoto, *Chem. Phys. Lett.*, **188**, 254 (1992).

34) A. Tsuchida, W. Sakai, M. Nakano, and M. Yamamoto, *J. Phys. Chem.*, **96**, 8855 (1992).

35) D. A. Parthenopoulos and P. M. Rentzepis, *Science*, **245**, 843 (1989).

36) W. Denk, J. H. Strickler, and W. W. Webb, *Science*, **248**, 73 (1990).

37) R. Chen and Y. Kirsh, *"Analysis of Thermally Stimulated Processes"*, Pergamon Press, Oxford (1981).

38) J. T. Randall and M. H. Wilkins, *Proc. R. Soc. London, Ser. A*, **184**, 390 (1945).

39) P. Debye and J. O. Edwards, *J. Chem. Phys.*, **20**, 236 (1952).

40) Kh. S. Bagdasar'yan, R. I. Milyutinskaya, and Yu. V. Kovalev, *Khim. Vysok. Energii*, **1**, 127 (1967).

41) J. R. Miller, *Chem. Phys. Lett.*, **22**, 180 (1973).

42) W. H. Hamill, *J. Chem. Phys.*, **71**, 140 (1979).

43) G. C. Abell and A. Mozumder, *J. Chem. Phys.*, **56**, 4079 (1972).

44) W. H. Hamill and K. Funabashi, *Phys. Rev. B*, **16**, 5523 (1977).

45) H. Scher and E. W. Montroll, *Phys. Rev. B*, **12**, 2455 (1975).

46) E. W. Montroll and G. H. Weiss, *J. Math. Phys.*, **6**, 167 (1965).

47) F. Kieffer, C. Meyer, and J. Rigaut, *Chem. Phys. Lett.*, **11**, 359 (1971).

48) F. Kieffer, C. Meyer, and J. Rigaut, *Int. J. Radiat. Phys. Chem.*, **6**, 79 (1974).

49) A. I. Mikhailov, *Dokl. Akad. Nauk SSSR*, **197**, 136 (1970).

50) M. Tachiya and A. Mozumder, *Chem. Phys. Lett.*, **28**, 87 (1974).

51) F. S. Dainton, M. J. Pilling, and S. A. Rice, *J. Chem. Soc. Faraday Trans.* 2, **71**, 1311 (1975).

52) M. Tachiya and A. Mozumder, *Chem. Phys. Lett.*, **34**, 77 (1975).

53) M. J. Pilling and S. A. Rice, *J. Phys. Chem.*, **79**, 3035 (1975).

54) J. T. Randall and M. H. Wilkins, *Proc. R. Soc. London, Ser. A*, **184**, 366 (1945).

55) P. D. Townsend and Y. Kirsh, *Comtem. Phys.*, **30**, 337 (1989).

56) V. G. Nikolskii and N. Ya. Buben, *Dokl. Akad. Nauk SSSR*, **134**, 134 (1960).

57) A. Charlesby and R. H. Partridge, *Proc. R. Soc. London, Ser. A*, **271**, 170 (1963).

58) R. H. Partridge, in *"The Radiation Chemistry of Macromolecules"*, Vol. I, ed. M. Dole, Academic Press, New York (1972), Chap. 10, p. 194.

59) T. Hashimoto, H. Shimada, and T. Sakai, *Nature*, **268**, 255 (1975).

60) R. J. Fleming, *J. Therm. Anal.*, **36**, 331 (1990).

61) R. J. Fleming, *Radiat. Phys. Chem.*, **36**, 59 (1990).

62) A. Mozumder and J. L. Magee, *J. Chem. Phys.*, **47**, 939 (1967).

63) A. Mozumder, *J. Chem. Phys.*, **48**, 1659 (1968).

64) G. C. Abell and K. Funabashi, *J. Chem. Phys.*, **58**, 1079 (1973).

65) J. M. Warman and S. J. Rzad, *J. Chem. Phys.*, **52**, 485 (1970).

66) A. Mozumder, *J. Chem. Phys.*, **60**, 4305 (1974).

67) R. J. Friauf, J. Noolandi, and K. M. Hong, *J. Chem. Phys.*, **71**, 143 (1979).

68) T. W. Scott and C. L. Braun, *Chem. Phys. Lett.*, **127**, 501 (1986).

69) H. Miyasaka and N. Mataga, *Chem. Phys. Lett.*, **134**, 480 (1987).

70) Y. Yoshida, S. Tagawa, and Y. Tabata, *Radiat. Phys. Chem.*, **23**, 279 (1984).

71) Y. Yoshida, S. Tagawa, and Y. Tabata, *Radiat. Phys. Chem.*, **28**, 201 (1986).

72) Y. Yoshida and S. Tagawa, in *"Dynamics and Mechanisms of Photoinduced Electron Transfer and Related Phenomena"*, eds. N. Mataga, T. Okada, and H. Masuhara, Elsevier, Amsterdam (1992), p. 435.

73) Y. Hama, Y. Kimura, H. Tsumura, and N. Omi, *Chem. Phys.*, **53**, 115 (1980).

74) Y. Hama and K. Gouda, *Radiat. Phys. Chem.*, **21**, 185 (1983).

75) A. Charlesby, *"Atomic Radiation and Polymers"*, Pergamon Press, Oxford (1960).

76) A. Chapiro, *"Radiation Chemistry of Polymeric Systems"*, Wiley Interscience, New

York (1962).

77) *"The Radiation Chemistry of Macromolecules"*, Vol. I, II, ed. M. Dole, Academic Press, New York (1973).

78) W. Schnabel, *"Polymer Degradation —Principles and Practical Applications— "*, Carl Hanser Verlag, Munch (1982).

79) A. R. Schultz, P. I. Roth, and G. B. Rathman, *J. Polym. Sci.*, **22**, 195 (1956).

80) C. David, D. Fuld, and G. Geuskens, *Makromol. Chem.*, **139**, 269 (1970).

81) C. David, D. Fuld, and G. Geuskens, *Makromol. Chem.*, **160**, 135 (1972).

82) C. David, D. Fuld, and G. Geuskens, *Makromol. Chem.*, **160**, 347 (1972).

83) W. W. Parkinson, C. D. Bopp, D. Binder, and J. E. White, *J. Phys. Chem.*, **69**, 828 (1965).

84) J. H. O'Donnell and P. J. Pomery, *J. Polym. Sci., Polym. Symp.*, **55**, 269 (1976).

85) T. Ichikawa and H. Yoshida, *J. Polym. Sci., Polym. Chem. Ed.*, **28**, 1185 (1990).

86) T. Ichikawa and H. Yoshida, *Radiat. Phys. Chem.*, **37**, 367 (1991).

87) H. Yoshida and T. Ichikawa, in *"Recent Trends in Radiation Polymer Chemistry"*, Advances in Polymer Science, Vol. 105, ed. S. Okamura, Springer-Verlag, Berlin (1993), p. 3.

88) W. Sakai, A. Tsuchida, M. Yamamoto, T. Matsuyama, H. Yamaoka, and J. Yamauchi, *Macromol. Rapid Commun.*, **15**, 551 (1994).

89) W. Sakai, A. Tsuchida, M. Yamamoto, and J. Yamauchi, *J. Polym. Sci., Polym. Chem. Ed.*, **33**, 1969 (1995).

90) H. Ahne, R. Leuschner, and R. Rubner, *Polym. Adv. Tech.*, **4**, 217 (1993).

91) J. Guillet, *"Polymer Photophysics and Photochemistry"*, Cambridge University Press, Cambridge (1985), Chap. 9.

92) J. M. Pearson and M. Stolka, *"Poly(N-vinylcarbazole)"*, Gordon and Beach Science Publishers, New York (1981).

93) K. Okamoto, A. Itaya, and S. Kusabayashi, *Chem. Lett.*, 1167 (1974).

94) F. C. De Schryver, P. Collart, J. Vandendriessche, R. Goedeweeck, A. Swinnen, and M. V. der Auweraer, *Acc. Chem. Res.*, **20**, 159 (1987).

95) W. Klöpffer, *J. Chem. Phys.*, **50**, 2337 (1969).

96) G. Rippen, G. Kaufmann, and W. Klöpffer, *Chem. Phys.*, **52**, 1265 (1980).

97) W. Klöpffer, *Chem. Phys.*, **57**, 75 (1981).

98) H. Masuhara, J. Vandendriessche, K. Demeyer, N. Boens, and F. C. De Schryver, *Macromolecules*, **15**, 1471 (1982).

99) A. Itaya, H. Sakai, and H. Masuhara, *Chem. Phys. Lett.*, **138**, 231 (1987).

100) A. Itaya, H. Sakai, and H. Masuhara, *Chem. Phys. Lett.*, **146**, 570 (1988).

101) H. Miyasaka, T. Moriyama, S. Kotani, R. Muneyasu, and A. Itaya, *Chem. Phys. Lett.*, **225**, 315 (1994).

102) T. Ueda, R. Fujisawa, H. Fukumura, A. Itaya, and H. Masuhara, *J. Phys. Chem.*, **99**, 3629 (1995).

103) K. Watanabe, T. Asahi, and H. Masuhara, *Chem. Phys. Lett.*, **233**, 69 (1995).

104) H. Masuhara, K. Yamamoto, N. Tamai, K. Inoue, and N. Mataga, *J. Phys. Chem.*, **88**, 3971 (1984).

105) H. Masuhara, N. Tamai, N. Mataga, F. C. De Schryver, and J. Vandendriessche, *J. Am. Chem. Soc.*, **105**, 7256 (1983).

106) Y. Tsujii, A. Tsuchida, M. Yamamoto, and Y. Nishijima, *Macromolecules*, **21**, 665 (1988).

107) M. Yamamoto, Y. Tsujii, and A. Tsuchida, *Chem. Phys. Lett.*, **154**, 559 (1989).

108) A. Tsuchida, A. Nagata, M. Yamamoto, H. Fukui, M. Sawamoto, and T. Higashimura, *Macromolecules*, **28**, 1285 (1995).

Part I

Chapter 2

Photoionization and Thermoluminescence in Poly(alkyl methacrylate) Films

2.1. Introduction

Multiphoton excitation of an aromatic dopant in a polymer solid ejects an electron from the dopant to the polymer matrix, producing a dopant radical cation and a photoejected electron. For example, intense laser pulse excitation of *N,N,N',N'*-tetramethyl-*p*-phenylenediamine (TMPD) doped in a poly(methyl methacrylate) (PMMA) solid develops the Wurster's blue color of the TMPD radical cation ($TMPD^{\bullet+}$). The $TMPD^{\bullet+}$ formed in the PMMA matrix is so stable that the color can be recognized even after a one-year storage at room temperature. The color fades when the temperature of the sample is raised near the glass transition temperature (T_g) of PMMA (378 K). Therefore, this photochromism is a reversible phenomenon. The backward charge recombination process is also observed through isothermal luminescence (ITL, preglow) and thermoluminescence (TL, glow).

Historically, Lewis found the two-photon ionization of TMPD in an EPA glass at 77 K.[1] Later, Albrecht studied extensively ITL, TL, and photoconductivity for the TMPD/3-methylpentane system (77 K), the mechanism of which was elucidated to be the recombination of the parent cation with an ejected electron.[2] Tsubomura also examined ITL and TL of TMPD in a rigid glass at 77 K in detail.[3] As for ITL and TL in polymer solids, Nikolskii and Buben were the first to measure the TL from irradiated polymer samples.[4] They found that the TL glow curve from the irradiated polymer bulk well reflects the polymer chain motion. Later, Charlesby and Partridge extensively studied TL of non-polar polymers such as polyethylene and polypropylene.[5,6] Hama *et al.* studied ITL and TL from γ-irradiated polymers.[7–10] They showed that the initial distribution function of an ejected electron from the parent cation just after the irradiation can be given

by the Laplace inverse transformation of the experimental ITL decay function, which has been reported to be inversely proportional to time, assuming the electron tunneling recombination of the geminate ion pair.

In this chapter, recent findings on the photochromism of chromophores doped in polymer films through two-photon ionization, and the ITL and TL resulting from the charge recombination of dopant radical cations with photoejected electrons[11–14] are demonstrated.

2.2. Experimental Section

2.2.1. Samples

Polymer samples used in this chapter were poly(methyl methacrylate) (PMMA, M_n = 7.0 – 7.5 × 10^5, Nacalai Tesque), poly(ethyl methacrylate) (PEMA, M_w = 2.8 × 10^5, Scientific Polym. Prod.), poly(*n*-butyl methacrylate) (PnBMA, M_w = 10^5, Scientific Polym. Prod.), and polystyrene (PSt, M_n = 1.6 – 1.8 × 10^5, Wako Pure Chem. Ind., Ltd.). All these polymers were purified by reprecipitation from a benzene solution into methanol twice. The glass transition temperatures of the polymers are 378 K (PMMA), 339 K (PEMA), 293 K (PnBMA), and 373 K (PSt).[15]

Perylene (Pe, Aldrich Chem.) and *N,N,N',N'*-tetramethylbenzidine (TMB, Wako Pure Chem. Ind., Ltd.) were used as the dopant chromophore. Perylene was purified by silica-gel flash column chromatography eluted with dichloromethane and TMB was purified by recrystallization several times.

Sample films for measurements were prepared by the solution cast method. A Pe chromophore was dissolved in benzene (Dojin Spectrosol) with polymer powder to make the concentration in the final polymer film 3 × 10^{-3} mol/L. The solution was cast on a glass plate in a dry box under a nitrogen atmosphere for two days and then dried by evacuation for one day at room temperature. The film was peeled off from the glass plate and finally dried by evacuation above the T_g for more than 10 h to remove the remaining trace of the casting solvent. No change of the Pe absorption or emission spectra was observed after the above heating procedure.

2.2.2. Measurements

Measurements of ITL and TL were done in a sample chamber of a cryostat *in vacuo*. The polymer sample film was covered with a quartz plate and set tightly on a copper cold finger of a cryostat (Iwatani Plantech Corp., CRT510). The sample film was cooled down to 20 K and the dopant Pe chromophore was selectively photoirradiated by 351-nm light pulses from a XeF excimer laser (Lambda Physik, EMG101MSC, *ca.* 20 ns fwhm and *ca.* 60 mJ/pulse) repeatedly. None of the polymers used in this work have absorption at 351 nm. Immediately after the disappearance of the Pe prompt luminescence, the isothermal luminescence (ITL) from the sample film was measured from 1 min to 25 h after the photoexcitation at 20 K. A photon-counting system was used for the emission intensity measurement, which consists of a photomultiplier (Hamamatsu, R585) and a photon counter (Hamamatsu, C-1230) connected to a personal computer. The ITL from the sample film became almost negligible 25 h after the photoexcitation. Then the film temperature was raised from 20 to 300 K at a heating rate of 5 K/min in the cryostat using a PID temperature control unit (Iwatani Plantech, TCU-4). The temperature was monitored by a calibrated Au + 0.07 % Fe / chromel thermocouple at the sample film position using an indium gasket. The thermoluminescence (TL) intensity from the sample film stimulated by heating was recorded using the photon-counting apparatus in the same manner as described above. The control experiment where the polymer films with no Pe dopant were excited by the same procedure gave neither ITL nor TL.

The steady state absorption and emission spectra of the sample films were measured by a spectrophotometer (Hitachi, U-3210) and a spectrofluorophotometer (Hitachi, 850), respectively, using a 2-nm slit width in the cryostat.

2.3. Results and Discussion

2.3.1. Photoionization of Perylene

The present experimental system of ITL and TL caused by the two-photon ionization has an advantage that the ionization condition can be easily controlled by selecting the proper excitation wavelength, dopant chromophore molecule, and the chromophore concentration. Many aromatic amines and polynuclear aromatic compounds

have been proved to be ionized by the two-photon excitation in a variety of polymer matrices.[11-14] In this chapter, perylene was used mainly as a dopant chromophore. Perylene has a large fluorescence quantum yield ($\Phi_f \approx 0.9$), which is desirable for the emission measurements.[16] The lack of the temperature dependence of this Φ_f of Pe was checked by the steady-state emission measurement over the temperature range from 20 to 300 K. The contribution of Pe phosphorescence ($\lambda_p \approx 800$ nm) to the present photon-counting measurement was considered to be negligible because of the small intersystem-crossing quantum yield of the excited singlet Pe and of the lack of the photomultiplier sensitivity in the red region. In practice, the emission spectra of ITL and TL measured by spectrofluorophotometry were the same as that of Pe fluorescence.

Figure 2–1 shows the absorption spectra of a PnBMA film doped with a Pe chromophore after the photoexcitation by the intense 351-nm laser pulses at 20 K. The

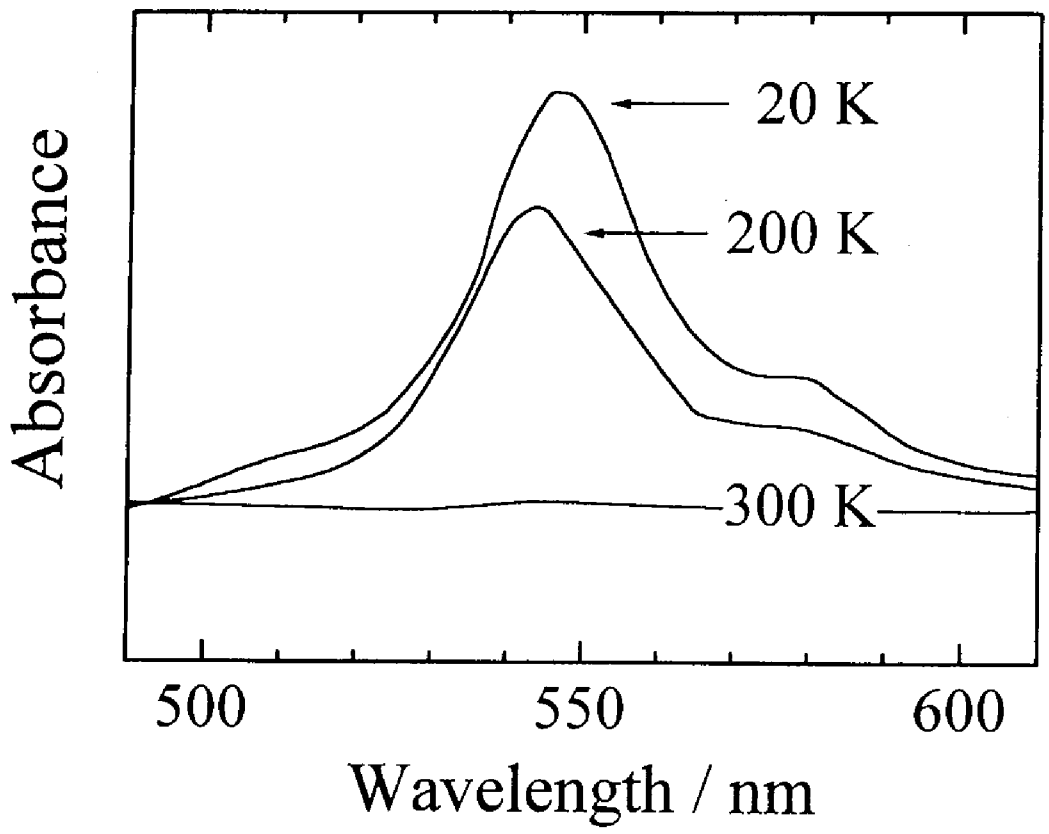

Figure. 2–1. Absorption spectra of $Pe^{\bullet+}$ formed through two-photon ionization in a PnBMA film measured at 20, 200, and 300 K.

sharp absorption band appearing around 545 nm after the photoexcitation was ascribed to that of Pe radical cation ($Pe^{\bullet+}$).[17,18] Owing to the formation of this $Pe^{\bullet+}$, the photoexcited sample film was colored purple. This $Pe^{\bullet+}$ is considered to be formed through the two-photon ionization by the intense laser excitation; the two-photon nature of this $Pe^{\bullet+}$ formation is obvious by the fact that no appreciable $Pe^{\bullet+}$ is produced by the prolonged photoexcitation with a Xe lamp, whose photon density is not sufficient to feed another photon to the excited Pe within the lifetime.[11-14] As shown in Figure 2-1, the absorption band of $Pe^{\bullet+}$ decreased with the temperature rise to 200 K, and finally it almost disappeared at 300 K, above the T_g of PnBMA.

2.3.2. Thermoluminescence (TL)

Figure 2-2 shows the TL glow curves for the Pe doped poly(alkyl methacrylate)s and PSt observed with the temperature rise from 20 to 300 K at a heating rate of 5 K/min. The measurements were done 25 h after the laser photoexcitation to avoid the participation of the ITL.

Although the TL intensity of PSt was weak as shown in the figure, all polymers studied gave the glow peaks around 100 – 200 K. These glow peaks are considered to be caused by the side group rotation of poly(alkyl methacrylate)s and PSt. Wada *et al.* studied the transition temperature of poly(alkyl methacrylate)s by NMR, and reported that the ester methyl group relaxation appears at 90 K (50 MHz), the methyl at the end of the alkyl group at 130 – 140 K (20 MHz), and α-methyl group at 240 – 260 K (20 MHz).[19] Also the transition temperature of the phenyl group rotation of PSt was reported to exist at 180 K (10 kHz) by the dynamic mechanical relaxation measurements.[20]

The good correlation of the glow peaks with the transition temperature has already been reported for γ-irradiated polymers.[4] In the present system of laser photoexcited polymers, the polymer chain local motions are also considered to enhance the recombination of the hole-electron pair produced through the two-photon process. As shown in Figure 2-2, PnBMA gave a large glow peak around 200 – 300 K. This glow peak is considered to be caused by the local mode relaxation of the polymer main chain, which is an incoherent oscillation of a polymer main chain. The number of the monomer units participating in this relaxation has been reported to be about 10 – 50.[21] This correlation chain length is of the same order as an estimated distance of 30 – 40 Å from a

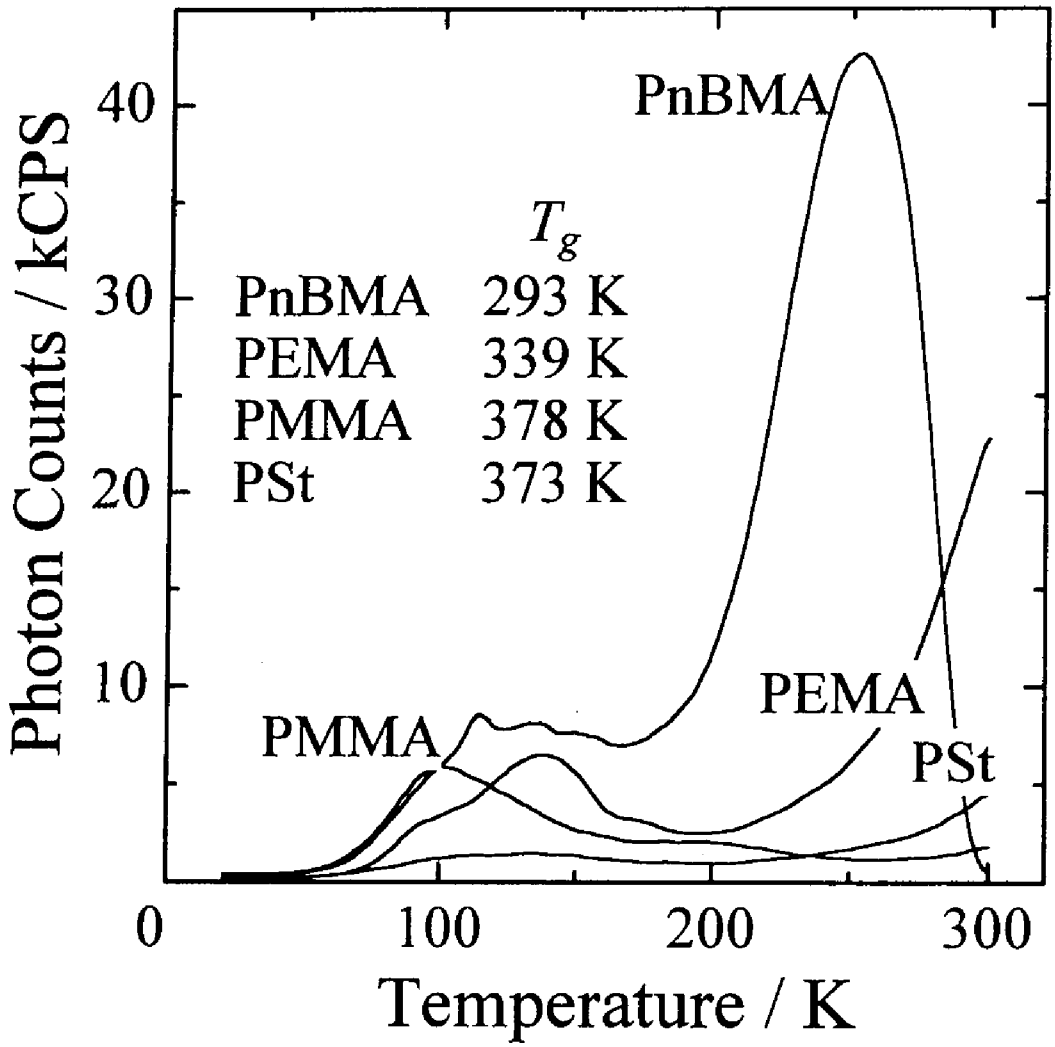

Figure. 2–2. Thermoluminescence (TL) glow curves of the polymer films doped with Pe measured after 25 h from 351-nm photoexcitation at 20 K. Heating rate was 5 K/min.

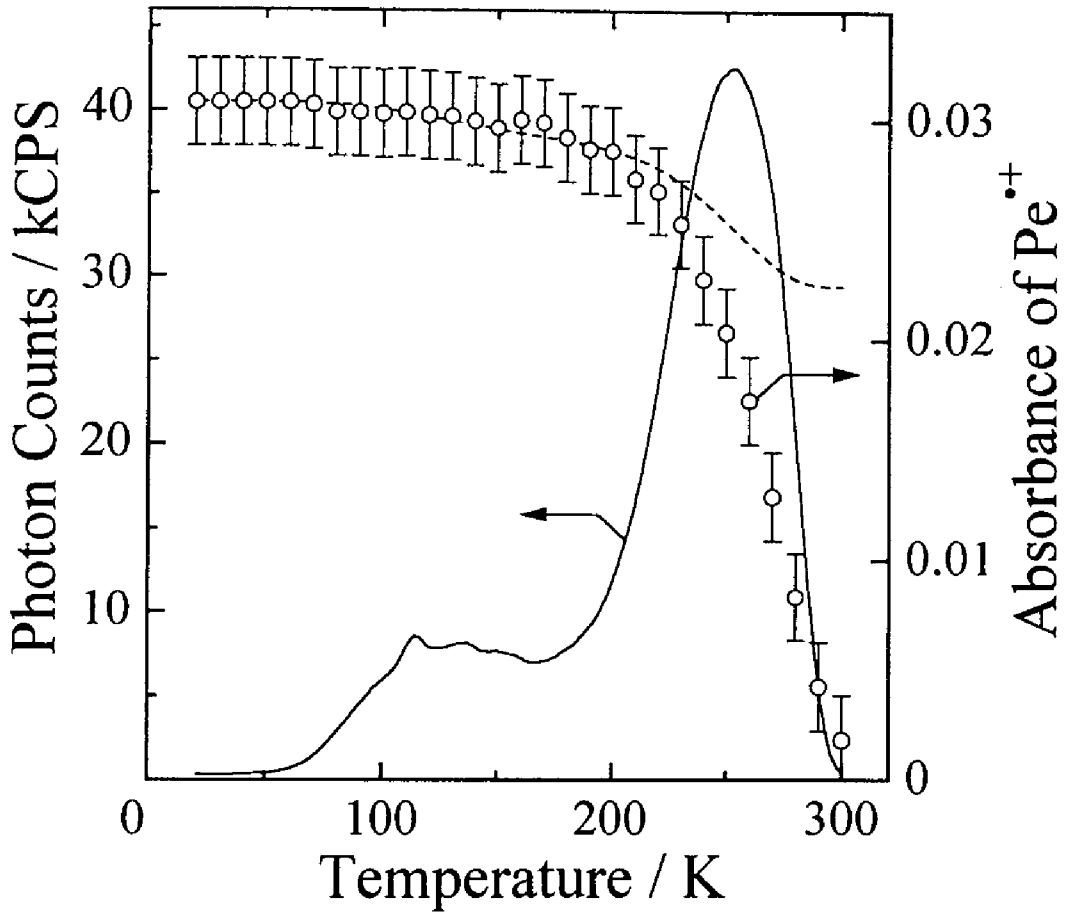

Figure. 2–3. Relationship between the thermoluminescence (TL) glow curve (solid line) and the absorbance (545 nm) of $Pe^{\bullet+}$ (open circles) produced through two-photon ionization at 20 K in a PnBMA film. Error bar shows the resolution limit of the spectrophotometer. The broken line shows the expected decay of the $Pe^{\bullet+}$ from the integration of the glow curve.

photoejected electron to the parent radical cation by the two-photon excitation.[11-14] The stimulation of this local main chain motion of the polymer matrices was strong enough to cause the charge recombination of all the hole-electron pairs. Other polymers of PMMA, PEMA, and PSt have a higher T_g and hence a higher relaxation temperature of the local main chain motion than those of PnBMA. Therefore, the corresponding glow peak was expected to shift to the higher temperature side above 300 K. In practice, the glow curves for PMMA, PEMA, and PSt in Figure 2–2 show a tendency to increase around 300 K, which is considered to be the onset of the glow peak induced by the main chain local relaxation.

To obtain the direct evidence that the glow was caused by the charge recombination of a photoejected electron with the parent radical cation, absorption measurement was done for a PnBMA film. Figure 2–3 shows the glow curve (solid line) and the absorbance of $Pe^{\bullet+}$ (open circles) for a PnBMA film doped with Pe. This figure shows that the decrease in the $Pe^{\bullet+}$ absorbance is related closely to the glow peaks around 100 – 200 K and 200 – 300 K. The broken line in the figure shows the expected curve of the $Pe^{\bullet+}$ decay from the integration of the glow curve. Although the expected $Pe^{\bullet+}$ decay deviated from the experimental curve above 200 K, both curves gave roughly the same tendency. This means that the charge recombination of $Pe^{\bullet+}$ with the ejected electron was the cause of the TL of Pe. The deviation above 200 K seen in the figure may be attributed to the change of the energy level of trapped electron, which has been shown by the ESR measurements.[22]

To demonstrate the recombination mechanism of ITL and TL, the electric field effect on ITL was examined for the TMB doped PMMA film. Figure 2–4 shows the electric field effect on ITL; the ITL was enhanced by an electric field. Both plus and minus polarities were effective to enhance the luminescence intensity. The intensity gradually decreased with the repeated application of an electric field. This decrease in intensity is probably because the amount of trapped electrons is constant upon photoionization and they are released by application of an electric field.

The present photochromism has two features: one is a threshold intensity due to two-photon ionization and the other is very fast response because the mechanism is an electron transfer process. Both ITL and TL may be used as the information storage where the read-out is made in an emissive way. Recent detectors such as single photon-counting technique have a very high sensitivity, thus ITL and TL system may make a unique image

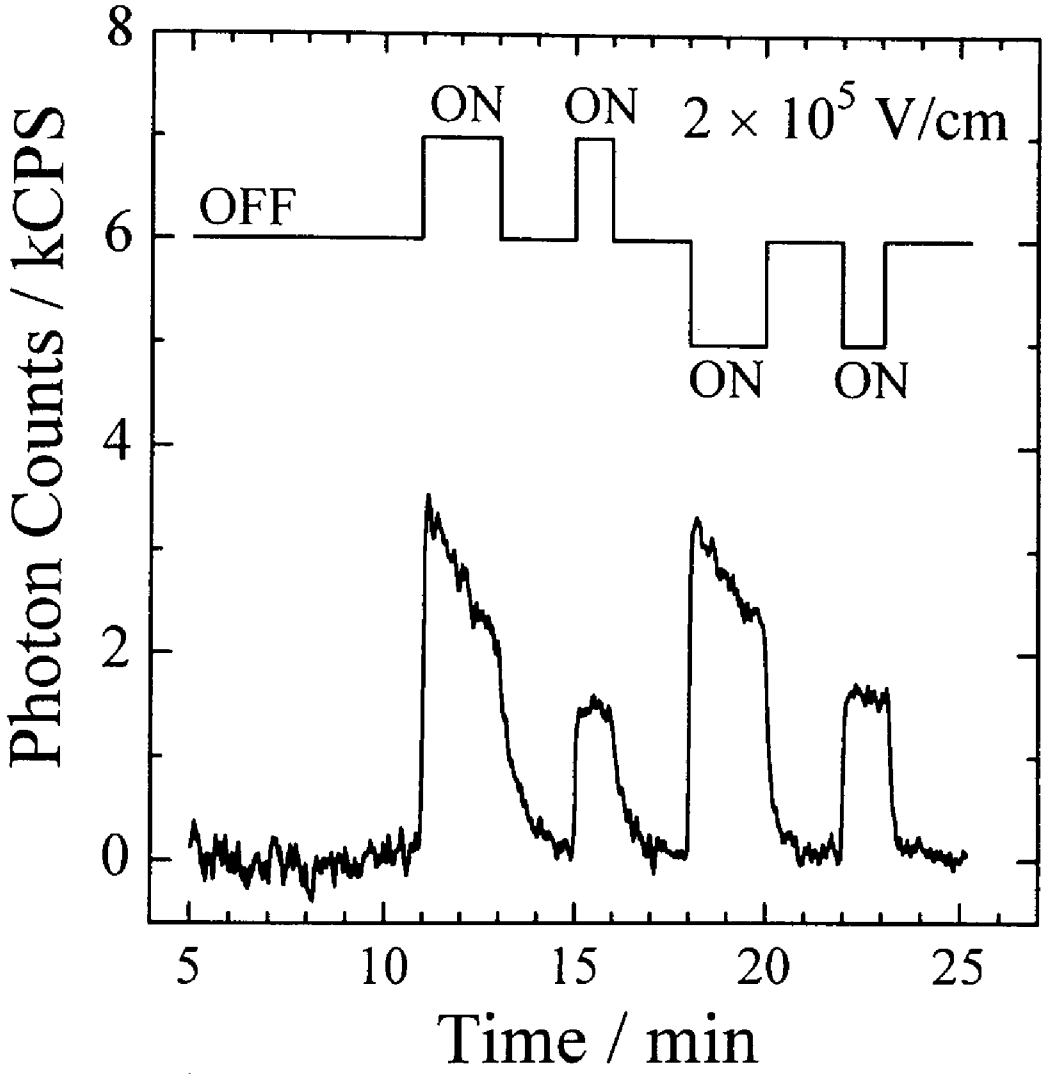

Figure. 2–4. Electric field effect on ITL for the TMB/PMMA system at 77 K. The upper signal is applied electric field; the polarity was reversed in the third step. The lower signal is ITL intensity enhanced.

storage device. The electric field effect can be used for intensification of the ITL and TL. When two-photon ionization is induced at a low temperature through a mask, one can store a photochromic or latent image in the film, and this image can be read out in an emissive way by applying heat or an electric field.

2.4. Conclusion

ITL and TL as well as photochromism upon photoirradiation by an intense pulse laser were observed on the polymer films doped with a chromophore. The photochromism was induced by two-photon ionization of a dopant chromophore, and ITL and TL were caused by the charge recombination of an ejected electron with the chromophore radical cation. Some applications of ITL and TL as well as photochromism have been presented.

References

1) J. E. Willard, in "*Fundamental Processes in Radiation Chemistry*", ed. P. J. Ausloos, Interscience, New York (1969), Chap. 9.
2) A. C. Albrecht, *Acc. Chem. Res.*, **3**, 238 (1970).
3) K. Yoshinaga, N. Yamamoto, M. Ozaki, and H. Tsubomura, *Nippon Kagaku Zasshi*, **92**, 124 (1971).
4) V. G. Nikolskii and N. Ya. Buben, *Dokl. Akad. Nauk SSSR*, **134**, 134 (1960).
5) A. Charlesby and R. H. Partridge, *Proc. R. Soc. London, Ser. A*, **271**, 170 (1963).
6) A. Charlesby and R. H. Partridge, *Proc. R. Soc. London, Ser. A*, **283**, 312 (1965).
7) Y. Hama, K. Nishi, K. Watanabe, and K. Shinohara, *J. Polym. Sci., Polym. Chem. Ed.*, **12**, 1109 (1974).
8) M. Tsumura, S. Takahashi, N. Omi, and Y. Hama, *Radiat. Phys. Chem.*, **16**, 67 (1980).
9) Y. Hama, Y. Kimura, H. Tsumura, and N. Omi, *Chem. Phys.*, **53**, 115 (1980).
10) Y. Hama and K. Gouda, *Radiat. Phys. Chem.*, **21**, 185 (1983).
11) A. Tsuchida, M. Nakano, M. Yoshida, M. Yamamoto, and Y. Wada, *Polym. Bull.*, **20**, 297 (1988).
12) M. Yamamoto, A. Tsuchida, and M. Nakano, *MRS Int. Meeting Adv. Mater.*, **12**, 243 (1989).
13) A. Tsuchida, W. Sakai, M. Nakano, M. Yoshida, and M. Yamamoto, *Chem. Phys. Lett.*, **188**, 254 (1992).
14) A. Tsuchida, W. Sakai, M. Nakano, and M. Yamamoto, *J. Phys. Chem.*, **96**, 8855 (1992).
15) P. Peyser, in "*Polymer Handbook* ", 3rd ed., eds. J. Brandrup and E. H. Immergut, John Wiley & Son, New York (1989).
16) J. B. Birks, "*Photophysics of Aromatic Molecules*", Wiley Interscience, New York (1970), Chap. 6, p. 252.
17) G. J. Hoijtink and W. P. Weijland, *Recueil*, **76**, 836 (1957).
18) K. H. Grellmann, A. R. Watkins, and A. Weller, *J. Phys. Chem.*, **76**, 469 (1972).
19) Y. Tanabe, J. Hirose, K. Okano, and Y. Wada, *Polym. J.*, **1**, 107 (1970).
20) O. Yano and Y. Wada, *J. Polym. Sci., Part A-2*, **9**, 669 (1971).

21) K. Yamafuji, *J. Phys. Soc. Jpn.*, **15**, 2295 (1960).

22) W. Sakai, A. Tsuchida, M. Yamamoto, and J. Yamauchi, *J. Polym. Sci., Polym. Chem. Ed.*, **33**, 1969 (1995).

Chapter 3

Charge Recombination via Electron Tunneling after Two-Photon Ionization of Dopant Chromophore in Poly(n-butyl methacrylate) Film at 20 K

3.1. Introduction

The luminescence having an extremely long lifetime is observed when a solid matrix is irradiated at a low temperature by high energy radiation such as γ- and X-rays. The decay of this isothermal luminescence (ITL) intensity has been reported to obey an inverse power function of time t,[1-4] that is, the t^{-m} law with $m \approx 1$, which is also called the Debye-Edwards law by Hamill.[5] This phenomenon has been explained as the luminescence resulting from the charge recombination of trapped electrons with the parent cation produced by the irradiation. Historically, Debye and Edwards[2] applied, for the first time, a diffusion mechanism to the ion-recombination reaction under a spatial distribution of ejected electrons. However, in their model, the total amount of produced ionic species is infinite because the distribution function is not normalized. Although Abell and Mozumder[6] resolved this problem using a normalized distribution function, only at an intermediate time scale can the t^{-1} decay be reproduced even in their model. In other words, the t^{-1} decay kinetics cannot be explained in terms of a simple diffusion mechanism for trapped electrons. In a simple diffusion model, the number of trapped electrons $N(t)$ is proportional to the square root of the inverse of time $t^{-1/2}$ in the long time region and thus the ITL intensity $I(t)$ is proportional to $t^{-3/2}$; the t^{-m} law cannot be explained by a simple diffusion model.

Hamill and Funabashi[7] insisted that one can explain the t^{-m} decay of the recombination luminescence as a non-Gaussian diffusion process with a hopping time

distribution of the asymptotic type proposed by Scher and Montroll. Scher and Montroll[8] adopted the Montroll-Weiss[9] model of continuous-time random walk (CTRW) to explain the long tail of the transient photocurrent in amorphous solids. They found that the hopping time distribution $\varphi(t)$ for localized electrons in disordered systems is an asymptotic type ($\varphi(t) \sim t^{-(1+\alpha)}$, $0 < \alpha < 1$), not an exponential type ($\varphi(t) = \lambda e^{-\lambda t}$, $\lambda =$ *const.*) leading to the familiar Gaussian diffusion. The hopping time distribution of the asymptotic type reflects the distribution for space and/or energetic depth of the trap sites. If activation energy for trapped electrons has a distribution, the rate of thermal activated electron transfer from one trap to another depends largely upon the temperature changes.

Kieffer, Meyer, and Rigaut[10,11] showed that the decay kinetics of the ITL in an irradiated rigid solution of methylcyclohexane is independent of temperature between 4 and 77 K. These experimental results indicate that trapped electrons are transferred to the parent cation without thermal activation. Thus, many authors[12–16] have explained the electron transfer independent of temperature using an electron tunneling model. Hama *et al.* found that, with the assumption of the electron tunneling, the Laplace inverse transformation of an empirical ITL decay function leads to the initial distribution function of a distance between a trapped electron and the parent cation just after the irradiation.[17,18] They used eq 3–1 as an empirical ITL decay function and insisted that the value of m should be more than unity to avoid the divergence of the total amount of ionic species.

$$I(t) = \frac{I_0}{(1+\alpha t)^m} \qquad (3\text{–}1)$$

Here, the ITL was observed for a photoirradiated polymer solid doped with a low molecular weight aromatic chromophore. An intense near-UV light pulse from an excimer laser (351 nm) was used for the selective photoexcitation of the dopant chromophore. The laser pulse is intense enough to feed another photon to the excited chromophore within the lifetime. Consequently, the dopant chromophore is excited to a higher level and then ejects an electron to the polymer matrix. The parent radical cation thus formed and the trapped electron in the polymer have already been reported to be so stable that the color of the parent radical cation can be seen even after a one-year storage from the photoexcitation at room temperature.[19–22]

Although the ITL from the irradiated polymers has been postulated to be caused

by the charge recombination of an electron with the parent cation, the direct evidence has been scarce to show that the emission intensity of ITL corresponds to the decay of the cationic species. For the case of the excitation by high energy radiation, this is probably due to the difficulty of the absorption measurement for the produced polymer cation with a very small molar absorption coefficient. In the present system, the use of a chromophore the radical cation of which has strong absorption in the visible region enables one to observe directly the decay of the radical cation by absorption spectroscopy. Thus, the decay of radical cation as well as the ITL decay was observed.

In this chapter, the mechanism of the ITL resulting from the recombination of electron-cation pairs formed in a polymer solid through two-photon ionization of dopant chromophores was elucidated. The effect of multi-shot photoirradiation on the ITL decay kinetics was examined by the ITL and TL measurement.

3.2. Experimental Section

3.2.1. Chemicals

The polymer sample used in this chapter was poly(*n*-butyl methacrylate) (PnBMA, $M_w = 10^5$, Scientific Polym. Prod., Inc.). The polymer was purified by reprecipitation from a benzene solution into methanol three times. The glass transition temperatures (T_g) of PnBMA is 293 K.[23]

Dopant chromophores used were perylene (Pe, Aldrich Chem. Co., Inc.) or *N,N,N',N'*-tetramethylbenzidine (TMB, Wako Pure Chem. Ind., Ltd.). Perylene was purified by silica-gel flash column chromatography eluted with dichloromethane and TMB was purified by recrystallization several times.

3.2.2. Sample Preparation

Polymer films for measurements were prepared by the solution cast method. A dopant chromophore was dissolved in a benzene (Dojin Spectrosol) solvent with a polymer powder so as to make a dopant concentration of *ca.* 3×10^{-3} mol/L in the final polymer film. The solution was cast on a glass plate in a dry box under a nitrogen atmosphere for two days and then was dried by evacuation for one day at room temperature. The film was

peeled off from the glass plate and was finally dried under vacuum above the T_g for more than 10 hours to remove the remaining trace of the solvent. No change of the absorption or emission spectra of the dopant was observed for the doped polymer films after the above heating procedure.

3.2.3. General Procedures

The ITL was measured in a sample chamber of a cryostat *in vacuo*. The polymer sample film was covered with a quartz plate and set tightly on a copper cold finger of a cryostat (Iwatani Plantech Corp., CRT510). The sample film was cooled down to 20 K and the temperature was kept constant using a PID temperature control unit (Iwatani Plantech Corp., TCU-4). The film temperature was monitored with a calibrated Au + 0.07 % Fe / chromel thermocouple at the sample film position using an indium gasket.

A dopant chromophore was selectively photoirradiated by a 351-nm light pulse from a XeF excimer laser (Lambda Physik, EMG101MSC, *ca.* 20 ns fwhm, and *ca.* 30 mJ/cm^2). The emission from the sample film (this is ITL or preglow) was measured from 1 min to 25 h after the photoexcitation at 20 K. A photon-counting system was used for the emission intensity measurement, which consists of a photomultiplier (Hamamatsu, R585) and a photon counter (Hamamatsu, C-1230) connected to a personal computer. The ITL from the sample film became almost negligible 25 h after the photoirradiation.

Subsequently, the film temperature was raised from 20 to 300 K at a heating rate of 5 K/min in the cryostat using the PID temperature control unit. Emission from the sample film was observed again with increase in the sample temperature. This thermal stimulated emission is called thermoluminescence (TL or glow). The TL intensity was recorded in the same manner as described above. The ITL and TL were not observed at all in the control experiments where the polymer films without dopant chromophores were excited in the same procedure as mentioned above.

The absorption spectra of the photoirradiated sample films were measured in the cryostat with a spectrophotometer (Hitachi, U-3500) using a 2-nm slit width. Ten sheets of the sample films prepared freshly were put together so as to gain high absorbance of the radical cation; total thickness is *ca.* 2 mm. The absorption spectra were measured from 5 min to 25 h after the photoirradiation at 20 K. The monitor light was shut off between the measurements to prevent the sample film from being photobleached.

3.2.4. Dependence on the Number of Photoirradiation Shots at a Fixed Fluence

A Pe doped PnBMA film was photoirradiated at 20 K and then ITL and TL were measured by the procedure mentioned above. The photoirradiation conditions were changed as follows: the energy density for a 1-shot laser pulse was *ca.* 3 mJ/cm^2; the laser pulse interval was set at 2 Hz; the number of photoirradiation shots was 1, 10, 50, 100, 500, 1000, 5000, and 10000, that is, the total number of photoirradiation shots was 1, 11, 61, 161, 661, 1661, 6661, and 16661, respectively. The sample film was used repeatedly in this experiment after an adequate annealing at 300 K above the T_g. This procedure can avoid the difference in the ITL intensity among sample films.

3.3. Results and Discussion

3.3.1. ITL Decay and Absorbance Decay of TMB Radical Cation under 1-Shot Photoirradiation Condition

In the beginning, the relationship between the ITL decay and the absorbance decay of TMB radical cation ($TMB^{\bullet+}$) produced through two-photon ionization is considered from the viewpoint of decay kinetics. Figure 3–1 shows the ITL decay of a PnBMA film doped with a TMB chromophore measured after the laser photoexcitation at 20 K. The log-log plots of the observed ITL intensity $I(t)$ *vs.* time t gave a straight line. This linear relationship (the t^{-m} law) was observed over the time range from 1 min to 25 h: of three or four orders of magnitude for time t.

The ITL decay profile after irradiation is empirically expressed[17,18] by

$$I(t) = \frac{I_0}{(1+\alpha t)^m}, \qquad (3\text{–}1)$$

where $I(t)$ is the ITL decay, I_0 is the ITL intensity at $t = 0$ just after the irradiation, and α and m are parameters. This empirical equation is theoretically explained in terms of the geminate charge recombination of a trapped electron with the parent radical cation on the basis of electron tunneling.[15,17,18] The ITL decay shown in Figure 3–1 was fitted to eq 3–1 using the least-squares method with I_0, α, and m as fitting parameters. The solid line in the figure shows the best fitting and one of the best-fit values is as follows: $I_0 = 1.3 \times 10^9$ CPS, $\alpha = 23.0$ s^{-1}, and $m = 1.11$. The values of I_0 and α have some ambiguity because the

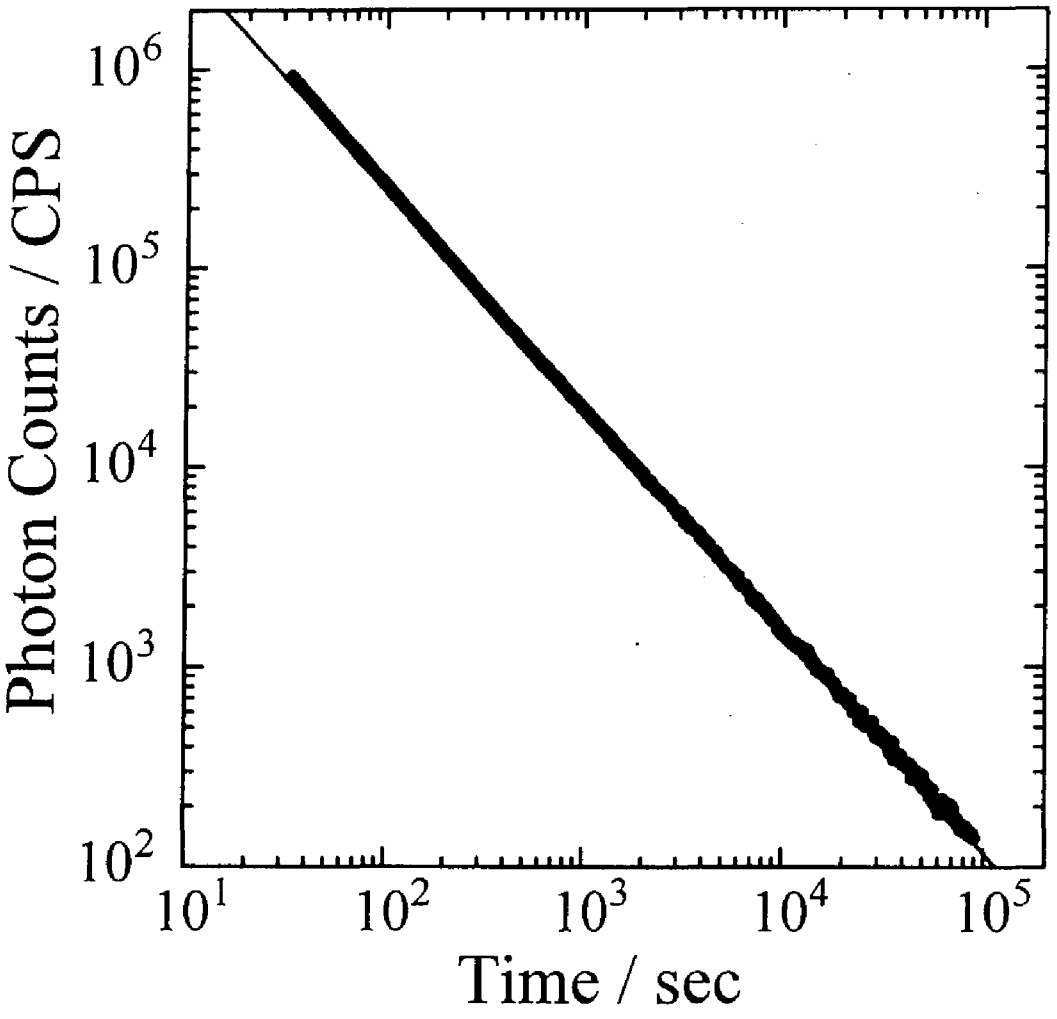

Figure 3–1. The ITL decays of a PnBMA film doped with a TMB chromophore measured from 1 min to 25 h after the 351-nm photoirradiation at 20 K. The solid line shows the fitting results using eq 3–1. The fitting parameters are as follows: $I_0 = 1.3 \times 10^9$ CPS, $\alpha = 23.0\ s^{-1}$, and $m = 1.11$.

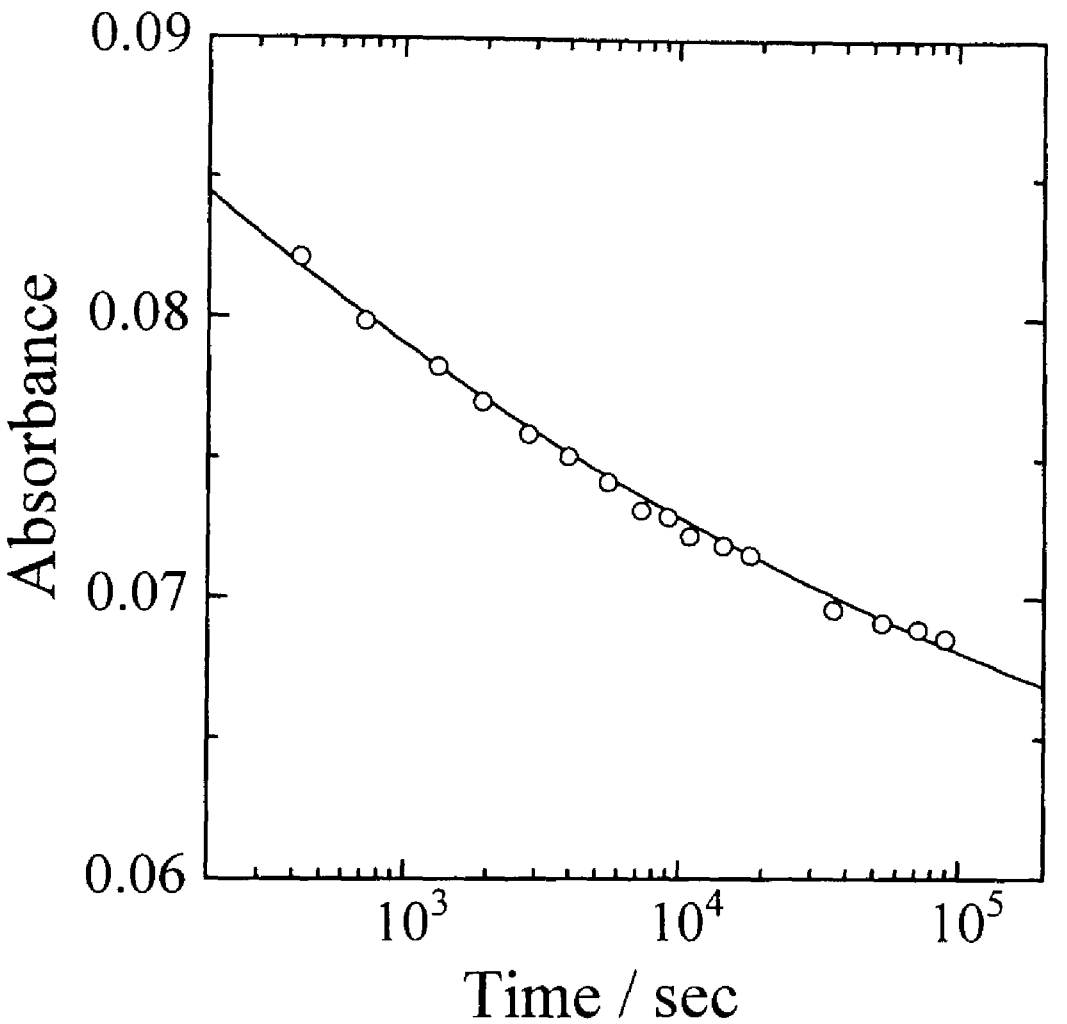

Figure 3–2. The fitting result for the absorbance decay of TMB radical cation $TMB^{\bullet+}$ formed in a PnBMA film through a two-photon ionization at 20 K. The observed wavelength was 475 nm which is the absorption peak wavelength of $TMB^{\bullet+}$. The solid line shows the result of the best fitting for the absorbance of $TMB^{\bullet+}$ denoted by open circles, using eq 3–4 with the same parameters used in the ITL fitting: $I_0 = 1.3 \times 10^9$ CPS, $\alpha = 23.0\ s^{-1}$, and $m = 1.11$. In other words, the solid line is drawn by the following equation: $Abs(t) = 0.135 - 0.0836[1 - 1/(1 + 23t)^{1.11}]$.

same quality of fitting is attained using other pair values of I_0 and α. On the contrary, the value of m is unique and close to unity.

Open circles shown in Figure 3–2 denote the absorbance decay of $TMB^{\bullet+}$ measured at 475 nm in a PnBMA film after the laser photoexcitation at 20 K. The dopant $TMB^{\bullet+}$ has a strong absorption peak at 475 nm, where the molar absorption coefficient can be as large as *ca.* 4×10^4 M^{-1} cm^{-1}.[24,25] Thus, the use of TMB as a dopant chromophore enables one to observe the radical cation produced in polymer solids through two-photon ionization by absorption spectroscopy. Plots of the absorbance of $TMB^{\bullet+}$ *vs.* log t gave an approximately linear relationship[26], and the absorbance of $TMB^{\bullet+}$ decreased from *ca.* 0.08 to *ca.* 0.07 over the time range from 3 min to 25 h. In other words, only twenty percent of trapped electrons produced through two-photon ionization recombined with the parent cations during a period of 25 hours at 20 K; eighty percent of trapped electrons remained without charge recombination.

Since ITL decay and the absorbance decay of $TMB^{\bullet+}$ result from the charge recombination of a photoejected electron with the parent cation, they should obey the same kinetics. The ITL is caused by the charge recombination, then eq 3–2 will hold

$$I(t) = -\lambda \frac{dN(t)}{dt}, \tag{3–2}$$

where $N(t)$ is the number of electron-hole pairs and λ is a constant that relates to the apparent emission quantum efficiency. Combining and integrating eqs 3–1 and 3–2, we obtain the following equation:

$$N(t) = N_0 - \frac{I_0}{\lambda\alpha(m-1)}\left[1 - \frac{1}{(1+\alpha t)^{m-1}}\right]. \tag{3–3}$$

According to the Lambert-Beer law, $N(t)$ is proportional to the absorbance $Abs(t)$ of $TMB^{\bullet+}$ at 475 nm, and therefore eq 3–3 leads to

$$Abs(t) = Abs_0 - \frac{I_0 \varepsilon}{\lambda\alpha S N_A (m-1)}\left[1 - \frac{1}{(1+\alpha t)^{m-1}}\right], \tag{3–4}$$

where ε is the molar absorption coefficient of $TMB^{\bullet+}$ at 475 nm, S is the sample film area, and N_A is the Avogadro constant. This eq 3–4 connects the ITL decay to the decrease in the absorbance of $TMB^{\bullet+}$ with the assumption that the ITL is caused by the charge recombination of a photoejected electron with the parent $TMB^{\bullet+}$.

As shown in Figure 3–2, the experimental data were well fitted using eq 3–4 (solid

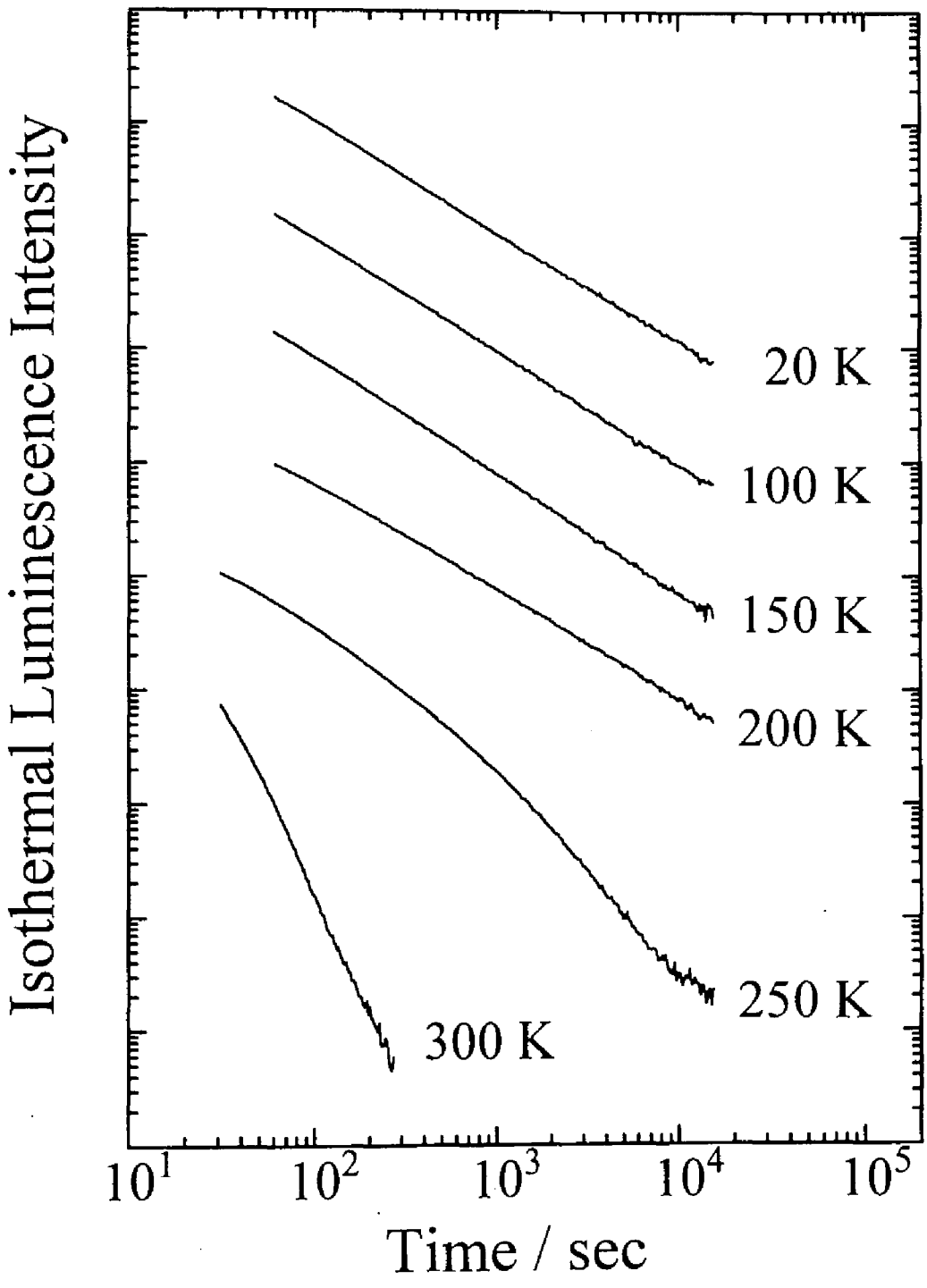

Figure 3–3. The ITL decays for Pe/PnBMA system photoirradiated and measured at 20, 100, 150, 200, 250, and 300 K. Each ITL decay is shifted arbitrarily in the direction of the ordinate.

line) with the same parameters used in the ITL fitting: $I_0 = 1.3 \times 10^9$ CPS, $\alpha = 23.0\ s^{-1}$, and $m = 1.11$. This finding clearly shows that both the ITL decay and the absorbance decay of $TMB^{\bullet+}$ can be explained on the basis of the same kinetics; the ITL is caused by the charge recombination of a photoejected electron with the parent $TMB^{\bullet+}$.

3.3.2. Temperature Dependence of ITL Decays at Temperatures from 20 to 300 K

The striking feature of the ITL is that the luminescence has an extremely long lifetime and the decay kinetics is independent of temperature at low temperatures. Here, perylene was used as a dopant chromophore, because its fluorescence quantum yield is independent of temperature between 20 and 300 K.[27] Figure 3–3 shows the ITL decays of Pe/PnBMA at temperatures from 20 to 300 K. The unit of the ordinate is arbitrary; each ITL decay is shifted arbitrarily in the direction of the ordinate. The ITL decays below 200 K obeyed the t^{-m} law, that is, the decay kinetics was the same in the temperature range below 200 K. This strongly suggests that the ITL decay mechanism remains the same below 200 K. Since the thermal energy at 20 K is no more than 1.7×10^{-3} eV, the electron transfer due to thermal activation hardly occurs at 20 K. However, the electron transfer due to electron tunneling mechanism can occur even at a temperature as low as 20 K. On the contrary, the ITL decays above 200 K did not obey the t^{-m} law. This deviation observed above 200 K suggests that the scheme for the ITL changes above this temperature.

The concentration of dopant chromophores in the present experiment is so dilute that the charge recombination of a photoejected electron with the parent radical cation can be considered to be a geminate recombination.

Thus, it is concluded that the ITL decays below 200 K results from the geminate charge recombination of a trapped electron with the parent radical cation by electron tunneling, not by thermal activation.

3.3.3. Dependence of Charge Recombination Luminescence on the Number of Photoirradiation Shots at a Fixed Fluence

First, the dependence of the ITL decay on the number of photoirradiation shots was examined. A PnBMA film doped with a Pe chromophore was photoirradiated at 20 K under multi-shot photoirradiation. To suppress degradation of sample films by multi-shot

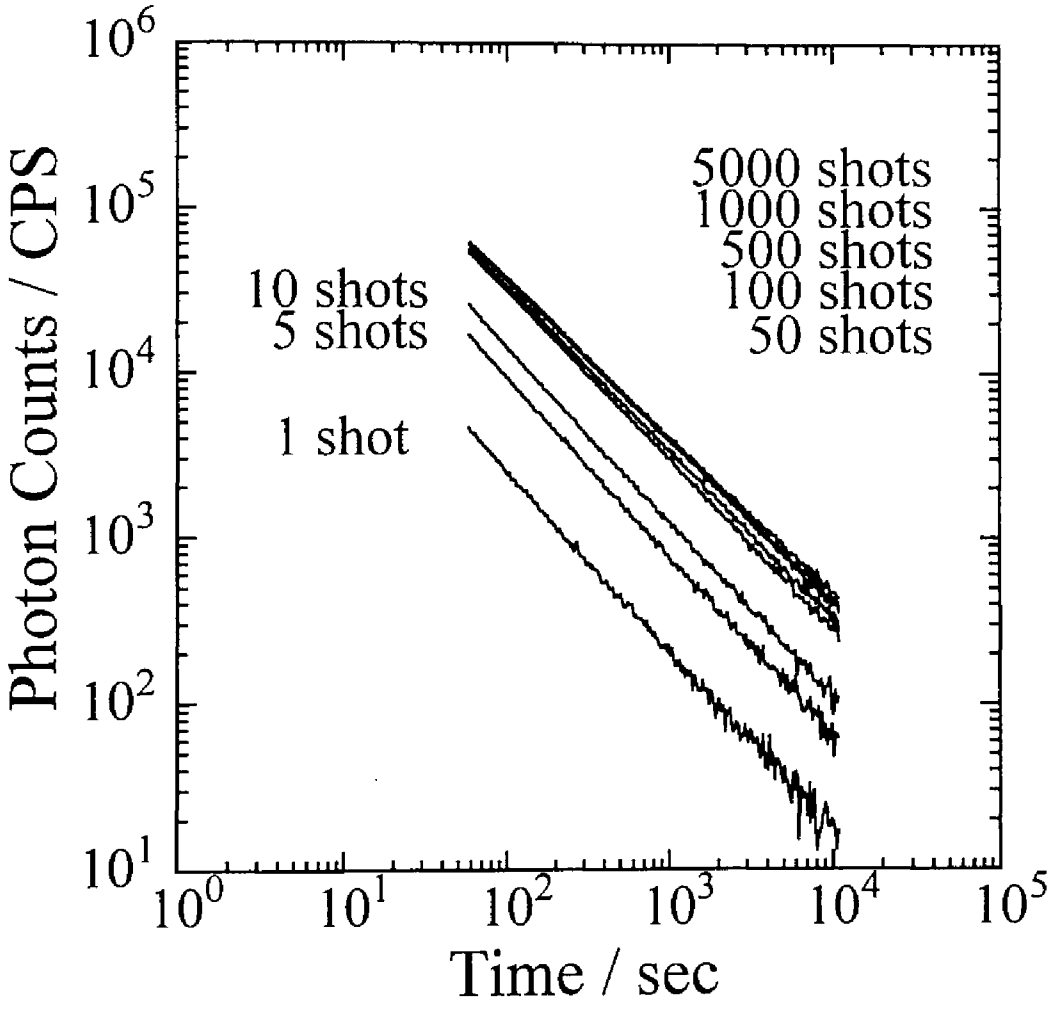

Figure 3–4. The ITL decays of Pe/PnBMA photoirradiated at 20 K. The number of photoirradiation shots was 1, 10, 50, 100, 500, 1000, and 5000.

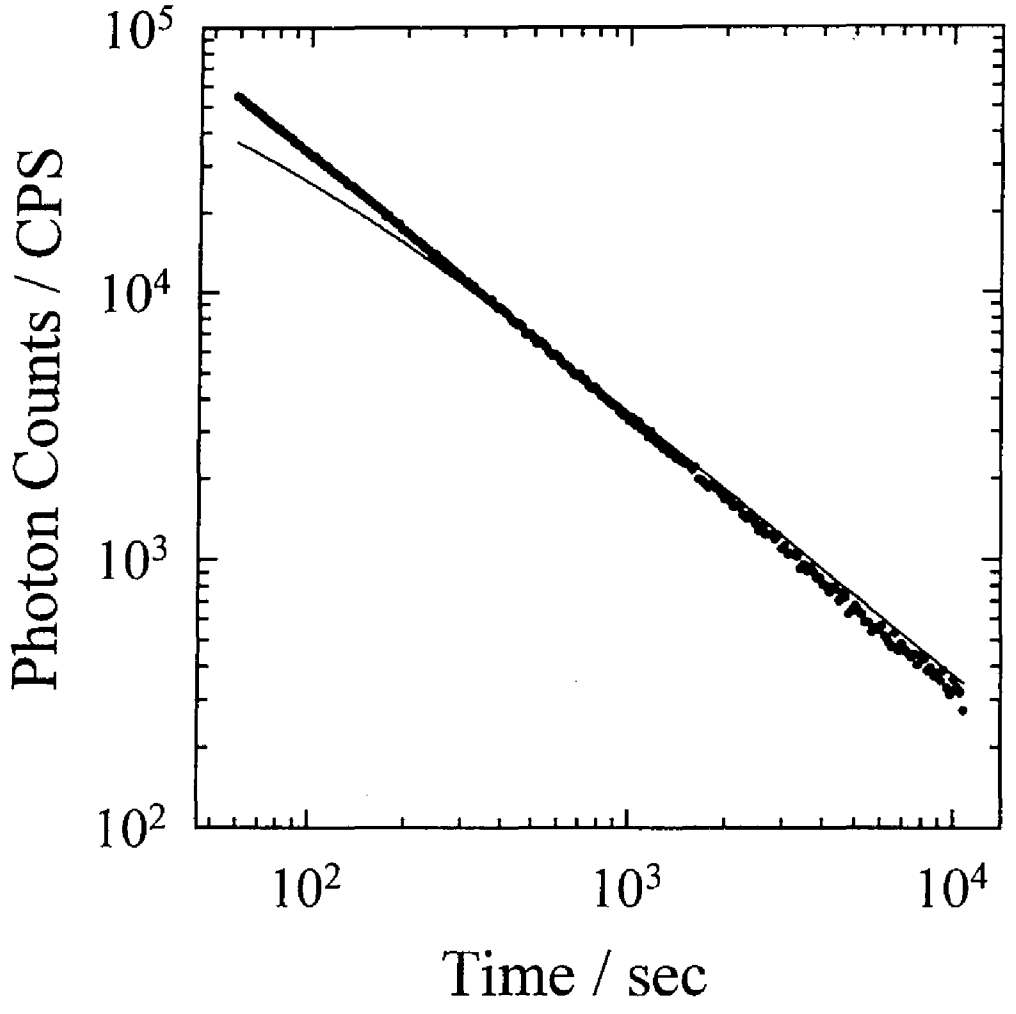

Figure 3–5. The closed circles represent the ITL decay of Pe/PnBMA under a 100-shot irradiation. The solid line is the summation of eq 3–1 with the fitting parameters obtained from the ITL decay of Pe/PnBMA under a 1-shot irradiation, resulting in eq 3–5.

irradiation, the photon density of the excitation light (*ca.* 3 mJ/cm^2) was made about one tenth of that in the previous section (*ca.* 30 mJ/cm^2). Also under the photoirradiation conditions, a two-photon ionization was confirmed; the radical cation of the dopant Pe chromophore was observed by absorption spectroscopy.

Figure 3–4 shows two tendencies; 1) the ITL intensity increased with the number of photoirradiation shots and 2) the slope of the ITL decay became gentle, that is, the value of m decreased with an increase in the number of photoirradiation shots. It is noticed that the ITL decay kinetics deviates from the t^{-m} law at more than 100-shot irradiation as the open circles in Figure 3–7 shows; the value of m is less than unity.

It was examined whether the ITL for multi-shot irradiation can be reproduced with the summation of the ITL for 1-shot irradiation,

$$I(t) = \sum_{i=0}^{99} \frac{I_0}{(1+\alpha(t+0.5i))^m}, \qquad (3\text{–}5)$$

that is to say, whether the 100-shot ITL can be explained as a superposition of the 1-shot ITLs for each photoirradiation. As shown in Figure 3–5, the superposition of the ITL for the 1-shot photoirradiation ($m \approx 1.09$) reproduces a smaller slope ($m \approx 0.99$) of the ITL for the 100-shot photoirradiation in a certain range, but not over the wide time range. This indicates that each ionization process is not independent; the subsequent irradiation changes the trapping form of electrons photoejected at the previous photoirradiation.

Next, the glow curves (thermoluminescence, TL) were examined in succession after the ITL decay measurement shown in Figure 3–4. Figure 3–6 shows the glow curves measured 3 h after the photoirradiation. As shown in the figure, the TL intensity increased with the number of photoirradiation shots and the increase in the TL intensity was larger at higher temperatures. This enhancement of the ITL intensity shows that the photon energy of irradiation is accumulated as the chemical energy of the charge separated state of ionic species. It is noteworthy that the increase in glow peak intensity at around 250 K corresponds to the decrease in the value of m with the increase in the number of photoirradiation shots as shown in Figure 3–7.

These changes in both ITL and TL indicate that the fraction of electron-cation pairs with a slow recombination rate increases with photoirradiation times. Two interpretations are possible for the slow recombination rate. One is that the distance between a photoejected electron and the parent cation increases with the number of

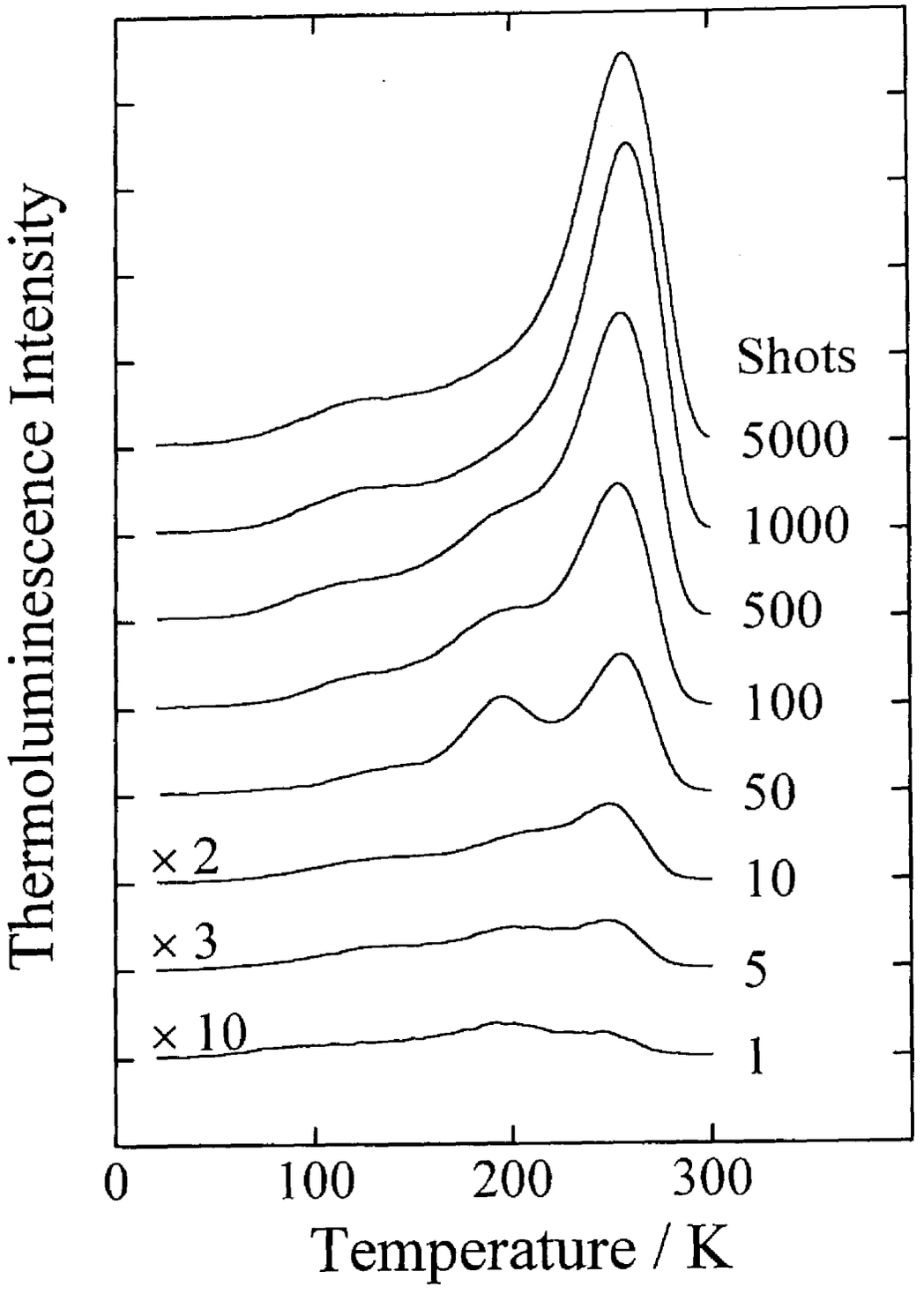

Figure 3–6. The TL glow curves of Pe/PnBMA photoirradiated at 20 K under several photoirradiation conditions were observed in succession after the ITL decay measurement. The number of photoirradiation shots was 1, 10, 50, 100, 500, 1000, and 5000.

photoirradiation shots. The other is that trap depth is deepened with the increase in the number of photoirradiation shots. The former indicates that some trapped electrons captured in a matrix polymer are released and kicked away by photo- or thermal-excitation.[28] The latter suggests that some trapped electrons are stabilized by transfer to more stable trap sites and by small scale structural relaxation of the matrix polymer even at 20 K.

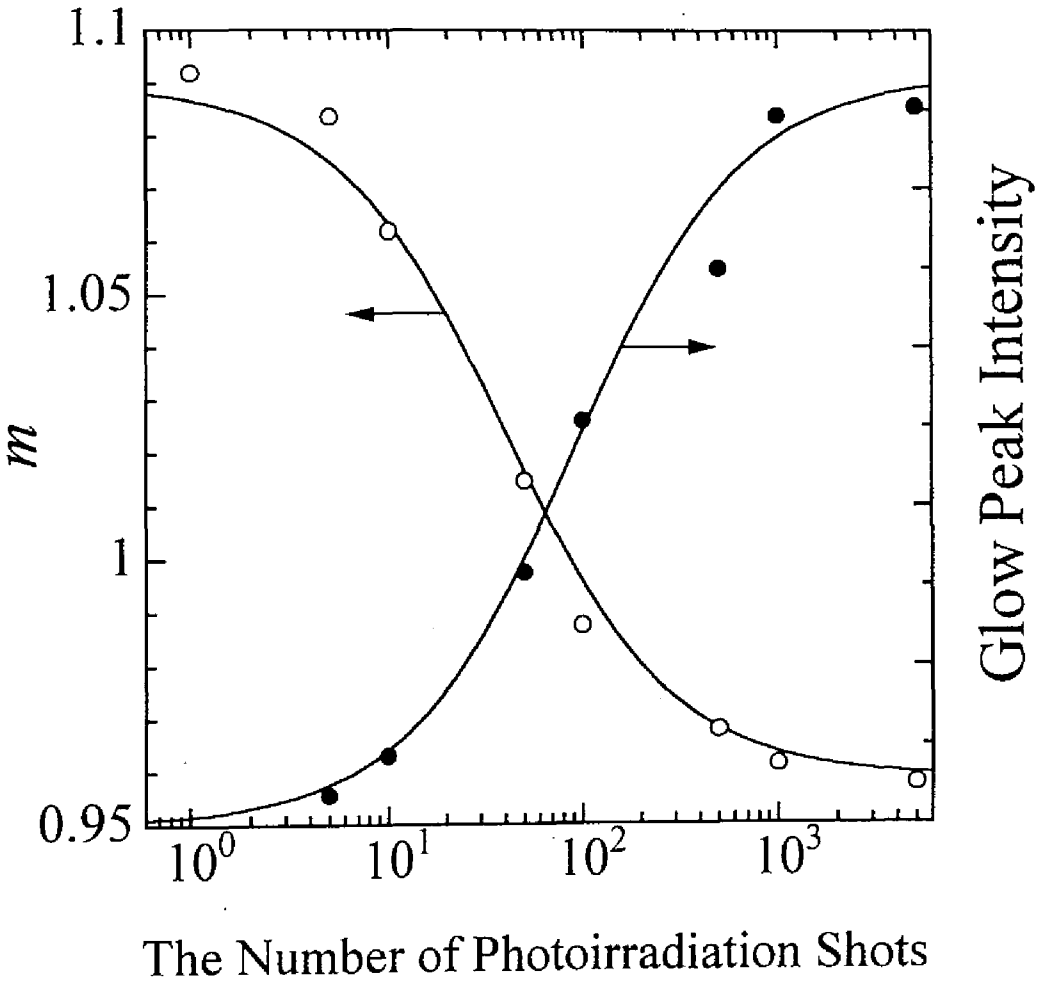

Figure 3–7. Plots of the value of m against the number of photoirradiation shots. Open circles denote the slope m of the ITL decay curves obtained from fitting using eq 3–1. Closed circles represent the glow peak intensity around 250 K. The solid curves are drawn arbitrarily

3.4. Conclusion

The charge recombination of electron-hole pairs formed in a polymer matrix was observed at 20 K by emission (ITL) as well as absorption measurement. The ITL decay kinetics corresponds to the absorption decay of the ionic species and obeys the same decay kinetics, the t^{-m} law, at temperatures from 20 to 200 K far below the T_g of PnBMA. It is concluded that the ITL decay at low temperatures results from the geminate charge recombination of a photoejected electron with the parent cation by electron tunneling. Multi-shot irradiation causes the deviation of the ITL decay from the t^{-m} law. This deviation results from the increase in the distance between a photoejected electron and the parent cation and/or the deepening of the trap depth.

References and Notes

1) J. T. Randall and M. H. Wilkins, *Proc. R. Soc. London, Ser. A*, **184**, 390 (1945).

2) P. Debye and J. O. Edwards, *J. Chem. Phys.*, **20**, 236 (1952).

3) Kh. S. Bagdasar'yan, R. I. Milyutinskaya, and Yu. V. Kovalev, *Khim. Vysok. Energii*, **1**, 127 (1967).

4) J. R. Miller, *Chem. Phys. Lett.*, **22**, 180 (1973).

5) W. H. Hamill, *J. Chem. Phys.*, **71**, 140 (1979).

6) G. C. Abell and A. Mozumder, *J. Chem. Phys.*, **56**, 4079 (1972).

7) W. H. Hamill and K. Funabashi, *Phys. Rev. B*, **16**, 5523 (1977).

8) H. Scher and E. W. Montroll, *Phys. Rev. B*, **12**, 2455 (1975).

9) E. W. Montroll and G. H. Weiss, *J. Math. Phys.*, **6**, 167 (1965).

10) F. Kieffer, C. Meyer, and J. Rigaut, *Chem. Phys. Lett.*, **11**, 359 (1971).

11) F. Kieffer, C. Meyer, and J. Rigaut, *Int. J. Radiat. Phys. Chem.*, **6**, 79 (1974).

12) A. I. Mikhailov, *Dokl. Akad. Nauk SSSR*, **197**, 136 (1970).

13) M. Tachiya and A. Mozumder, *Chem. Phys. Lett.*, **28**, 87 (1974).

14) F. S. Dainton, M. J. Pilling, and S. A. Rice, *J. Chem. Soc. Faraday Trans. 2*, **71**, 1311 (1975).

15) M. Tachiya and A. Mozumder, *Chem. Phys. Lett.*, **34**, 77 (1975).

16) M. J. Pilling and S. A. Rice, *J. Phys. Chem.*, **79**, 3035 (1975).

17) Y. Hama, Y. Kimura, H. Tsumura, and N. Omi, *Chem. Phys.*, **53**, 115 (1980).

18) Y. Hama and K. Gouda, *Radiat. Phys. Chem.*, **21**, 185 (1983).

19) A. Tsuchida, M. Nakano, M. Yoshida, M. Yamamoto, and Y. Wada, *Polym. Bull.*, **20**, 297 (1988).

20) M. Yamamoto, A. Tsuchida, and M. Nakano, *MRS Int. Meeting Adv. Mater.*, **12**, 243 (1989).

21) A. Tsuchida, W. Sakai, M. Nakano, M. Yoshida, and M. Yamamoto, *Chem. Phys. Lett.*, **188**, 254 (1992).

22) A. Tsuchida, W. Sakai, M. Nakano, and M. Yamamoto, *J. Phys. Chem.*, **96**, 8855 (1992).

23) P. Peyser, in *"Polymer Handbook"*, 3rd ed., eds. J. Brandrup and E. H. Immergut, John Wiley & Son, New York (1989).

24) J. P. Jaget and V. Plichon, *Bull. Soc. Chim. Fr.*, 1394 (1964).

25) S. A. Alkaitis and M. Grätzel, *J. Am. Chem. Soc.*, **98**, 3549 (1976).

26) When the value of m is close to unity, equation 3–4 can be approximately given by

$$Abs(t) = Abs_0 - \frac{I_0 \varepsilon}{\lambda \alpha S N_A} \ln(1 + \alpha t). \qquad (3\text{–}6)$$

Thus, the plots of $Abs(t)$ *vs.* log t show a linear relationship when the value of m is close to unity.

27) M. Yamamoto, H. Ohkita, W. Sakai, and A. Tsuchida, *Synth. Metals*, **81**, 301 (1996).

28) T. W. Scott and C. L. Braun, *Can. J. Chem.*, **63**, 228 (1985).

Chapter 4

Charge Recombination of Electron-Cation Pairs Formed in Polymer Solids at 20 K through Two-Photon Ionization

4.1. Introduction

There have been various investigations on the charge recombination of geminate ion pairs in a condensed phase, which is a primary process following an ionization.[1] In solution systems, the WAS equation[2-5] (an empirical equation) and the square-root law[6] (a first order approximated equation) have been proposed and widely used for the analysis of experimental results. Historically, Onsager derived for the first time the steady-state solution of the Smoluchowski equation for geminate charged particles in a Coulomb potential under the influence of an external field.[7] Currently, a strict solution has been developed for the time-dependent Smoluchowski equation.[6] The decay of ejected electrons in the picosecond order is in agreement with that of the parent radical cation and the decay kinetics obeys the Smoluchowski equation. On the contrary, the decay of ejected electrons in the nanosecond order is inconsistent with that of radical cations owing to the participation of side reactions;[8-10] ejected electrons and radical species produced by irradiation are so reactive that side reactions occur subsequently.

On the other hand, the charge recombination of an ejected electron and the parent cation formed in irradiated solids at a low temperature causes luminescence with an extremely long lifetime. This emission is called isothermal luminescence (ITL) or preglow and the decay kinetics cannot be explained in terms of either the first order or the second order kinetics. This ITL intensity $I(t)$ obeys the power kinetics, *i.e.*, the t^{-m} law: $I(t) \propto t^{-m}$, with $m \approx 1$.[11]

There have been proposed mainly two mechanisms for the ITL power decay resulting from the charge recombination of an ejected electron with the parent cation

formed in irradiated solids. One is based on the diffusion process of trapped electrons.[12] The long lifetime emission is explained in terms of a small diffusion constant resulting in slow charge recombination rate; the trap depth is much larger than the thermal energy at a low temperature. Debye and Edwards[11] derived theoretically the t^{-m} relationship for the first time in terms of the diffusion mechanism considering a spatial distribution of ejected electrons. However, as Abell and Mozumder[13] pointed out, their model has an inherent weakness in that the initial emission intensity diverges at $t = 0$ just after the irradiation owing to neglect of the normalization of the spatial distribution. Abell and Mozumder reconsidered the Debye-Edwards model using the normalized distribution function and demonstrated the t^{-m} law only on an intermediate time scale; their model also shows the square-root law on a long time scale. After all, the simple diffusion mechanism based on the random walk of trapped electrons results in the square-root law on a long time scale, not the t^{-m} law. Hamill and Funabashi[14] showed that the t^{-m} behavior can be reproduced over the whole time range using the continuous-time random walk (CTRW) model,[15] by which Scher and Montroll[16] explained the long tail of the transient photocurrent in amorphous solids.

The other mechanism is based on long-range electron transfer by electron tunneling.[17-21] The key assumptions of this mechanism are a spatial distribution of ionic species and the exponential decrease in the rate of electron transfer with increasing distance of electron-cation pairs. It is debatable which mechanism is dominant because there is no conclusive experimental evidence at present. Many authors explained the ITL decay in terms of an electron tunneling model when the ITL decay kinetics is independent of temperature at low temperatures,[22,23] because the hopping rate in the diffusion depends strongly on temperature. Later, Hama *et al.*[24,25] have proposed a modified equation $I(t) = I_0 / (1 + \alpha t)^m$ of the empirical equation[26] $I(t) = I_0 / (1 + \alpha t)$ to avoid the divergence of ionic species produced at $t = 0$. They showed that the initial spatial distribution of ejected electrons can be calculated from the Laplace inverse transformation of the modified empirical equation when the value of m is more than unity. If the value of m is less than unity, the distribution function loses its physical meaning because the total amount of ionic species produced diverges into infinity at $t = 0$ just after the irradiation.

Most studies on the ITL have been discussed from the viewpoint of the kinetics of the charge recombination and little attention has been given to chemical reactions. Thus,

in an ordinary electron tunneling model, ejected electrons are assumed to be captured in a unique depth trap. However, such an assumption cannot be readily accepted considering the spatially inhomogeneous structure of polymer solids and chemical reactions. Actually, there have been reported many investigations on radiation-induced chemical reactions by ESR measurements.[27-30] For confirmation of this assumption, it is necessary to show a quantitative agreement of the kinetics between the ITL decay and the absorbance decay of ionic species.

In the present study, ionic species were produced through the two-photon ionization of a dopant chromophore in polymer solids, not high energy radiation. An intense near-UV light pulse from an excimer laser (351 nm) was used for the selective photoexcitation of the dopant chromophore. The laser pulse is intense enough to feed another photon to the excited chromophore within the lifetime. Consequently, the dopant chromophore is excited to a higher energy level than the ionization potential and then ejects an electron to the polymer matrix. The parent radical cation and the trapped electron thus formed in the polymer are so stable that the color of the parent radical cation can be seen even after a one-year storage from the photoexcitation at room temperature.[31-34]

In this chapter, the decay kinetics of the ITL is compared with the absorbance decay of dopant cation resulting from the charge recombination of electron-cation pairs formed by two-photon ionization of the dopant chromophore.

4.2. Experimental Section

4.2.1. Chemicals

Polymer samples used here were poly(methyl methacrylate) (PMMA, $M_w = 3.95 \times 10^5$, Scientific Polym. Prod., Inc.), poly(ethyl methacrylate) (PEMA, $M_w = 2.8 \times 10^5$, Scientific Polym. Prod., Inc.), poly(*n*-butyl methacrylate) (PnBMA, $M_w = 10^5$, Wako Pure Chem. Ind., Ltd.), and polystyrene (PSt, $M_n = 1.6 - 1.8 \times 10^5$, Wako Pure Chem. Ind., Ltd.). All these polymers were purified by reprecipitation from a benzene solution into methanol three times. The glass transition temperatures (T_g) of the polymers are 378 K (PMMA), 339 K (PEMA), 293 K (PnBMA), and 373 K (PSt).[35] The dopant chromophore used here was *N,N,N',N'*-tetramethylbenzidine (TMB, Wako Pure Chem. Ind.,

Ltd.), which was purified by recrystallization several times.

4.2.2. Sample Preparation

Sample films for measurements were prepared by the solution cast method. A TMB chromophore was dissolved in a benzene (Dojin Spectrosol) solvent with a polymer powder so as to become *ca.* 3×10^{-3} mol/L in the final polymer film. The solution was cast on a glass plate in a dry box for two days and then was dried by evacuation for one day at room temperature. The film was peeled off from the glass plate and was finally dried under vacuum above the T_g until no absorption of the casting solvent was observed with a spectrophotometer. No change in the absorption or emission spectra of the dopant chromophore was observed for the prepared polymer films after the above heating procedure.

4.2.3. Measurements

A sample film was covered with a quartz plate and set tightly on a copper cold finger of a cryostat (Iwatani Plantech Corp., CRT510). The sample film was, *in vacuo*, cooled down to 20 K and the temperature was kept constant using a PID temperature control unit (Iwatani Plantech Corp., TCU-4). The sample temperature was monitored with a calibrated Au + 0.07 % Fe / chromel thermocouple at the sample film position using an indium gasket.

The polymer film doped with TMB was photoirradiated at 20 K by only one 351-nm light pulse from a XeF excimer laser (Lambda Physik, EMG101MSC, *ca.* 20 ns fwhm, and *ca.* 30 mJ/cm^2). After the prompt fluorescence and phosphorescence of the TMB chromophore disappeared, the emission from the sample film at a fixed temperature of 20 K (this is ITL or preglow) was measured from 1 min to 25 h after the end of the photoirradiation at 20 K. A photon-counting system was used for the emission intensity measurement, which consists of a photomultiplier (Hamamatsu, R585) and a photon counter (Hamamatsu, C-1230) connected to a personal computer. No ITL was observed in the control experiments where the polymer films without dopant chromophores were excited by the same procedure.

The steady-state absorption spectra of the photoirradiated sample films were measured in the cryostat with a spectrophotometer (Hitachi, U-3500) using a 2-nm slit

width. Ten sheets of sample films prepared freshly, with a total thickness of *ca.* 2 mm, were put together to gain absorbance of the dopant radical cation high enough to detect. The sample films were photoirradiated at 20 K under the conditions mentioned above. Then the absorption spectra were measured from 3 min to 25 h after the photoirradiation at 20 K. During the intervals of each measurement, the monitor light of the spectrophotometer was shut off to prevent the sample film from being photobleached.

4.3. Results and Discussion

The kinetics of the geminate recombination by electron tunneling has been theoretically explained by Tachiya and Mozumder.[20] Assuming a proper distribution function of the distance between trapped electrons and solute cations, they demonstrated that the t^{-m} decay profile can be reproduced over the wide time range using an electron tunneling model. On the other hand, Hama *et al.*[24,25] showed that the Laplace inverse transformation of an empirical ITL decay function (eq 4–1) enables one to obtain directly the initial distribution function of the distance between a trapped electron and the parent cation. Their model is also essentially based on the geminate recombination by electron tunneling.

$$I(t) = \frac{I_0}{(1+\alpha t)^m} \qquad (4\text{–}1)$$

Here let us summarize the assumptions in the electron tunneling model used by Hama *et al.*: (i) the charge recombination occurs for geminate pairs; (ii) the recombination reaction proceeds through electron tunneling whose rate constant decreases exponentially with a separation distance r between a trapped electron and the parent cation, $k(r) = \nu \exp(-\beta r)$; (iii) the spatial distribution of ejected electrons is taken into account. The first assumption is valid for this system because the concentration of dopant chromophore is so low (*ca.* 3×10^{-3} mol/L) that each chromophore is considered to be isolated. The second is also reasonable: the above equation holds in most electron transfer reactions. The second and third assumptions are essential to an interpretation of the extremely long lifetime of ITL. In particular, the second assumption enables one to obtain the initial distribution function of the distance between an ejected electron and the parent cation from

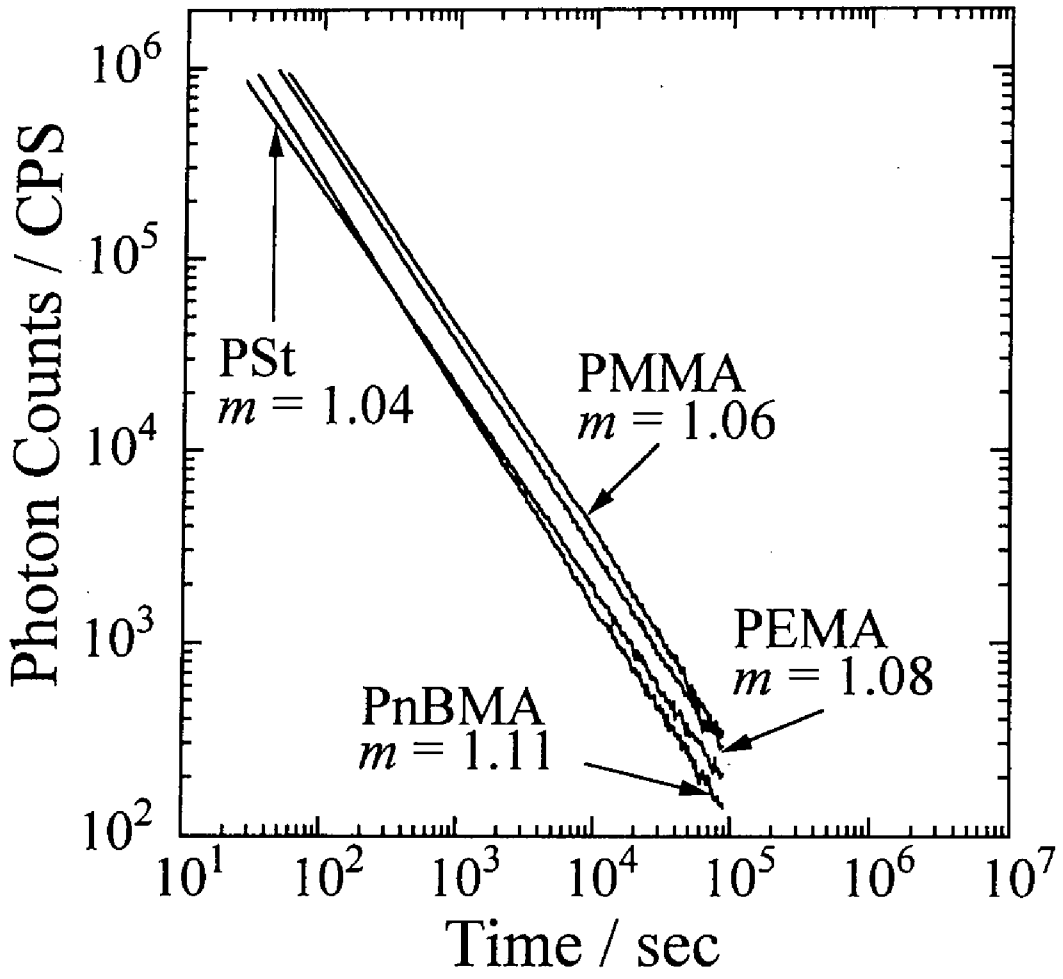

Figure 4–1. The ITL decay of TMB doped in polymer solids photoirradiated at 20 K. The values of m represent the slope of the ITL decay; see eq 4–1.

the Laplace inverse transformation of the ITL decay function. The initial distribution function is connected with the ITL decay through the Laplace inverse transformation, because the electron transfer rate is expressed in an exponential form that remains similar one after a differential operation regarding distance r. The third assumption, a spatial distribution, can be replaced with a trap depth distribution, because the electron transfer rate is also expressed in an exponential form that remains similar one after a differential operation regarding a trap depth V. One can, therefore, obtain the initial distribution function of trap depth in the same procedure as the spatial distribution function; see Appendix.

Table 4–1. Fitting Parameters for ITL Decay of TMB Doped Polymer Films under 1-Shot Photoirradiation Condition using Eq 4–1

	I_0 / CPS	α / s^{-1}	m
PnBMA	1.3×10^9	23.0	1.11
PEMA	1.9×10^8	2.8	1.08
PMMA	5.0×10^8	7.0	1.06
PSt	1.1×10^7	0.39	1.04

To begin with, the empirical eq 4–1 was fitted to the observed ITL decay and the fitting parameters I_0, α, and m were obtained . Figure 4–1 shows the ITL decays of TMB doped in PnBMA, PEMA, PMMA and PSt after the photoirradiation at 20 K. The fitting parameters using eq 4–1 are summarized in Table 4–1. The value of m is uniquely obtained whereas there are many combinations of I_0 and α which can reproduce the observed ITL decay. According to eq 4–1, the ITL intensity shows a constant value I_0 when the value of αt is ignored in comparison with unity, and it obeys the t^{-m} law when the value of αt is much higher than unity. In other words, the value of α gives the time when the ITL decay starts to obey the t^{-m} law.

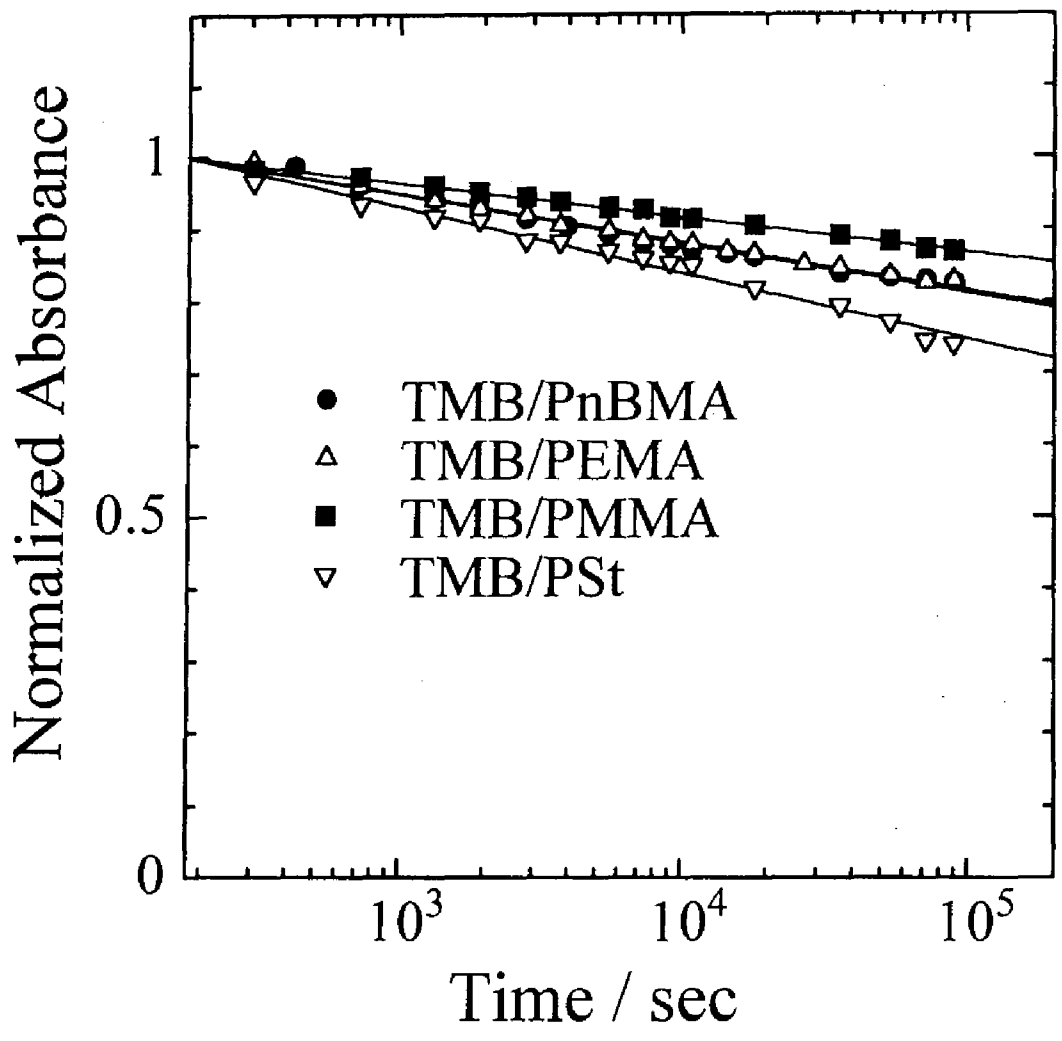

Figure 4–2. The absorbance decay of $TMB^{\bullet+}$ at 20 K formed through photoionization of the TMB chromophore doped in polymer solids. The ordinate is normalized with the absorbance at t = 180 s (3 min after the photoirradiation).

The ITL deviated from the t^{-m} law has been reported to be observed over a short time range in the radiation chemistry.[24,25] Thus, the deviation gives information on I_0 and α. On the contrary, such deviation was not observed at all in this system; the ITL decay obeyed the t^{-m} law over the whole time range of measurement. Therefore, the ITL decay in this system has no information on I_0 and α. Although the values of I_0 and α from the fitting cannot be determined precisely, these parameters are not so important in the later discussion.

Next, the absorbance decay of the TMB radical cation was measured for 1-shot irradiation from 3 min to 25 h after the photoirradiation at 20 K; the ordinate is normalized with the absorbance at t = 3 min. As shown in Figure 4–2, the plots of the absorbance of $TMB^{\bullet+}$ in several polymer films *vs.* log t gave an approximately linear relationship. This approximated linear relationship shows that the ITL decay and the decay of $TMB^{\bullet+}$ obey the same kinetics, which can be, as mentioned in the previous Chapter 3, explained in terms of long-range electron transfer by electron tunneling.[36] Therefore, the discussion on the basis of the distribution function obtained from the Laplace inverse transformation is valuable; the scheme for the charge recombination used by Hama *et al.* can be also applied to this experimental results.

4.3.1. Initial Distribution Function of Distance between Photoejected Electron and Parent Radical Cation

First, the initial spatial distribution function[37] of the distance between a photoejected electron and the parent cation is discussed from the Laplace inverse transformation of the empirical ITL decay function with the fitting parameters. Figure 4–3 shows the initial distribution functions for TMB/PnBMA, TMB/PEMA, TMB/PMMA and TMB/PSt. According to Hama *et al.*, when ITL decay can be fitted with the empirical equation 4–1, the initial distribution function $n(r, 0)$ is given by eq 4–2 using $k(r) = \nu \exp(-\beta r)$ as the electron transfer rate

$$n(r,0)\mathrm{d}r = \frac{\beta I_0}{\lambda \alpha^m \Gamma(m)} \nu^{m-1} \exp\left[-(m-1)\beta r - \frac{\nu}{\alpha}\exp(-\beta r)\right]\mathrm{d}r, \qquad (4\text{–}2)$$

where frequency factor ν and damping factor β are assumed to be 10^9 s^{-1} and 1 $Å^{-1}$, respectively.[38]

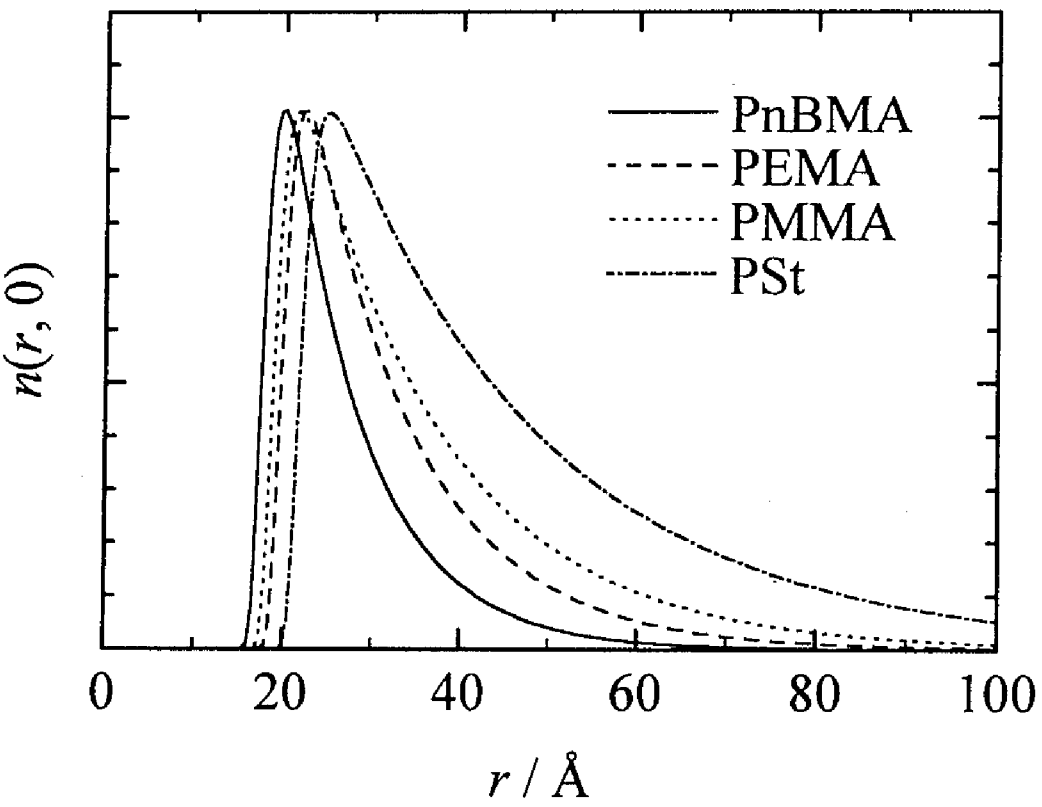

Figure 4–3. The initial distribution function $n(r, 0)$ of the distance between an ejected electron and the parent cation calculated using eq 4–2 obtained from the Laplace inverse transformation of the observed ITL decay function fitted to eq 4–1.

Here, it is considered how the initial spatial distribution function $n(r, 0)$ depends on the fitting parameters I_0, α, and m. Equation 4–2 shows that the value of I_0 affects the ordinate of the initial distribution function but not the shape of the initial distribution function. On the contrary, the value of α may influence the shape of the initial distribution function, because the value of α is comparable with that of ν if the ITL decay still obeys the t^{-m} law in a short time range of 10^{-10} s after the photoirradiation. One cannot, therefore, obtain the exact initial distribution function just after the photoirradiation from the observed ITL decay.

Nevertheless, one can partly discuss the initial distribution function obtained from the ITL decay. It should be noticed that the shape of the initial distribution function depends on only the exponential part in eq 4–2; the pre-exponential term changes only the ordinate. The first term in the exponential brackets characterizes the decay profile of the initial distribution function. On the other hand, the second term characterizes the rising profile of the initial distribution function. Thus, one can discuss the decay part of the initial distribution function, which is dependent upon the value of m, although one cannot discuss the rising part of the initial distribution function.

The initial distribution obtained from the Laplace inverse transformation of the ITL decay function shows that TMB/PSt system has the most long-range distribution. Trap depth is assumed to be unique for all the polymer matrices used here. However, polystyrene is expected to have a shallower trap than poly(alkyl methacrylate)s having an ester side-chain whose electron affinity is higher than that of the phenyl group. Considering the difference in trap depth between them, TMB/PSt system has a much more long-range distribution.

Comparing the distribution of trapped electrons among poly(alkyl methacrylate)s, photoejected electrons are farther distributed in the following order: PnBMA < PEMA < PMMA. According to the Wigner-Seitz model, which was applied to the study of the stability criterion for the localization of an excess electron in a nonpolar fluid,[39] trap binding energy V_0 is expressed by a function of the density of solids; its absolute value $|V_0|$ decreases with an increase in the density of solids. Scattering cross section σ increases with the absolute value of trap binding energy $|V_0|$.[40] Since PMMA has the highest density among poly(alkyl methacrylate)s used here, that is, has the smallest $|V_0|$, TMB/PMMA system has the smallest scattering cross section σ. Therefore, if the

photoejection in this solid system can be interpreted in terms of discussion on the behavior of excess electrons in nonpolar liquids, the difference in the initial distribution may be explained in terms of the difference in the trap binding energy V_0. In Figure 4–3, the difference in the trap binding energy V_0 is disregarded but, if it was taken into account, polymers with higher density would have much farther distribution of trapped electrons; the difference in the distribution of trapped electrons among poly(alkyl methacrylate)s would be larger.

Next, let us focus our attention on the change in the spatial distribution function $n(r, t)$ with time t. In the present experiment, the concentration of dopant chromophore is so dilute that the charge recombination of a photoejected electron with the parent cation can be considered to be a geminate recombination. The geminate recombination obeys the first order kinetics with assumption that the one-step electron transfer process is dominant compared with the electron detrap-retrap processes. Therefore, the spatial distribution function $n(r, t)$ at time t is given by

$$\begin{aligned} n(r,t)\mathrm{d}r &= n(r,0)\exp\left[-k(r)t\right]\mathrm{d}r \\ &= \frac{\beta I_0}{\lambda\alpha^m\Gamma(m)}\nu^{m-1}\exp\left[-(m-1)\beta r-\frac{\nu}{\alpha}\exp(-\beta r)(1+\alpha t)\right]\mathrm{d}r \end{aligned} \qquad (4\text{–}3)$$

According to eq 4–3, the shape of the distribution function is independent of the value of α when the observation time t is much more than the inverse of α. Since the inverse of α corresponds to the time when the t^{-m} law starts to hold; the ITL decay obeyed the t^{-m} law over the time range measured from 10^2 to 10^5 s, therefore, the inverse of α is at least more than of the order of 10^2 s. Thus, it is safe to say that the shape of the distribution function for observation time scale is mainly dependent upon the value of m. One can, therefore, discuss the distribution function within the observed time range even if the value of I_0 and α cannot be determined.

Although the shape of the distribution function within the observed time range is, as described above, mainly characterized by the value of m, it also depends on the values of ν and β. These parameters are not observed values but assumed ones. Thus, it will be considered how the values of ν and β affect the shape of the distribution function.

Multiplication of ν by $e^{\beta a}$ makes the distribution function $n(r, t)$ moved parallel in the direction of the r-axis by a. Namely, this procedure is equivalent to the variable transformation of r into $r - a$. Thus, there is no change in the shape of the distribution

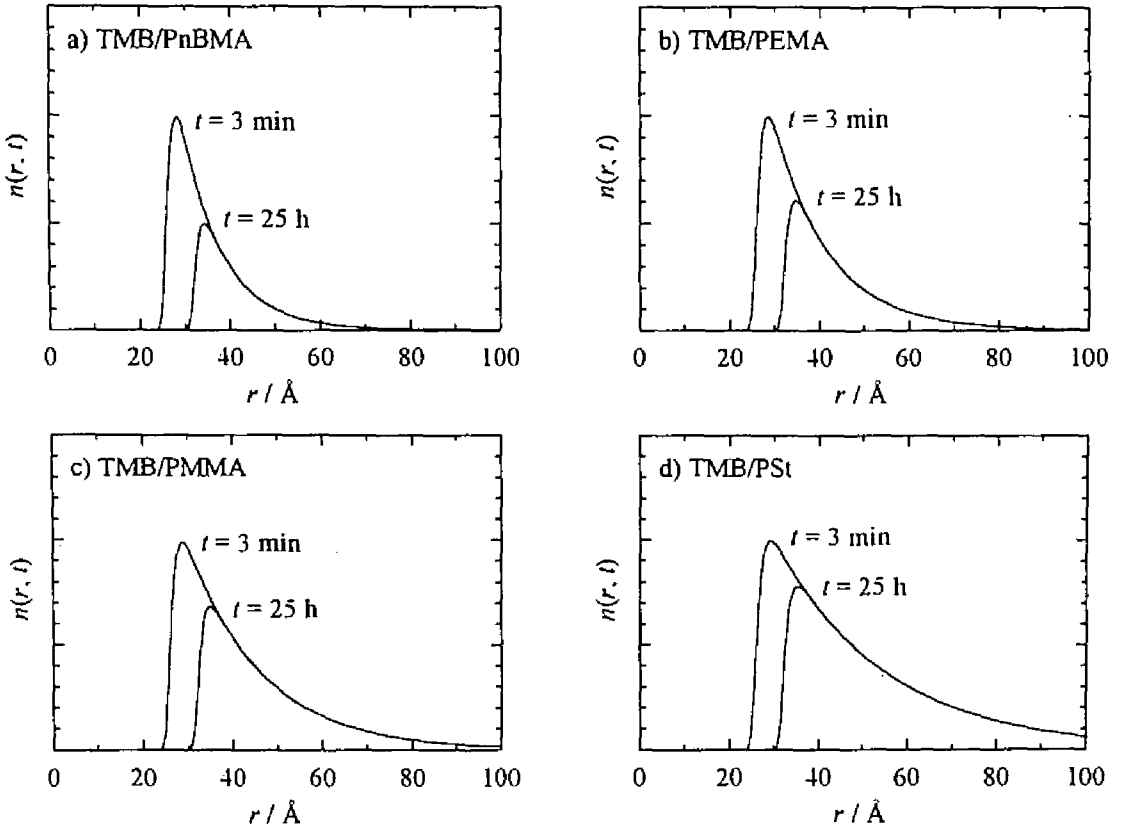

Figure 4–4. The distribution function $n(r, t)$ of the distance between an ejected electron and the parent cation calculated using eq 4–3 obtained from the Laplace inverse transformation of the observed ITL decay function fitted to eq 4–1. The distribution functions $n(r, t)$ at 3 min and 25 h after the photoirradiation at 20 K.

function with time t because such a procedure leads to not only the shift of the distribution function along the r-axis but also the change in the electron transfer rate $k(r)$ multiplied by $e^{\beta a}$. Therefore, the percentage of the decrease in a dopant cation within a certain time range is independent of the value of ν.

The replacement of β with βb is equivalent to the variable transformation of r into br leading to the expansion or contraction of r-axis. Consequently, it is reasonable to conclude that the percentage of the decrease in a dopant cation within a certain time range is also independent of the value of β, that is, the exact values of ν and β are not necessary when one discuss the percentage of the decrease in a dopant cation within a certain time range.

Then, the fraction of the decrease in radical cations evaluated from the ITL decay using the electron tunneling model is compared with that directly observed by the absorption spectroscopy. The changes in the distribution function $n(r, t)$ with time t shown in Figures 4–4 are calculated from eq 4–3. These figures represent the disappearance of electron-cation pairs from 3 min to 25 h after the photoirradiation.

On the other hand, when the ITL decay is expressed by eq 4–1, as described in Chapter 3, the absorbance decay $Abs(t)$ is given by

$$Abs(t) = Abs_0 - Abs_\infty^{\mathrm{dis}}\left[1 - \frac{1}{(1+\alpha t)^{m-1}}\right], \qquad (4\text{–}4)$$

where Abs_0 is the absorbance of $TMB^{\bullet+}$ at $t = 0$ and $Abs_\infty^{\mathrm{dis}}$ is the absorbance corresponding to the disappearance of $TMB^{\bullet+}$ between $t = 0$ and $t = \infty$.[36] The amount of radical cations at 3 min is defined as 100 percent and then the percentage of the disappearance from 3 min to 25 h was estimated using eq 4–4.

The second column in Table 4–2 is the percentage of the disappearance of electron-cation pairs from 3 min to 25 h calculated from the distribution function. The third column is the percentage of the disappearance of the parent cation from 3 min to 25 h directly obtained from the measurement of the absorbance decay of $TMB^{\bullet+}$.

The calculated value in the second column and the observed one in the third column show good agreement for polystyrene whereas they exhibit disagreement for poly(alkyl methacrylate)s. In the latter case, the decrease in radical cations was less than that expected from the ITL decay. This disagreement suggests that some photoejected electrons are captured in a deeper trap and cannot recombine with the parent cation at 20

K; there is another deep trap besides a shallow trap in photoirradiated poly(alkyl methacrylate)s even at 20 K.

Table 4–2. The Percentage of Decrease in $TMB^{\bullet+}$ Doped in Polymer solids over the Time Range from 3 min to 25 h after Photoirradiation at 20 K

	ITL / %[a)]	Abs / %[b)]	difference / %
PnBMA	48.2	19.6	28.6
PEMA	38.4	18.7	19.7
PMMA	28.9	13.2	15.7
PSt	23.9	23.1	0.8

a) Calculated from the distribution function of the distance between an ejected electron and the parent cation obtained from the Laplace inverse transformation of the observed ITL decay function fitted to eq 4–1.

b) Obtained from the fitting curve using eq 4–4 to the absorption measurement of $TMB^{\bullet+}$ decay at 20 K.

4.3.2. Initial Distribution Function of Trap Depth

As an example, the initial trap-depth distribution function $n(V, 0)$ of TMB/PnBMA was calculated from the Laplace inverse transformation of the ITL decay function; see eq 4–13. The parameters used here were as follows: $I_0 = 1.3 \times 10^9$ CPS, $\alpha = 23.0\ s^{-1}$, $m = 1.11$, $\nu = 10^9\ s^{-1}$, and $r_{DA} = 35$ Å. As shown in Figure 4–5, the explanation of the t^{-m} behavior over the wide time range requires a wide trap-depth distribution from 0.5 to 2.0 eV. An explanation can be made from the viewpoint of the very narrow spectral distribution of excitation laser pulses[41)] if the spatial distribution of electron-cation pairs is disregarded. However, the wide trap-depth distribution contradicts the temperature independence of the ITL decay kinetics. Besides, the decrease in ionic species calculated from the initial trap-depth distribution is too large compared with that obtained from the absorbance measurement given above; the former is about 50 % whereas the latter is about 20 %. Therefore, the trap-depth distribution model without a spatial distribution cannot be adopted.

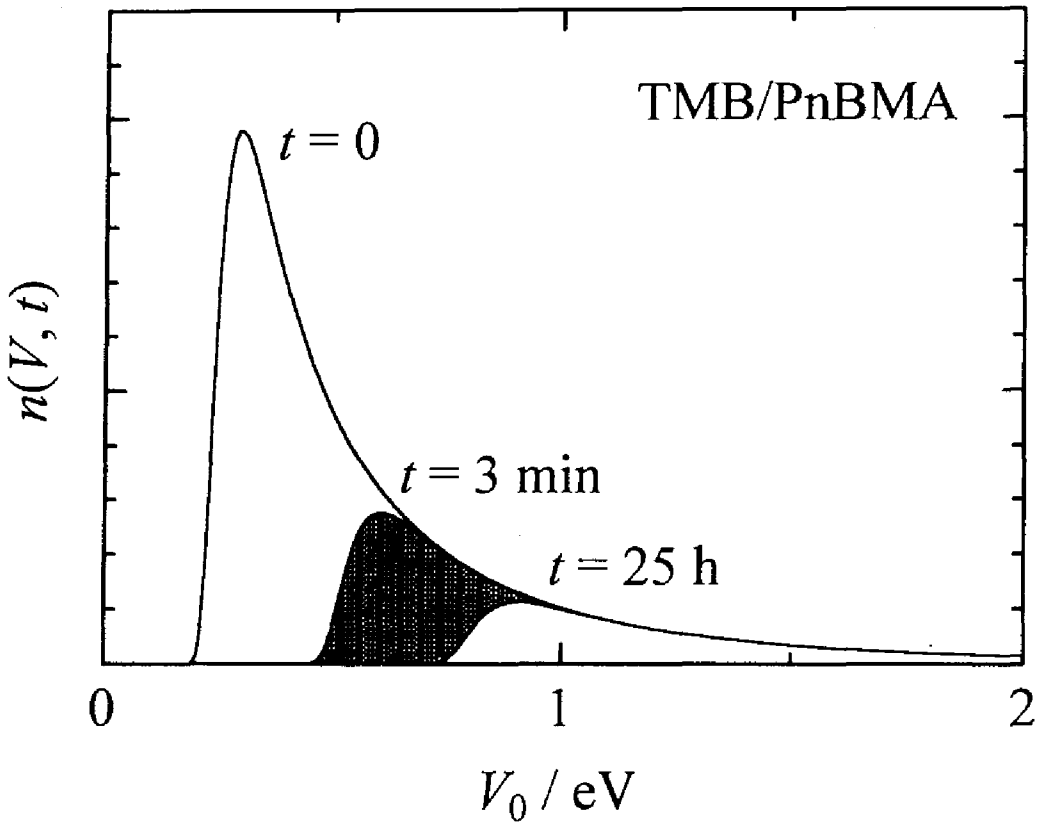

Figure 4–5. The distribution function of a trap depth (eq 4–13) calculated from the Laplace inverse transformation of the observed ITL decay function fitted to eq 4–1. The shaded portion in the figure represents the decrease in the $TMB^{\bullet+}$ due to the charge recombination over the time range from 3 min to 25 h after the photoirradiation at 20 K. The parameters used are as follows: $I_0 = 1.3 \times 10^9$ CPS, $\alpha = 23.0\ s^{-1}$, $m = 1.11$, $\nu = 10^9\ s^{-1}$, and $r_{DA} = 35$ Å.

4.3.3. Spatial Distribution of Photoejected Electrons in Shallow Trap and Deep Trap

In subsection 4.3.1, only a spatial distribution of photoejected electrons with a unique trap depth was considered. Here, to explain the difference between the ITL decay and the absorbance decay, another trap is added: the trap depth is so deep that the trapped electron cannot participate in the charge recombination with the parent cation. In other words, it is assumed that the ITL results from the charge recombination from a shallow trap and the absorbance is the sum of the shallow trap and deep trap not participating in the charge recombination.

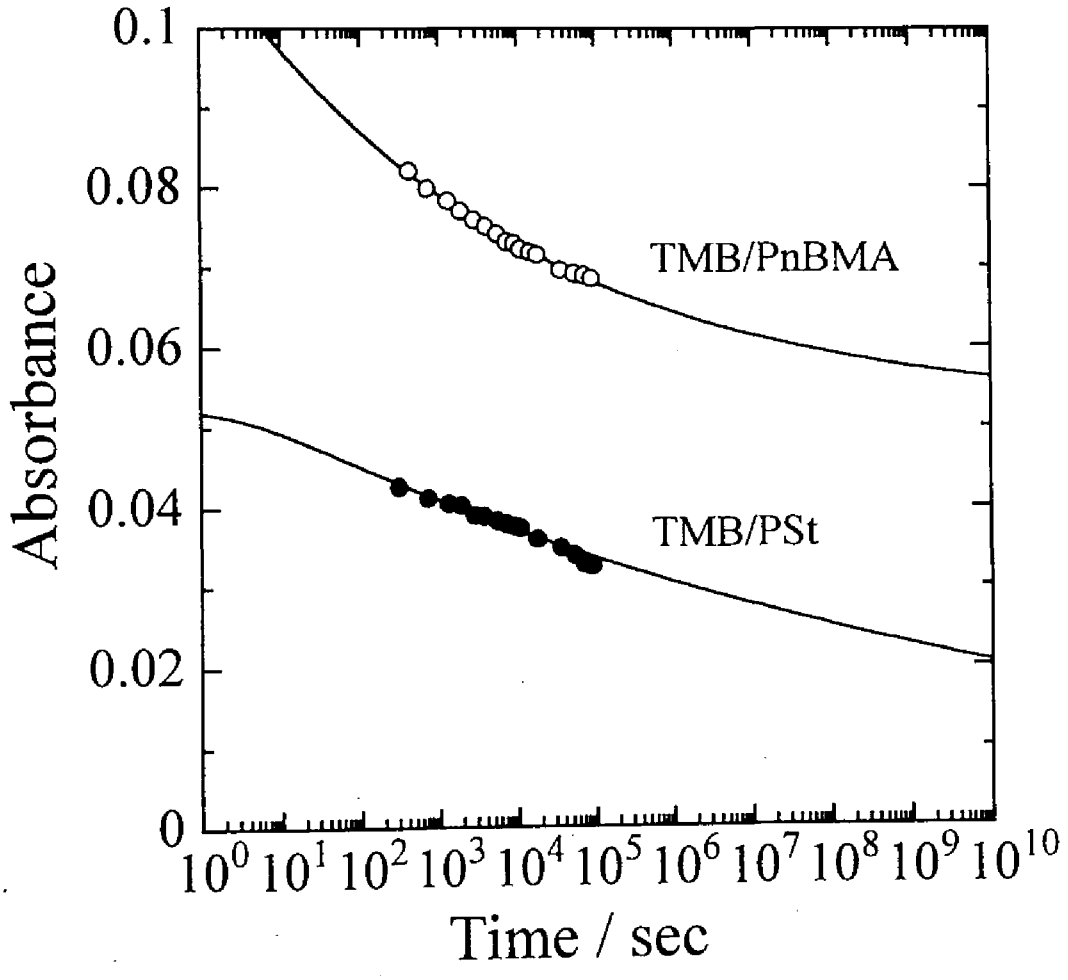

Figure 4–6. The absorbance decay of $TMB^{\bullet+}$ for TMB/PnBMA and TMB/PSt at 20 K. The solid lines are the fitting curves using eq 4–4 with the same parameters obtained from the ITL decay fitting: α = 23.0 s^{-1}, m = 1.11 for TMB/PnBMA; α = 0.39 s^{-1}, m = 1.04 for TMB/PSt. The fitting parameters for the absorbance decay are as follows: $Abs_0 = 0.135 > Abs_\infty^{dis} = 0.0838$ for PnBMA; $Abs_0 = 0.0526 \approx Abs_\infty^{dis} = 0.0548$ for PSt.

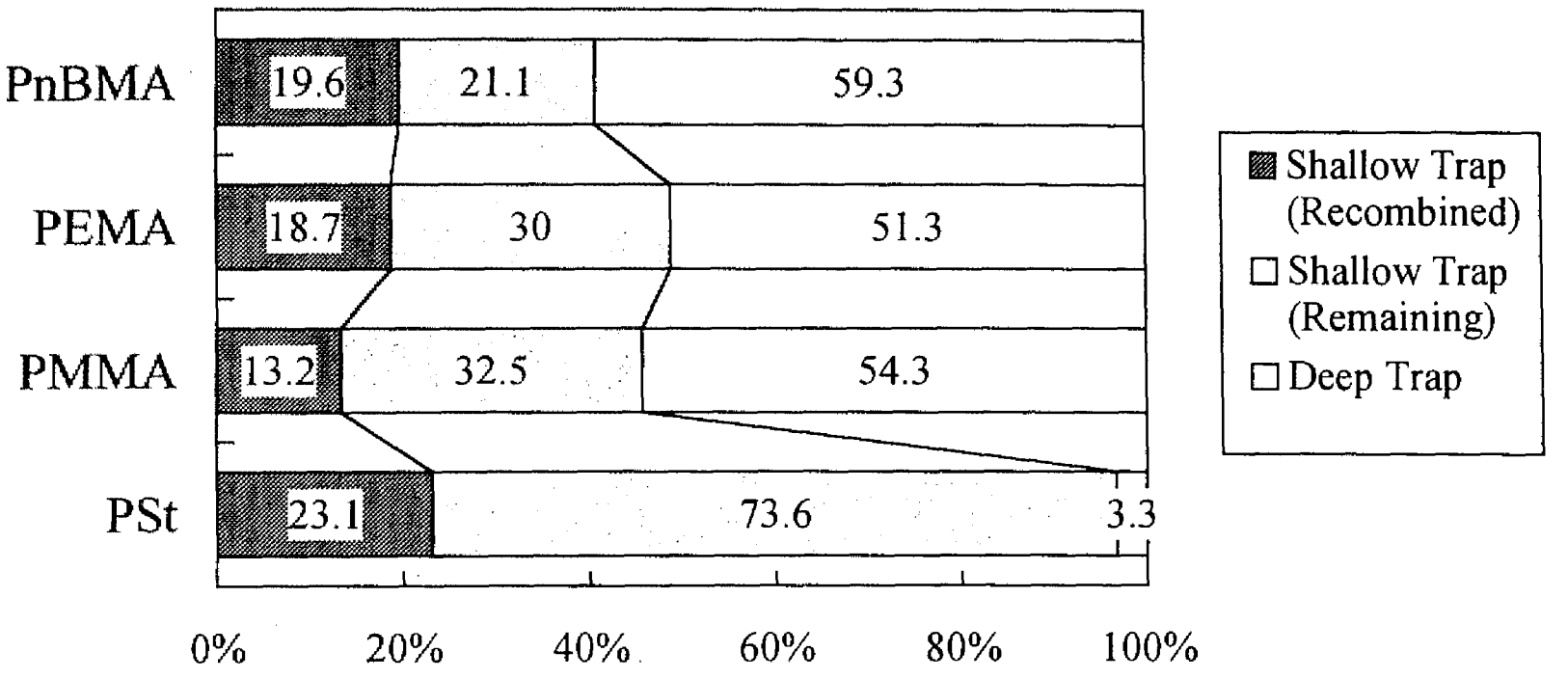

Figure 4–7. The bar charts for the proportion of shallow and deep traps. Photoejected electrons captured in a shallow trap can recombine with the parent cation at 20 K. On the contrary, photoejected electrons captured in a deep trap stay in the trap and cannot recombine with the parent cation at 20 K.

The absorbance decay of $TMB^{\bullet+}$ indicates the existence of a deep trap not participating in the charge recombination. Figure 4–6 shows the results for the fitting of eq 4–4 to the absorbance of $TMB^{\bullet+}$ in PnBMA and PSt as an example. The value of Abs_0 is higher than that of Abs_∞^{dis} for poly(alkyl methacrylate)s, while the value of Abs_∞^{dis} is almost equal to that of Abs_0 for polystyrene. A part of $TMB^{\bullet+}$ in poly(alkyl methacrylate) solids remains even at $t = \infty$. This finding also indicates the existence of a deep trap not participating in the charge recombination.

In Figure 4–7, the fraction of shallow trap (recombined) was that of the absorbance decay of $TMB^{\bullet+}$ from 3 min to 25 h after the photoirradiation when the absorbance at 3 min was defined as 100 %. The fraction of shallow trap (remaining) was calculated from the ratio of the disappearance to the remaining of distribution function obtained from the Laplace inverse transformation of the ITL decay during the same time domain. Then, the fraction of deep trap was estimated from the subtracting both of the above from 100 %. As shown in Figure 4–7, the ratio of the shallow and deep traps is about 40 : 60 ~ 50 : 50 for poly(alkyl methacrylate)s used here. This suggests that 50 – 60 % of photoejected electrons are captured in deep trap sites for poly(alkyl methacrylate)s. This estimation is very rough, but suggests that deep as well as shallow traps exist even at 20 K where major motions of the polymer chain are frozen.

In irradiated polymer solids, charged species produced by radiation was reported to cause side-chain elimination, main-chain scission, and crosslinking.[42] In poly(alkyl methacrylate)s solids, a main-chain scission was reported to be induced by photoionization of the dopant chromophore[29,30] as well as radiation.[27,28] On the other hand, polystyrene is more highly resistant to radiation than poly(alkyl methacrylate)s, although it is classified as a crosslinking type.[42,43] Thus, the disagreement in poly(alkyl methacrylate)s might be related to the photoinduced chemical reaction. However, a large scale chemical reaction might be impossible at a temperature as low as 20 K, because only small species such as electrons, protons, and methyl group can migrate and transfer at 20 K. One possible explanation is that the shallow trap is a physical trap, *e.g.*, a small cavity of polymer matrix, and the deep trap is a chemical trap, *e.g.*, ester anion radical,[29,30,44,45] which is a precursor of main-chain scission.

4.4. Conclusion

On the basis of an electron tunneling model, the initial distribution function of the distance between a photoejected electron and the parent cation was calculated from the Laplace inverse transformation of the observed ITL decay function. The decrease in ionic species estimated from the initial distribution was found to be consistent with that from the absorbance measurement of the dopant cation for polystyrene but not for poly(alkyl methacrylate)s. In the case of poly(alkyl methacrylate)s, some photoejected electrons are captured in a deep trap site and change into a precursor of chemical reaction, *e.g.*, ester anion radical, even at 20 K where major motion of the polymer chain is frozen.

Appendix

The following kinetics equation holds for the geminate charge recombination:

$$\begin{aligned} \frac{\mathrm{d}}{\mathrm{d}t} n(r,V,t)\mathrm{d}r\mathrm{d}V &= -k(r,V)n(r,V,t)\mathrm{d}r\mathrm{d}V \\ n(r,V,t)\mathrm{d}r\mathrm{d}V &= n(r,V,0)\exp\left[-k(r,V)t\right]\mathrm{d}r\mathrm{d}V , \end{aligned} \tag{4–5}$$

where $n(r, V, t)\mathrm{d}r\mathrm{d}V$ is the number of electron-cation pairs as a function of the distance between the electron-cation pairs r, trap depth V, and time t from the end of irradiation, and $k(r, V)$ is the rate of electron transfer.

Assuming that the trap-depth distribution is independent of the spatial distribution, $n(r, V, t)$ can be divided into the product of $n(r, t)$ and $n(V, t)$,

$$n(r,V,t) = n(r,t)n(V,t) . \tag{4–6}$$

Thus, we obtain the following equations with apparent quantum efficiency of emission λ:

$$\begin{aligned} I(t) &= -\lambda \frac{\mathrm{d}}{\mathrm{d}t} \iint n(r,v,t)\mathrm{d}r\mathrm{d}V \\ &= -\lambda \iint \frac{\mathrm{d}}{\mathrm{d}t} n(r,V,t)\mathrm{d}r\mathrm{d}V \\ &= \lambda \iint k(r,V)n(r,0)n(V,0)\exp\left[-k(r,V)t\right]\mathrm{d}r\mathrm{d}V . \end{aligned} \tag{4–7}$$

Here, we disregard the spatial distribution; the following delta function is introduced for the spatial distribution,

$$n(r,0) = n\delta(r - r_{\mathrm{DA}}) . \tag{4–8}$$

Then the ITL intensity $I(t)$ is given by

$$\begin{aligned} I(t) &= \lambda n \int k(r_{\mathrm{DA}},V)n(V,0)\exp\left[-k(r_{\mathrm{DA}},V)t\right]\mathrm{d}V \\ &= \lambda n \int k(V)n(V,0)\exp\left[-k(V)t\right]\mathrm{d}V \end{aligned} \tag{4–9}$$

where $k(V)$ is given by the WKB approximation,

$$k(V) = k(r_{\mathrm{DA}},V) = \nu \exp\left(-\frac{2\sqrt{2m_e(V-E)}}{\hbar} r_{\mathrm{DA}} \right) . \tag{4–10}$$

Then we carried out the following variable transformation from V into $k(V)$:

$$k(V)\mathrm{d}V = -\frac{\hbar}{r_{\mathrm{DA}}} \sqrt{\frac{V-E}{2m_e}} \mathrm{d}k(V) . \tag{4–11}$$

Finally, the ITL intensity can be expressed by

$$I(t) = -\lambda n \int_{v}^{0} n(V,0)\exp[-k(V)t]\frac{\hbar}{r_{DA}}\sqrt{\frac{V-E}{2m_e}}\mathrm{d}k(V)$$
$$= \frac{\lambda n\hbar}{r_{DA}\sqrt{2m_e}}\int_{0}^{\infty} n(V,0)\sqrt{V-E}\exp[-k(V)t]\mathrm{d}k(V). \quad (4\text{–}12)$$

Because this equation is satisfied with the Laplace transformation, the initial trap-depth distribution $n(V, 0)$ can be obtained from the Laplace inverse transformation of the ITL intensity function $I(t)$

$$n(V,0)\sqrt{V-E} = \frac{r_{DA}\sqrt{2m_e}}{\lambda n\hbar}\mathcal{L}^{-1}[I(t)]$$
$$n(V,0) = \frac{r_{DA}\sqrt{2m_e}}{\lambda n\hbar}\frac{1}{\sqrt{V-E}}\mathcal{L}^{-1}\left[\frac{I_0}{(1+\alpha t)^m}\right] \quad (4\text{–}13)$$
$$= \frac{r_{DA}\beta I_0 \nu^{m-1}}{n\hbar\lambda\alpha^m\Gamma(m)}\sqrt{\frac{2m_e}{V-E}}\exp\left[-(m-1)\beta r_{DA} - \frac{\nu}{\alpha}\exp(-\beta r_{DA})\right],$$

where β is given by the following equations:

$$\beta = \frac{2\sqrt{2m_e(V-E)}}{\hbar} = \frac{2\sqrt{2m_eV_0}}{\hbar}. \quad (4\text{–}14)$$

References and Notes

1) J. M. Warman, in *"The Study of Fast Processes and Transient Species by Electron Pulse Radiolysis"*, eds. J. H. Baxendale and F. Busi, Reidel, Dordrecht (1982).

2) J. M. Warman, K. -D. Asmus, and R. H. Schuler, *J. Phys. Chem.*, **73**, 931 (1969).

3) J. M. Warman and S. J. Rzad, *J. Chem. Phys.*, **52**, 485 (1970).

4) S. J. Rzad, P. P. Infelta, J. M. Warman, and R. H. Schuler, *J. Chem. Phys.*, **52**, 3971 (1970).

5) M. Tachiya, *J. Chem. Phys.*, **70**, 4701 (1979).

6) K. M. Hong and J. Noolandi, *J. Chem. Phys.*, **68**, 5163 (1978).

7) L. Onsager, *Phys. Rev.*, **54**, 554 (1938).

8) Y. Yoshida, S. Tagawa, and Y. Tabata, *Radiat. Phys. Chem.*, **28**, 201 (1986).

9) Y. Yoshida, S. Tagawa, M. Washio, H. Kobayashi, and Y. Tabata, *Radiat. Phys. Chem.*, **34**, 493 (1989).

10) Y. Yoshida and S. Tagawa, in *"Dynamics and Mechanisms of Photoinduced Electron Transfer and Related Phenomena"*, eds. N. Mataga, T. Okada, and H. Masuhara, Elsevier, Amsterdam (1992).

11) P. Debye and J. O. Edwards, *J. Chem. Phys.*, **20**, 236 (1952).

12) In this chapter, the term "a trapped electron" is defined as an electron captured in the matrix; including trapped electrons, solvated electrons, radical anions, and other anionic species.

13) G. C. Abell and A. Mozumder, *J. Chem. Phys.*, **56**, 4079 (1972).

14) W. H. Hamill and K. Funabashi, *Phys. Rev. B*, **16**, 5523 (1977).

15) E. W. Montroll and G. H. Weiss, *J. Math. Phys.*, **6**, 167 (1965).

16) H. Scher and E. W. Montroll, *Phys. Rev. B*, **12**, 2455 (1975).

17) A. I. Mikhailov, *Dokl. Akad. Nauk SSSR*, **197**, 136 (1970).

18) M. Tachiya and A. Mozumder, *Chem. Phys. Lett.*, **28**, 87 (1974).

19) F. S. Dainton, M. J. Pilling, and S. A. Rice, *J. Chem. Soc., Faraday Trans. 2*, **71**, 1311 (1975).

20) M. Tachiya and A. Mozumder, *Chem. Phys. Lett.*, **34**, 77 (1975).

21) M. J. Pilling and S. A. Rice, *J. Phys. Chem.*, **79**, 3035 (1975).

22) F. Kieffer, C. Meyer, and J. Rigaut, *Chem. Phys. Lett.*, **11**, 359 (1971).

23) F. Kieffer, C. Meyer, and J. Rigaut, *Int. J. Radiat. Phys. Chem.*, **6**, 79 (1974).

24) Y. Hama, Y. Kimura, H. Tsumura, and N. Omi, *Chem. Phys.*, **53**, 115 (1980).

25) Y. Hama and K. Gouda, *Radiat. Phys. Chem.*, **21**, 185 (1983).

26) Kh. S. Bagdasar'yan, R. I. Milyutinskaya, and Yu. V. Kovalev, *Khim. Vysok. Energii*, **1**, 127 (1967).

27) M. Tanaka, H. Yoshida, and T. Ichikawa, *Polym. J.*, **22**, 835 (1990).

28) H. Yoshida and T. Ichikawa, in *"Recent Trends in Radiation Polymer Chemistry"*, Advances in Polymer Science, Vol. 105, ed. S. Okamura, Springer-Verlag, Berlin (1993), p. 3.

29) W. Sakai, A. Tsuchida, M. Yamamoto, T. Matsuyama, H. Yamaoka, and J. Yamauchi, *Macromol. Rapid Commun.*, **15**, 551 (1994).

30) W. Sakai, A. Tsuchida, M. Yamamoto, and J. Yamauchi, *J. Polym. Sci., Polym. Chem. Ed.*, **33**, 1969 (1995).

31) A. Tsuchida, M. Nakano, M. Yoshida, M. Yamamoto, and Y. Wada, *Polym. Bull.*, **20**, 297 (1988).

32) M. Yamamoto, A. Tsuchida, and M. Nakano, *MRS Int. Meeting Adv. Mater.*, **12**, 243 (1989).

33) A. Tsuchida, W. Sakai, M. Nakano, M. Yoshida, and M. Yamamoto, *Chem. Phys. Lett.*, **188**, 254 (1992).

34) A. Tsuchida, W. Sakai, M. Nakano, and M. Yamamoto, *J. Phys. Chem.*, **96**, 8855 (1992).

35) P. Peyser, in *"Polymer Handbook"*, 3rd ed., eds. J. Brandrup and E. H. Immergut, John Wiley & Son, New York (1989).

36) The mechanism of the charge recombination has discussed in Chapter 3. The ITL decay results from the charge recombination of a photoejected electron with the parent cation formed in a polymer solid through two-photon ionization of a dopant chromophore.

H. Ohkita, W. Sakai, A. Tsuchida, and M. Yamamoto, *Bull. Chem. Soc. Jpn.*, submitted.

37) Correctly speaking, the initial distribution function $f(r)$ represents the probability density that an ejected electron exists at a distance r from the parent cation. Thus, the number of ejected electrons between r and $r + dr$ is proportional to $f(r)4\pi r^2 dr$ in

the three dimensions. The relationship between $f(r)$ and $n(r,0)$ is given by $n(r,0)dr \propto f(r)4\pi r^2 dr$. In this chapter, for the sake of convenience, $n(r,0)$ is also called initial distribution function.

38) According to the WKB approximation, the value of β can be expressed by eqs 4–14. Thus, the value of β is estimated to be *ca.* 1 $Å^{-1}$ using eqs 4–14 with the assumption that the binding energy for trapped electrons $V - E$ ($= V_0$) is about 1 eV.

39) B. E. Springett, J. Jortner, and M. H. Cohen, *J. Chem. Phys.*, **48**, 2720 (1968).

40) S. Basak and M. H. Cohen, *Phys. Rev. B*, **20**, 3404 (1979).

41) H. Miyasaka and N. Mataga, *Chem. Phys. Lett.*, **134**, 480 (1987).

42) W. Schnabel, *"Polymer Degradation —Principles and Practical Applications—"*, Carl Hanser Verlag, Munich (1982).

43) J. H. O'Donnell and P. J. Pomery, *J. Polym. Sci., Polym. Symp.*, **55**, 269 (1976).

44) A. Torikai, H. Kato, and Z. Kuri, *J. Polym. Sci., Polym. Chem. Ed.*, **14**, 1065 (1976).

45) A. Torikai and S. Okamoto, *J. Polym. Sci., Polym. Chem. Ed.*, **16**, 2689 (1978).

Chapter 5

Charge Recombination Luminescence via Photoionization of Dopant Chromophore in Polymer Solids

5.1. Introduction

The charge transport in solid systems is of scientific and practical interest, because it is a key process to photoconduction,[1] electroluminescence,[2] and photorefractive effect.[3] The charge recombination of electron-hole pairs formed in irradiated solids can be observed through the charge recombination luminescence, which is called isothermal luminescence (ITL) at a fixed temperature or thermoluminescence (TL) with increasing temperature.[4]

There have been various investigations on the ITL for irradiated organic glasses or polymer solids at low temperatures. The ITL decay kinetics has been reported to obey the t^{-1} law: the ITL intensity is proportional to an inverse power function of time t.[5-8] In most cases, the kinetics is independent of temperature.[7,8] Thus, many authors explained the ITL decay in terms of a long-range electron transfer by electron tunneling.[9-14] In this model, the trap depth is assumed to be unique and constant with time. However, the direct evidence for the assumptions is lacking because of the difficulty of the absorption measurements of the transient ionic species.

On the other hand, the TL method has been historically used to examine the energy level of impurities and defects in an insulator or a semiconductor. It is still a unique method for measuring the trap depth of organic or inorganic insulators. With the pioneer work of Randall and Wilkins,[15] a big step was made in theoretical analysis of the TL. Nikolski and Buben[16] studied TL of irradiated polymer solids. They found, for the first time, that the TL glow curve reflects sensitively polymer chain motions. Since then, it has been widely used in the field of polymer chemistry as an effective method for observing the motional relaxation of polymer solids. In particular, Partridge and Charlesby[17,18]

investigated the TL for non-polar polymer solids such as polyethylene and polypropylene. However, little is known about the mechanism since the nature of the trap for an ejected electron is not understood in detail.

The measurement system used in this study is different from the previously reported high energy irradiated system in the following two points.

An aromatic chromophore was doped in polymer solids to clarify the luminescence center; the dopant chromophore clearly acts as a luminescence center because the ITL and TL spectra consist of the fluorescence and phosphorescence of the dopant chromophore. Although several reports have been made on irradiated polymers doped with a chromophore, high energy irradiation might cause various side reactions because of the direct excitation of the polymer matrix. Thus, an excimer laser pulse was used as an excitation light source instead of the high energy radiation. The excimer laser pulse is so intense that it can feed two photons simultaneously or another photon within the lifetime of an electronic excited dopant chromophore. The chromophore that absorbed two photons is excited to a higher electronic excited state above the ionization potential and ejects an electron to the matrix polymer. This phenomenon is called two-photon ionization. The dopant aromatic chromophores used here have absorption at 351 nm, which is the wavelength of XeF excimer laser light, but none of the polymer matrices used have absorption at the excitation wavelength. Therefore, two-photon ionization enables one to ionize selectively a dopant chromophore in a polymer solid without the direct excitation of the polymer matrix.[19–22)]

The emission spectra of the charge recombination luminescence, not the total emission intensity, were observed Most of various attempts[23)] for obtaining information on the motional relaxation of polymer solids using the TL glow curve of the irradiated polymer, were made by measurement of the total emission intensity of the TL, not the emission spectra. The total emission intensity of TL, *i.e.*, the glow curve gives information on the motional relaxation of the polymer solids, but the emission spectra provide information on the change in a trap depth with temperature as well as the motional relaxation of the polymer solids. The intensity ratio of phosphorescence to fluorescence I_P/I_F changes with the trap depth. If the trap depth is constant, the emission spectra hardly change and the intensity ratio I_P/I_F remains the same.

In this chapter, the emission spectra of ITL at 20 K and TL in the wide temperature range from 20 to 300 K were observed for several photoirradiated polymer films doped

with an aromatic chromophore. Concerning ITL, let us focus our attention on the charge recombination process of a photoejected electron with the parent cation at a temperature as low as 20 K where major motions of polymer chains are frozen; whether the trap depth changes with time or not. The observed TL glow peaks for each polymer were assigned to the motional relaxation of the polymer, the relationship between the change in depth of trapped electrons[24] and the motional relaxation of the polymer with increasing temperature was elucidated, and the difference in the photoinduced chemical reactivity between poly(alkyl methacrylate)s and polystyrene was examined. Finally, a reaction scheme is proposed for the charge recombination of a photoejected electron with the parent cation in polymer solids produced through two-photon ionization. The trap depth is estimated from the TL spectral change with temperature.

5.2. Experimental Section

5.2.1. Sample Preparation

Polymer matrices used in the present work were poly(*n*-butyl methacrylate) (PnBMA, $M_w = 10^5$, Scientific Polym. Prod.), poly(ethyl methacrylate) (PEMA, $M_w = 2.8 \times 10^5$, Scientific Polym. Prod.), and polystyrene (PSt, $M_n = 1.6 - 1.8 \times 10^5$, Wako Pure Chem. Ind., Ltd.). Poly(alkyl methacrylate)s belong to the category of scission type to radiation.[25,26] Polystyrene is relatively resistant to radiation although it belongs to the category of crosslinking type.[25,26] The glass transition temperatures (T_g) of the polymers are 293 K (PnBMA), 339 K (PEMA), and 373 K (PSt).[27] These polymers were purified by reprecipitation from a benzene solution into methanol three times. *N,N,N',N'*-Tetramethylbenzidine (TMB, Wako Pure Chem. Ind., Ltd.) was used as a dopant chromophore and was purified by recrystallization several times.

The sample films were prepared by the solution cast method. The films were evacuated above the T_g to remove the remaining trace of the casting solvent (benzene, Dojin, Spectrosol) until no absorption of benzene was observed with a spectrophotometer (Hitachi, U-3500). The concentration of TMB in the final polymer film was *ca.* 3×10^{-3} mol/L. The thickness of the film was *ca.* 200 – 300 μm.

5.2.2. *Measurements*

The polymer film doped with TMB was covered with a quartz plate (20 × 30 × 0.5 mm), fixed tightly on a copper cold finger of a cryostat (Iwatani Plantech Corp., CRT510), and then, *in vacuo*, cooled down to 20 K. The temperature of the sample film was monitored with a calibrated thermocouple (Au + 0.07% Fe/chromel) and was kept constant using a PID temperature control unit (Iwatani Plantech Corp., TCU-4). The sample film was repeatedly photoirradiated by 351-nm light pulses from an excimer laser (Lambda Physik, EMG101MSC, *ca.* 20 ns fwhm, *ca.* 60 mJ/pulse). The 351-nm laser pulses allow one to ionize the TMB dopant chromophore selectively, because none of these polymers used in the present work have absorption at 351 nm. The emission spectra of the isothermal luminescence (ITL or preglow) were measured with a fluorescence spectrophotometer (Hitachi, 850) from 10 min to 10 h after the photoirradiation at 20 K. Subsequently, the temperature of the sample film was raised at a heating rate of 5 K/min using the PID temperature control unit. The emission spectra of the thermoluminescence (TL or glow) were measured at temperatures from 20 to 300 K.

5.2.3. *Temperature Dependence of Steady-State Emission Spectra of TMB Doped in Polymer Solids*

From the TMB chromophore doped in a polymer solid photoexcited with a Xe lamp, not an excimer laser, phosphorescence as well as fluorescence was observed with the fluorescence spectrophotometer even at room temperature. Figure 5–1 shows the total emission spectra of the TMB doped in a PnBMA film at temperatures from 20 to 300 K. The emission peaks observed around 400 and 530 nm are ascribable to fluorescence and phosphorescence, respectively. As the figure shows, the fluorescence intensity I_F was nearly constant at temperatures from 20 to 300 K while the phosphorescence intensity I_P decreased steeply above 200 K and disappeared near the T_g of the polymer matrix. Similar emission spectra were also obtained for the TMB doped in PEMA and PSt.

Figure 5–2 shows the dependence of the intensity ratio I_P/I_F on temperature for all the polymer matrices doped with TMB used. As shown in Figure 5–2, the intensity ratio I_P/I_F for steady-state emission decreased with an increase in temperature; the I_P decreased with increasing temperature because non-radiative deactivation of the dopant chromophore was enhanced at higher temperatures.

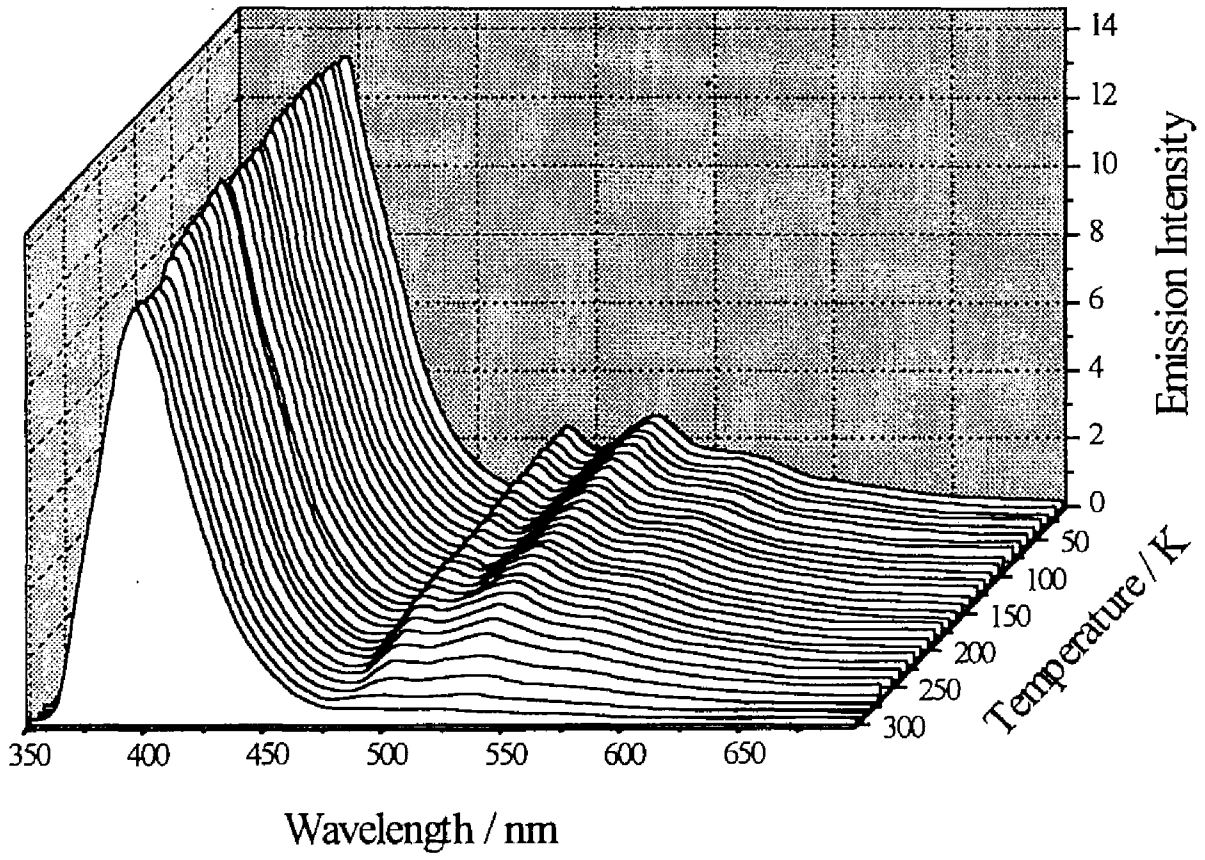

Figure 5–1. Steady-state emission spectra of the TMB doped in a PnBMA film over the temperature range from 20 to 300 K.

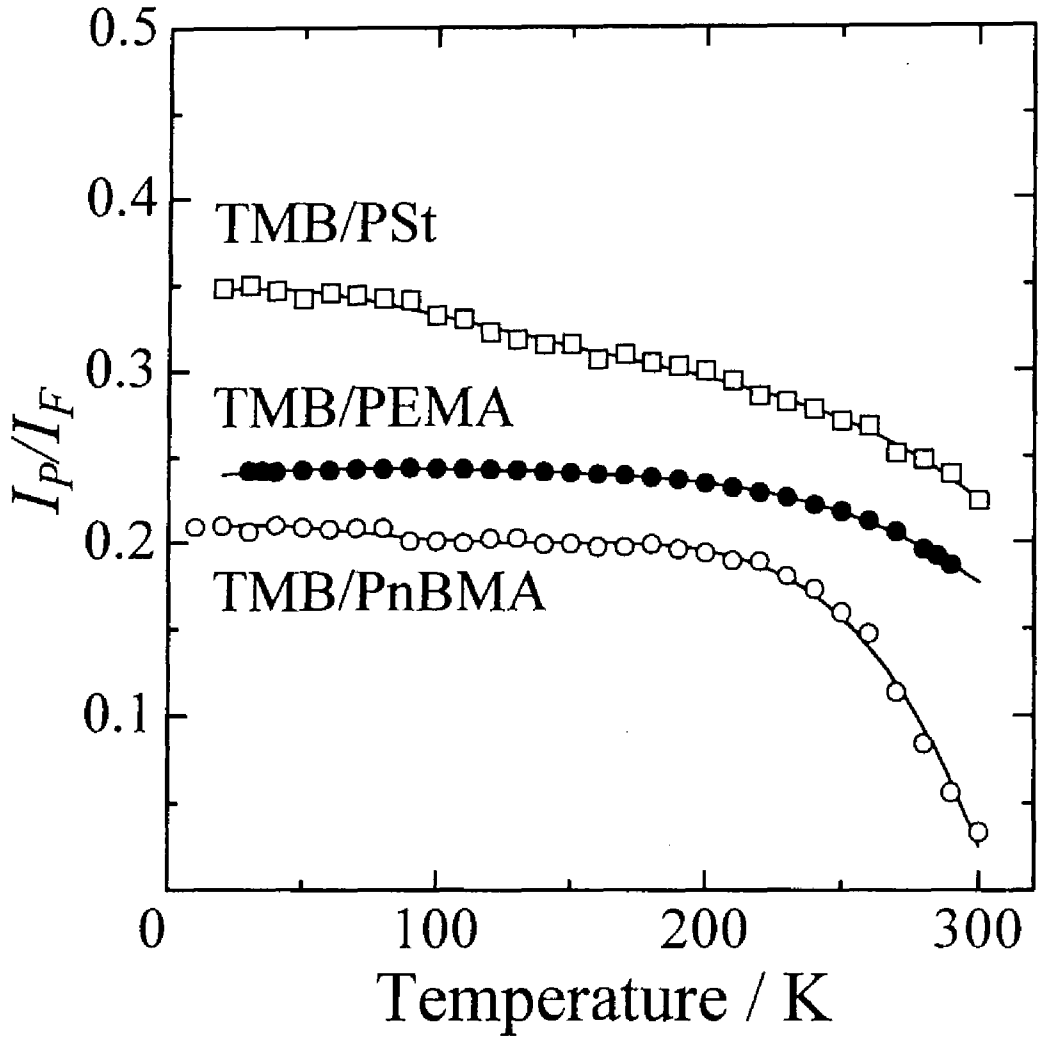

Figure 5–2. Temperature dependence of the intensity ratio of phosphorescence to fluorescence I_P/I_F for the TMB chromophore doped in polymer matrices: open circles TMB/PnBMA; closed circles TMB/PEMA; open squares TMB/PSt.

5.3. Results and Discussion

5.3.1. Spectral Change in Isothermal Luminescence (Preglow) with Time

Most ejected electrons through two-photon ionization are captured by the polymer matrix at a temperature as low as 20 K. However, some of them recombine with their parent-cation chromophores even at a fixed low temperature. As a result of the recombination, the chromophore is electronically excited again and emits fluorescence and/or phosphorescence. This emission is called isothermal luminescence (ITL) or preglow.

Figure 5–3 shows the spectral change in the ITL for the TMB doped in a PnBMA film which was photoirradiated at 20 K. The phosphorescence intensity I_P of the ITL was larger than the fluorescence intensity I_F of the ITL, contrary to the steady-state emission spectra shown in Figure 5–2. The intensity ratio I_P/I_F for the ITL was *ca.* 2 while that for the steady-state emission spectra was *ca.* 0.2. If the energy level of a trapped electron is much higher than the excited singlet state of the parent-cation chromophore, the charge recombination results in both excited singlet state and triplet state of the dopant chromophore. In the simplest case, the ratio of excited triplet state to excited singlet state reproduced by charge recombination will be three to one owing to the three-fold degeneracy of triplet state, because trapped electrons stay in traps for a much longer time than their spin relaxation time in the case of TL.[28,29]

Figure 5–4 shows the ITL decay at 20 K for the TMB doped in a PnBMA film; similar results were obtained for the other polymers. The log-log plots of I_F or I_P against time t from the end of the photoirradiation show straight lines; both decays of I_F and I_P for the ITL obeyed the t^{-1} law for all the polymer matrices used.[30] The t^{-1} law has been reported in the field of radiation chemistry.[5–8] This decay kinetics is often theoretically explained in terms of the long-range electron transfer model by electron tunneling,[9–14] because it is independent of the temperature.[7,8] The ITL was observed at 20 K where even the side-chain motion of a polymer seems to be almost frozen. Therefore, the ITL is also considered to take place through the charge recombination *via* electron tunneling.

The open squares shown in the figure denote the intensity ratio I_P/I_F. The intensity ratio I_P/I_F for all the polymers used is nearly constant over the time range from 10 min to 10 h after the photoirradiation, which indicates that the energy level of trapped electrons is

high enough to reproduce both excited singlet state and triplet state as a result of the charge recombination and the depth of trapped electrons involved in the charge recombination is nearly constant with time at 20 K.[31]

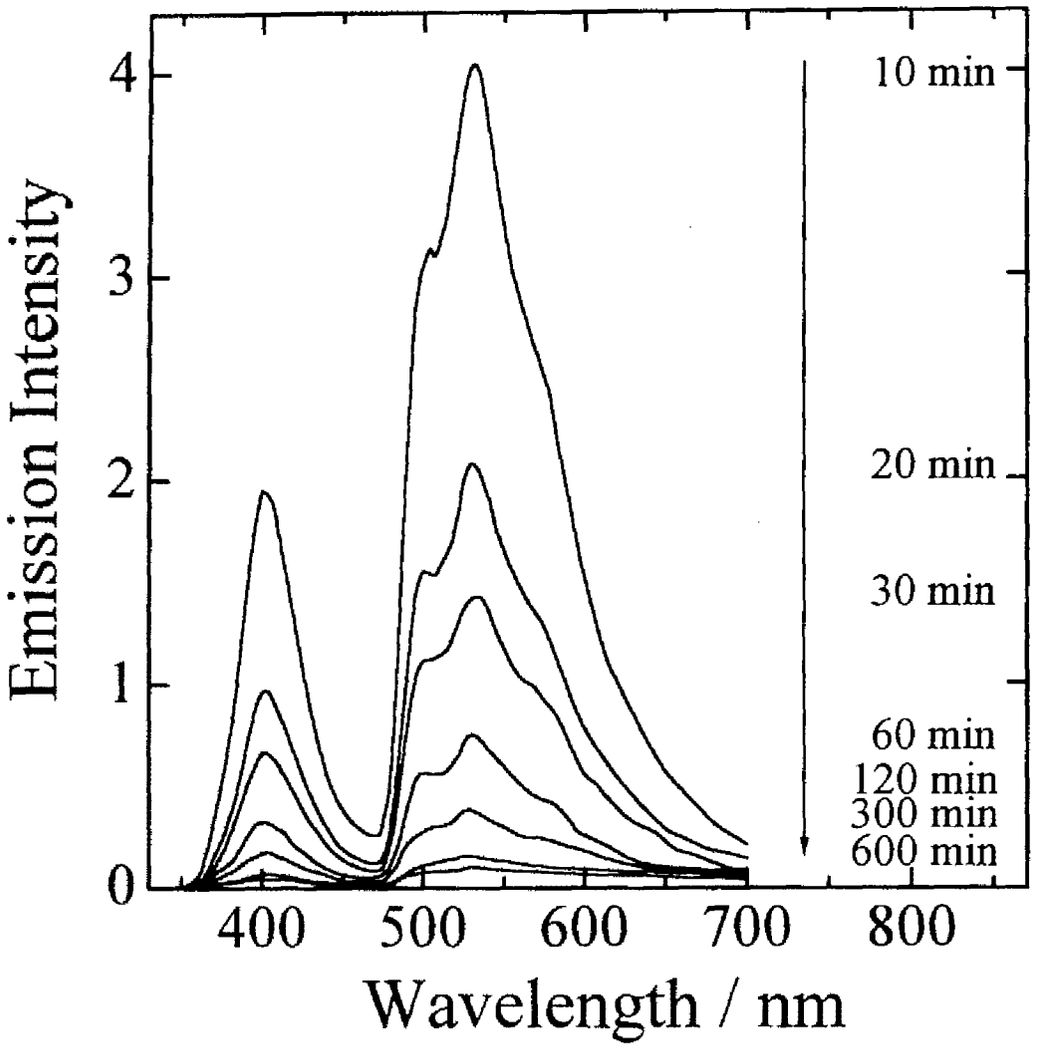

Figure 5–3. Emission spectral change in the ITL for the TMB chromophore doped in a PnBMA film over the time range from 10 to 600 min after the photoirradiation at 20 K.

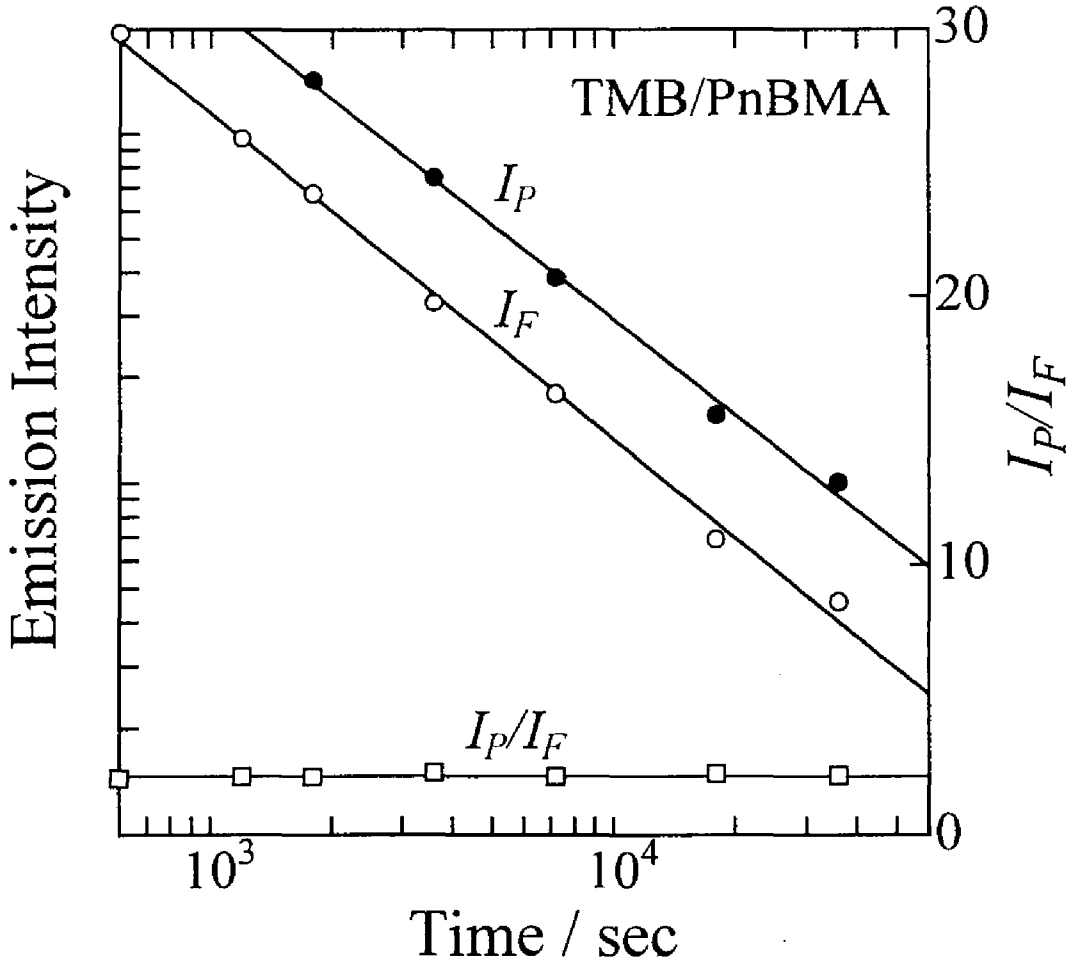

Figure 5–4. Dependence of the fluorescence intensity I_F (open circles), the phosphorescence intensity I_P (closed circles), and the intensity ratio I_P/I_F (open squares) on time, for the ITL at 20 K of the TMB chromophore doped in a PnBMA film. Solid lines in this figure are fitted using the least square methods.

5.3.2. *Spectral Change in Thermoluminescence (Glow) with Temperature*

5.3.2.1. *TMB/PnBMA*

After the ITL diminished, the emission was observed again as the photoirradiated film was heated. This emission is called thermoluminescence or glow. Figure 5–5 shows the spectral change in the TL for the TMB doped in a PnBMA film over the temperature range from 20 to 300 K. The emission spectrum of the TL at 20 K was similar to that of the ITL; the I_P was larger than the I_F. This enhancement of I_P shows that the TL is also based on the charge recombination of a photoejected electron with the parent cation.

First, the glow peaks in the I_F or the I_P were assigned to a motional relaxation of the polymer. Figure 5–6a shows the spectral glow curves for TMB/PnBMA; the I_F reached a peak around 100 K and then monotonically decreased while the I_P gave small peaks around 100 K and rose to the largest peak around 220 K. The TL method has been widely used to obtain information on the motional relaxation of polymer chains. However, the assignment of observed results to a motional relaxation is generally difficult because the sub-transition depends on the frequency of the stimuli of methods used to detect it. In the TL measurement, it is not measured directly as a function of time or frequency, but as a function of heating rate. Then, the frequency region observed in the TL measurement can be roughly estimated to be in the order of 10^{-1} Hz because the heating rate was 5 K/min at temperatures from 20 to 300 K. Thus, all the assignments of the TL results were based on the comparison with the results hitherto obtained from other measurements at low frequencies.

According to the dynamic mechanical measurements, the loss peaks appear at 100 – 120 K (~ 0.5 Hz) for most of the poly(alkyl methacrylate)s with a long side chain except for PEMA.[32] Wada *et al.* reported that the dielectric loss peak is observed at 120 K (10 – 100 Hz) for PnBMA.[33] They ascribed the loss peak to the rotation of *n*-propyl group accompanied by the rotation of the end ethyl group, which is called δ-relaxation. Therefore, the peak around 100 K is ascribable to the δ-relaxation, that is, the rotation of ester alkyl group.

On the other hand, the glow peak around 220 K would be observed at a higher temperature, if it were not for the decrease in the I_P of the TMB doped in a PnBMA film above 200 K as shown in Figure 5–2. Actually, the corresponding glow peak was

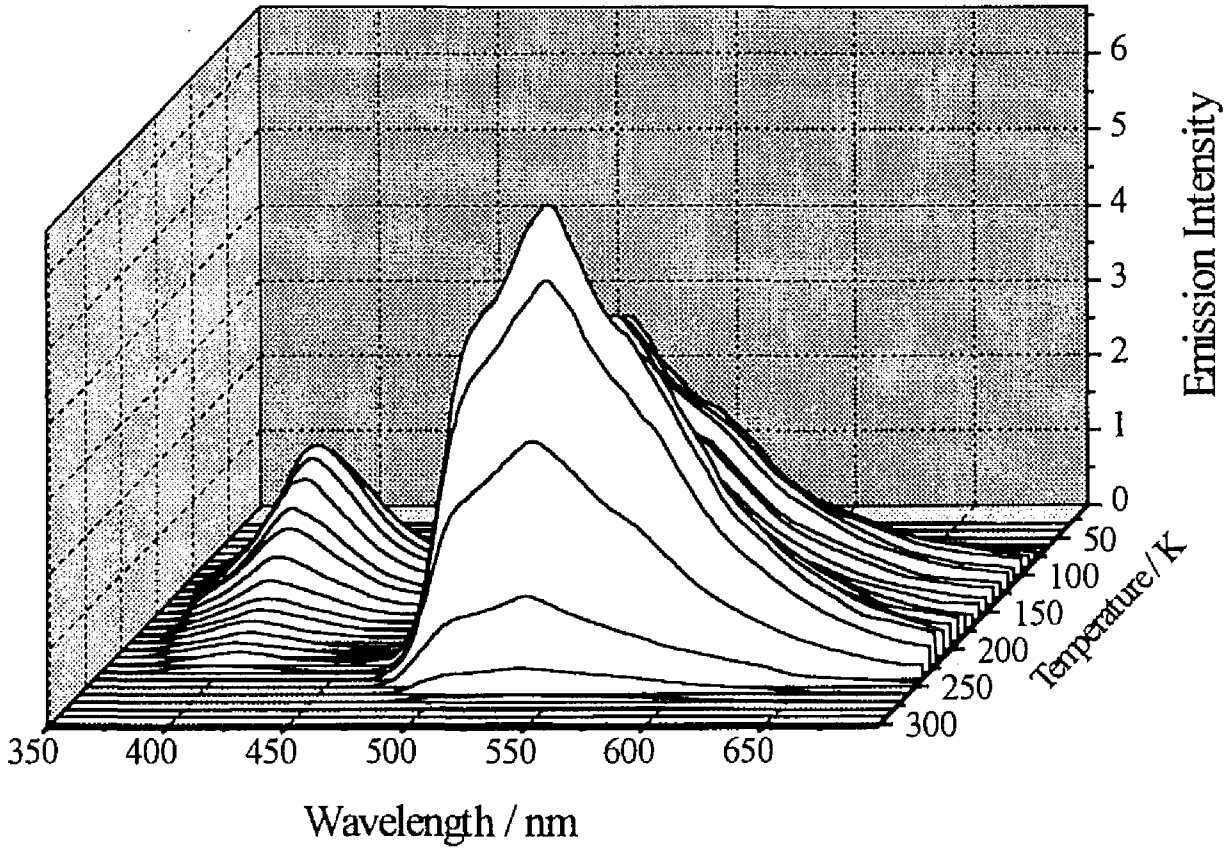

Figure 5–5. Emission spectral change in the TL of the TMB chromophore doped in a PnBMA film at temperatures from 20 to 300 K. Sample films were photoirradiated at 20 K. Heating rate was 5 K/min.

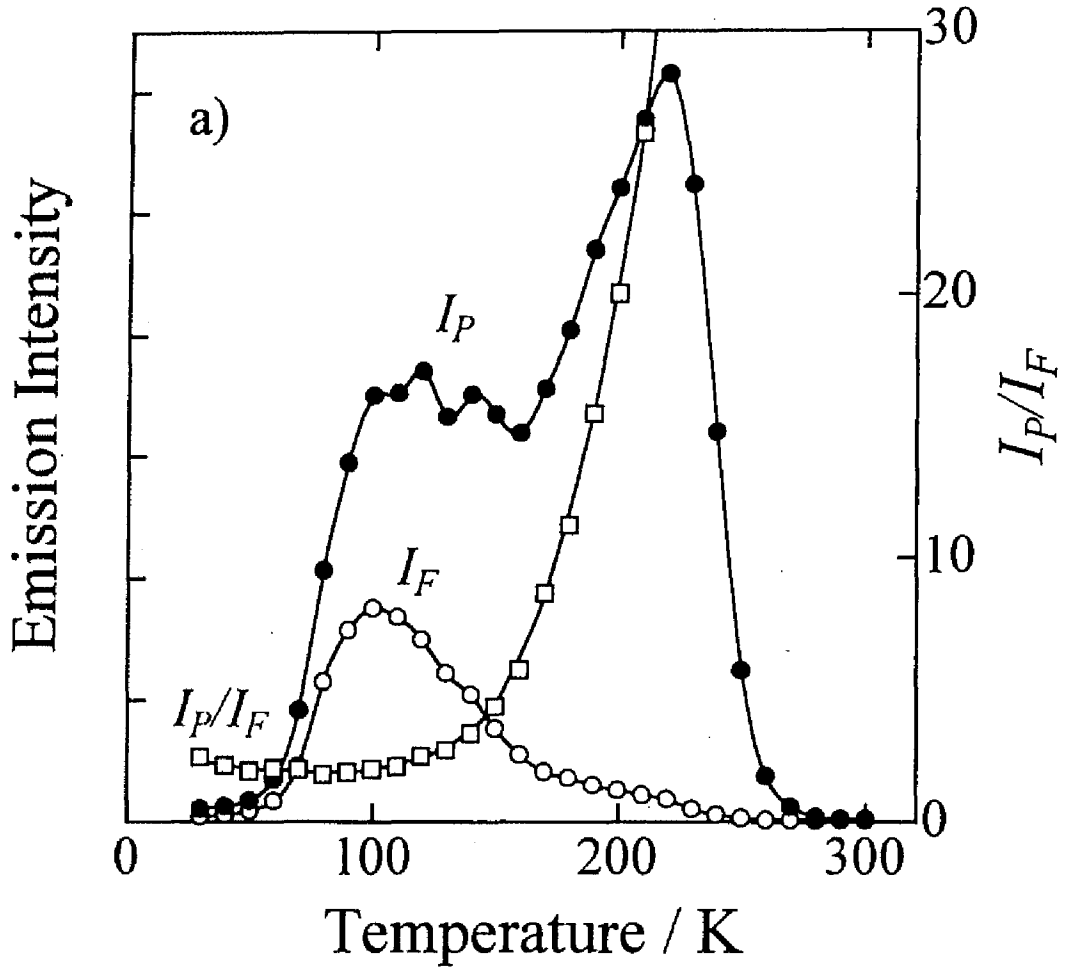

Figure 5–6a. Dependence of the fluorescence intensity I_F (open circles), the phosphorescence intensity I_P (closed circles), and intensity ratio I_P/I_F (open squares) on temperature for the TL of the TMB chromophore doped in a photoirradiated PnBMA film. Heating rate was 5 K/min.

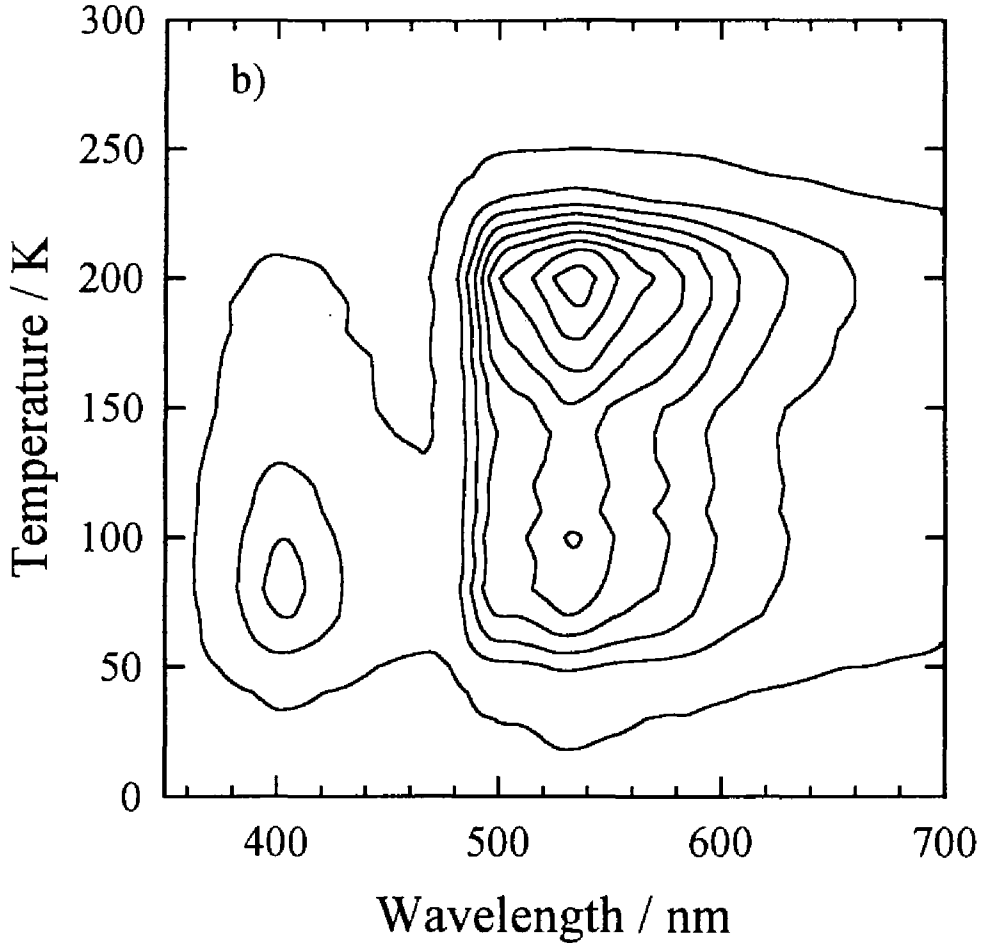

Figure 5–6b. A TL contour map for the PnBMA film doped with a TMB chromophore photoirradiated at 20 K. Heating rate was 5 K/min.

observed around 250 K for a photoirradiated PnBMA film doped with perylene, the fluorescence intensity of which is independent of temperature between 20 and 300 K.[34] The peak at 220 K here is probably ascribed to the side chain relaxation and/or the local mode relaxation of the main chain,[35-37] that is, the small scale motion of small segments of a main chain at a low temperature where the micro-Brownian motion of the main chain is frozen. This relaxation is generally observed below the T_g, although it can exist above and below the T_g in principle.[35] This assignment will be discussed later in comparison with the result for PEMA.

It is noteworthy that the intensity ratio I_P/I_F is constant below about 100 K and starts to increase steeply above about 130 K. Figure 5–6b shows clearly this tendency. Since the intensity ratio I_P/I_F decreased with an increase in temperature in the case of steady-state emission, the increase in the intensity ratio I_P/I_F is clearly due to the change in the energy level of electron trap sites with increasing temperature and not to the increase in the rate of non-radiative deactivation. This dependence of the intensity ratio I_P/I_F on temperature can be interpreted as 1) the deepening of trap depth with increasing temperature, and 2) the electron transfer from a shallow trap to a deeper trap, which is a possible explanation when there are many pre-existing trap sites with various energetic depths. Both mechanisms result in the increase in the intensity ratio I_P/I_F because ejected electrons firmly captured in deeper trap sites participate in the charge recombination at higher temperatures; the potential energy of electrons in deeper traps is insufficient to reproduce the excited singlet state of a dopant chromophore *via* the charge recombination. Radical species produced by the irradiation have been reported to take part in chemical reactions such as elimination of alkyl group and main-chain scission and consequently change into more stable chemical species with increasing temperature.[38,39] Therefore, the increase in the intensity ratio I_P/I_F can be mainly attributed to the deepening of trap depth caused by chemical reactions with increasing temperature.

5.3.2.2. TMB/PEMA

Here, the matrix polymer was changed from PnBMA to PEMA to examine the relationship between the energy level of trapped electrons and the motional relaxation of a polymer matrix. As shown in Figures 5–7a and 5–7b, two glow peaks were observed for the TMB doped in a PEMA film; the lower one at 130 K and higher one at 270 K.

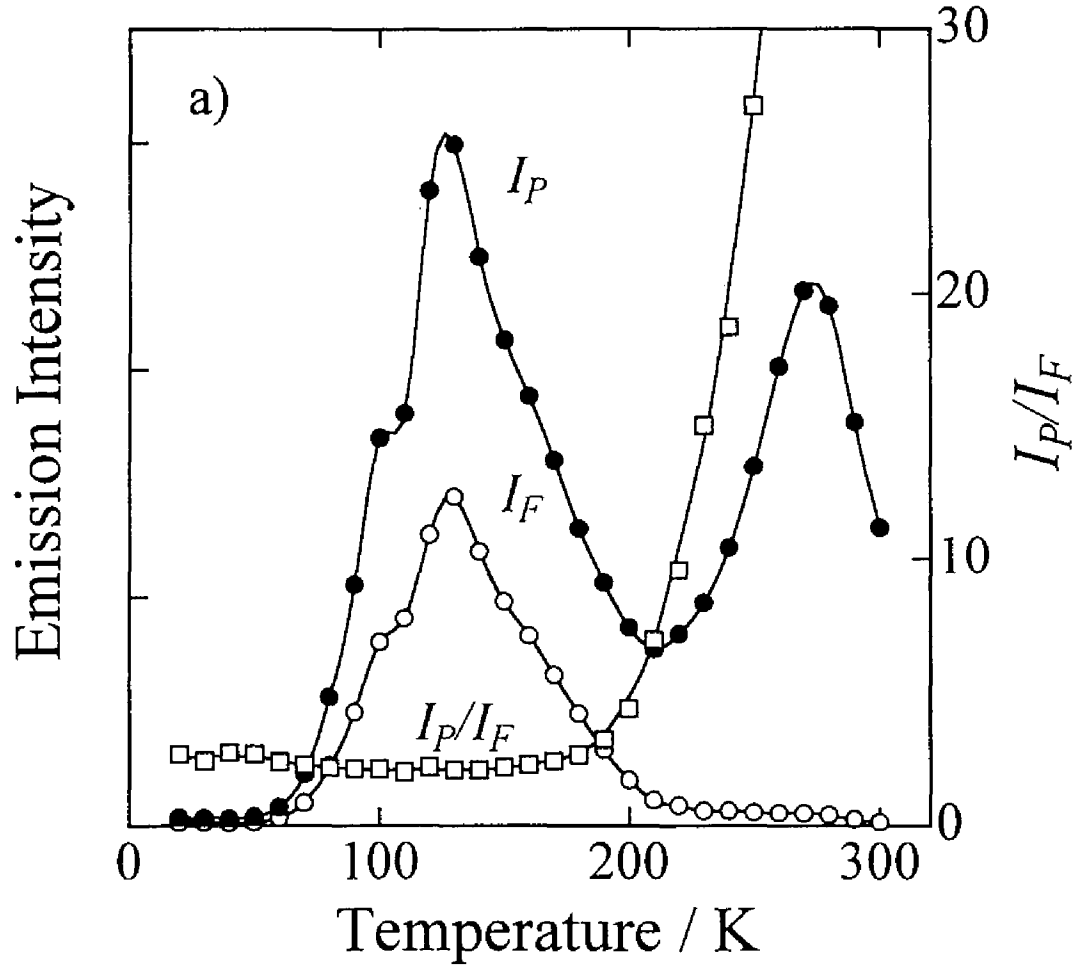

Figure 5–7a. Dependence of the fluorescence intensity I_F (open circles), the phosphorescence intensity I_P (closed circles), and the intensity ratio I_P/I_F (open squares) on temperature for the TL of the TMB chromophore doped in a photoirradiated PEMA film. Heating rate was 5 K/min.

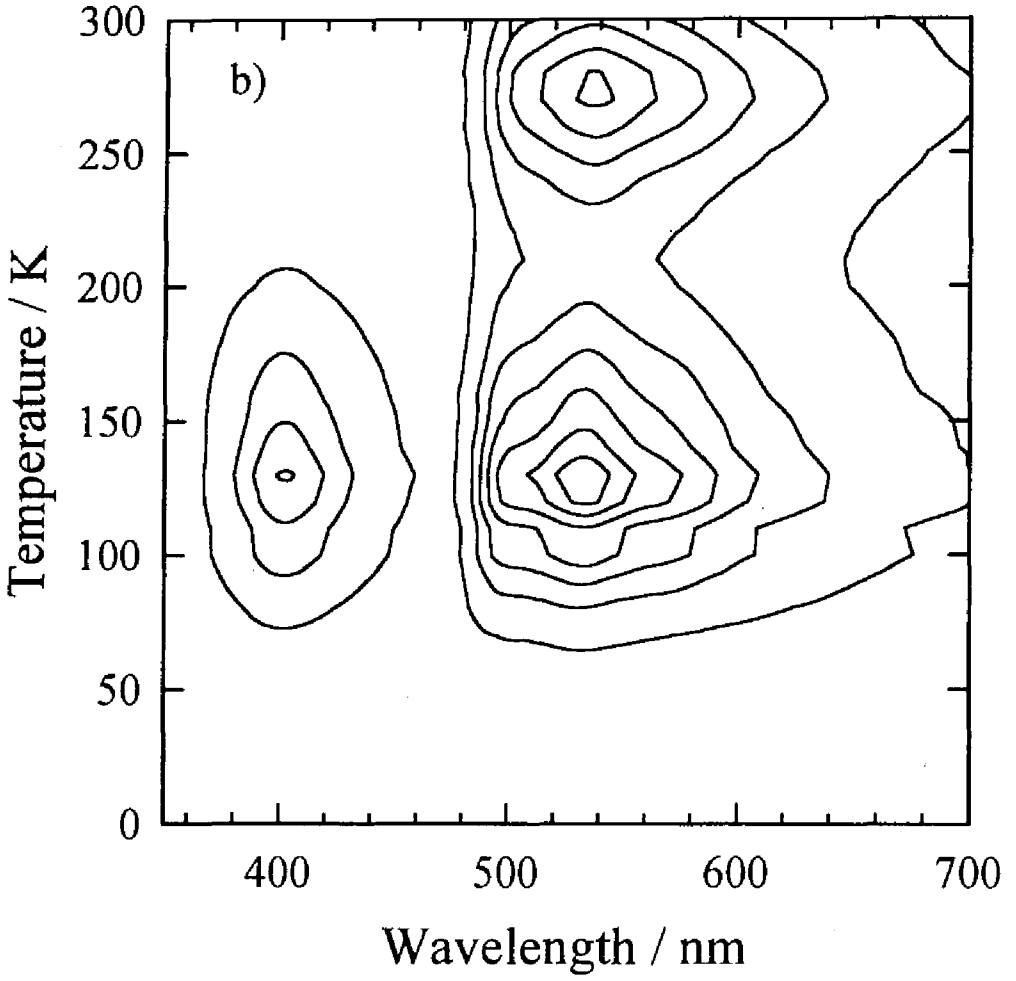

Figure 5–7b. A TL contour map for the PEMA film doped with a TMB chromophore photoirradiated at 20 K. Heating rate was 5 K/min.

The relaxation processes observed for a PEMA solid with increasing temperature are the rotation of ethyl group (δ-relaxation), the rotation of α-methyl group (γ-relaxation), the motion of the side-chain units including the carbonyl group (β-relaxation), and the micro-Brownian motion of the main chain (α-relaxation). The δ-peak of PEMA has been reported to be observed at 34 K (1.4 Hz),[40] 41 K (9.0 HZ),[41] 55 K (3 kHz),[42] 52 K (9.8 kHz),[43] 60 K (34 kHz),[44] and 75 K (3 MHz).[44] These results show that the peak position is strongly dependent upon the measuring frequency and the peaks at lower frequencies appear at lower temperatures. In the present system, the δ-peak of PEMA is expected to be observed below 30 K because of the low frequency in the TL measurement. However, the glow peak corresponding to the δ-peak was failed to be detected . This is probably because a photoirradiation temperature of 20 K was so close to the temperature region of the δ-peak of PEMA; most of the photoejected electrons captured in trap sites with the depth corresponding to the δ-relaxation disappear owing to the charge recombination even at a fixed temperature before the heating procedure. Thus, the glow peak observed at 130 K cannot be assigned to the δ-relaxation. Furthermore, it is too low in temperature to be ascribed to the β-relaxation, that is, the whole motion of side-chain units including the carbonyl group. Therefore, the glow peak at 130 K is ascribed to the γ-relaxation, that is, the rotation of α-methyl group. Furthermore, the result for TMB/PnBMA shown in Figure 5–6a was carefully re-examined and then it was noticed that glow peaks appear around 120 – 140 K. The glow peaks are also ascribable to the γ-relaxation as in TMB/PEMA, although a peak temperature of 130 K observed in this system is much lower than a γ-peak temperature of 220 K in both PMMA and PEMA by ultrasonic measurements at 10 MHz.[45]

The glow peak at 270 K is probably an apparent one owing to the decrease in the I_P at higher temperatures as in TMB/PnBMA. If it were not for the decrease in the I_P, the glow peak at 270 K would appear above 300 K; in the case of a photoirradiated PEMA film doped with a perylene chromophore, an upswing of the glow curve was observed extending over 300 K.[34] Possible assignment of the apparent glow peak at 270 K is the side-chain relaxation and/or the local mode relaxation of the main chain.

Historically, the β-relaxation for poly(alkyl methacrylate)s has been ascribed to the rotation of the side chain including the carbonyl group. According to the mechanical experiment, the loss modulus peak of β-relaxation at 1 Hz is observed around 280 K for

several poly(*n*-alkyl methacrylate)s: PMMA, PEMA, PnPMA, and PnBMA.[46] On the other hand, the dielectric loss peak at 1 kHz attributed to β-relaxation appears also at almost the same temperature for copolymers of methyl methacrylate with *n*-butyl methacrylate and *i*-butyl methacrylate.[47] Hence, the rotation of a side chain, β-relaxation, is believed to be governed mainly by the intrachain potential, not by the interchain interaction which affects the micro-Brownian motion of main chains. However, the effect of local mode motions of the main chain on the β-relaxation remains unknown.[35,48] Recently, Spiess and his co-workers investigated the β-relaxation in PMMA[49] and PEMA[50] by multidimensional NMR. They elucidated that 180° flips of the side chain are accompanied by main chain rotational readjustments with an amplitude of *ca.* ±20° around the local chain axis. Furthermore, Johari and Goldstein insisted that the β-relaxation in glassy state can arise solely from intermolecular processes; such molecular relaxations can be a universal feature of the glassy state.[51–54] Of course, they did not deny the explanations offered hitherto for the β-relaxation in polymers in terms of the rotation of side chain including the carbonyl group, but they also suggested that other molecular motions, *e.g.*, main-chain motions, take part to some extent in the β-relaxation and that a particular molecular motion, governed by an internal potential when the molecule is isolated, is opposed in the glassy state by a barrier that is primarily intermolecular in origin.

In Chapter 2 where perylene was used as a dopant chromophore,[34] a glow peak at a higher temperature appeared at 250 K for PnBMA while a rise of glow was observed up to 300 K for PEMA; the glow peak temperature increased with the decrease of side-chain length. This indicates that the glow at higher temperatures might be mainly dominated by local interchain interactions. It might be inappropriate to ascribe the glow only to the rotation of the side chain. Local mode relaxation is generally observed for linear polymers without long side chains and its motion is mainly governed by a local intrachain potential.[37] Thus, it might be also unreasonable to ascribe the glow peaks to the local mode relaxation governed by the local intrachain potential. It should be rather concluded that the glow at a higher temperature is ascribed to the small scale motion of the main chain governed by the interchain potential, as Johari and Goldstein pointed out.

Figures 5–7a and 5–7b show that in the TL spectra of PEMA above 200 K only phosphorescence was observed while fluorescence diminished. This tendency is consistent with the result for PnBMA; the onset of the increase in the intensity ratio I_P/I_F was observed

around 190 K, while in the case of PnBMA it was observed around 130 K. This increase in the intensity ratio I_P/I_F also suggests the deepening of trap depth caused by chemical reactions with increasing temperature just as in PnBMA. More noteworthy is that the temperature at which the intensity ratio I_P/I_F starts to increase is in correspondence with that of the upswing of the largest glow at higher temperatures in both PnBMA and PEMA. This finding indicates that the change in trap depth is closely related to the small scale motion of the main chain. Thus, the increase in the intensity ratio I_P/I_F results from chemical reactions, *e.g.*, elimination of ester alkyl group and main-chain scission induced by the photoirradiation and is related to the motional relaxation of polymer matrices.

5.3.2.3. TMB/PSt

Here, polystyrene was used as a matrix polymer. Although polystyrene is classified as a crosslinking-type,[25,26] it is more resistant to the radiation than poly(alkyl methacrylate)s. Figure 5–8a shows the spectral glow curves for the TMB doped in a PSt film; a small glow peak appeared at 120 K and an upswing of the glow curve up to 300 K. The former peak at 120 K is ascribed to the rotation of phenyl group and the latter rise observed up to 300 K to the local mode relaxation of the main chain. The γ-peak of PSt has been found by Schmieder and Wolf at 133 K (11.3 Hz)[55] and by Illers and Jenckel at 132 K (1 Hz).[56] On the other hand, the β-peak has been reported to be observed at 320 K by the dynamic mechanical measurements at 0.3 Hz.[57] Yano and Wada showed the relaxation map of PSt which consists of the results for mechanical and dielectric loss peaks, NMR narrowing, and the spin-lattice relaxation time.[58] They ascribed the β-peak at 350 K (10 kHz) to the local oscillation mode of main chains and the γ-peak at 180 K (10 kHz) to the rotation of phenyl groups. It can be seen that the glow curve observed for PSt in this system corresponds to their assignments considering the difference in measurement frequency.

As shown in Figures 5–8a and 5–8b, temperature dependence of the I_F was the same as that of the I_P; the intensity ratio I_P/I_F was constant over the whole temperature range measured from 20 to 300 K. Therefore, it can be seen that the energy level of trapped electrons in the PSt matrix does not change with the increase in temperature, in contrast to the poly(alkyl methacrylate)s.

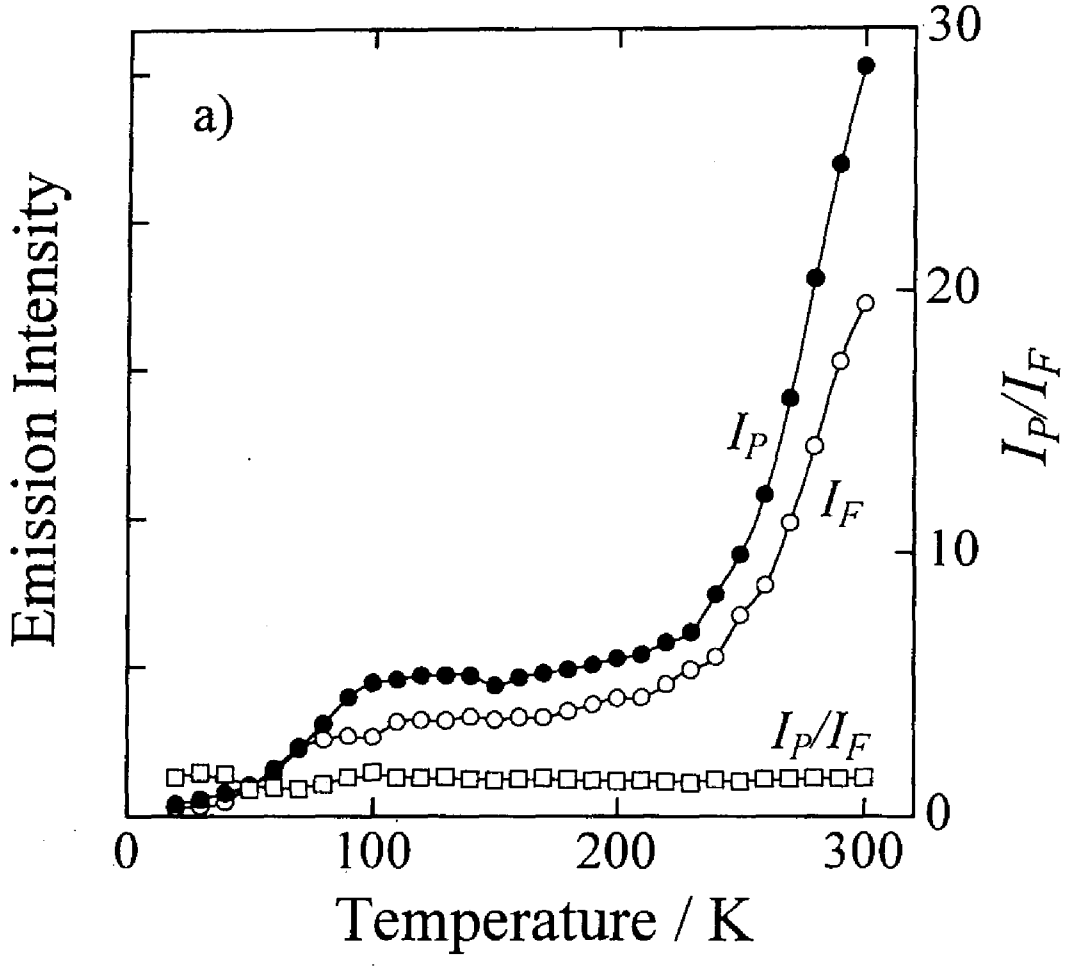

Figure 5–8a. Dependence of the fluorescence intensity I_F (open circles), the phosphorescence intensity I_P (closed circles), and the intensity ratio I_P/I_F (open squares) on temperature for the TL of the TMB chromophore doped in a photoirradiated PSt film. Heating rate was 5 K/min.

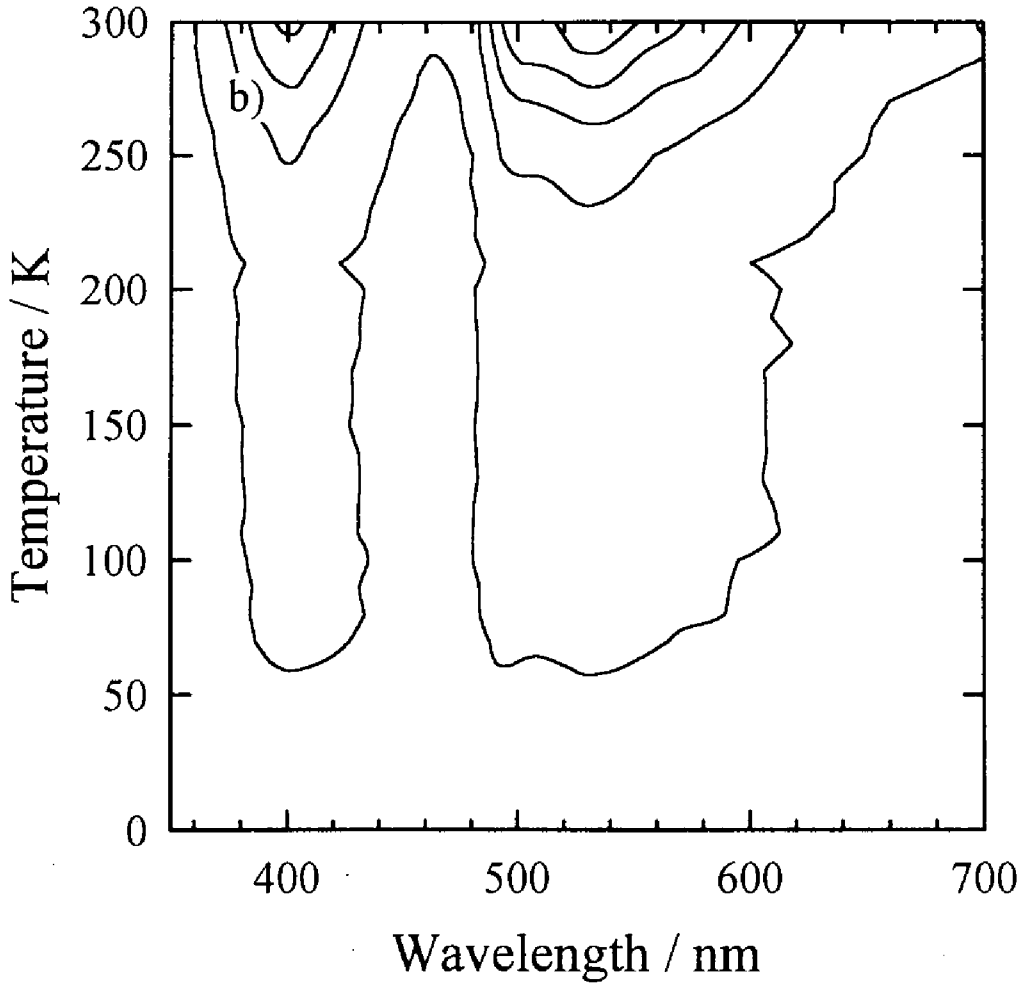

Figure 5–8b. A TL contour map for the PSt film doped with a TMB chromophore photoirradiated at 20 K. Heating rate was 5 K/min.

5.3.3. *Reaction Scheme for Charge Recombination of Photoejected Electron with Parent TMB Radical Cation in Polymer Solids.*

Since the I_P in the ITL was enhanced in comparison with that in the steady-state emission for all the polymers used in the present work and the intensity ratio I_P/I_F was almost constant over the whole time range measured from 10 min to 10 h, it is concluded that the observed ITL is due to the charge recombination from a shallow trap.

The TL showed differences between poly(alkyl methacrylate)s and polystyrene; the intensity ratio I_P/I_F increased with temperature for poly(alkyl methacrylate)s, but was constant for polystyrene at temperatures from 20 to 300 K. The increase in the intensity ratio I_P/I_F shows that the energy level of the excited singlet state of a dopant chromophore is higher than that of some trapped electrons participating in the charge recombination, that is, the energy of the trapped electrons is insufficient to reproduce the excited singlet state by the charge recombination, and consequently the fluorescence intensity I_F decreases.

The energy level of trapped electrons in PnBMA is roughly estimated as follows. The energy of electron-cation pairs formed in a condensed phase, E is expressed by

$$E = IP_g + P_+ + V_0. \qquad (5\text{–}1)$$

The gas phase ionization potential IP_g of TMB is reported to be *ca.* 6.5 eV.[59] The polarization energy P_+ can be evaluated using the Born equation:[60]

$$P_+ = -\frac{e^2}{8\pi\varepsilon_0 r_+}\left(1-\frac{1}{\varepsilon_S}\right), \qquad (5\text{–}2)$$

where e is the elementary charge, ε_0 the vacuum permittivity, r_+ the radius of cationic species, and ε_S the relative dielectric constant of the medium. The radius r_+ was roughly estimated[61] to be 3.88 Å from the van der Waals volume[62] of TMB. The dielectric constant ε_S of PnBMA has been reported to be 2.8 at 200 K (30 Hz)[63] where the TL glow consisted of only phosphorescence and fluorescence was almost diminished. Thus, the polarization energy was calculated using eq 5–2: $P_+ = -1.2$ eV. By inserting these values into eq 5–1, we obtain the energy of electron-cation pairs as a function of the electron trap depth V_0: $E = 5.3 - V_0$ (eV). On the other hand, the energy level of the excited singlet state of TMB chromophore was estimated to be *ca.* 3.5 eV from the absorption and emission spectrum of TMB. Consequently, the trap depth can be estimated to be more than 1.8 eV in PnBMA above 200 K where the fluorescence component in TL diminished and only phosphorescence was observed.

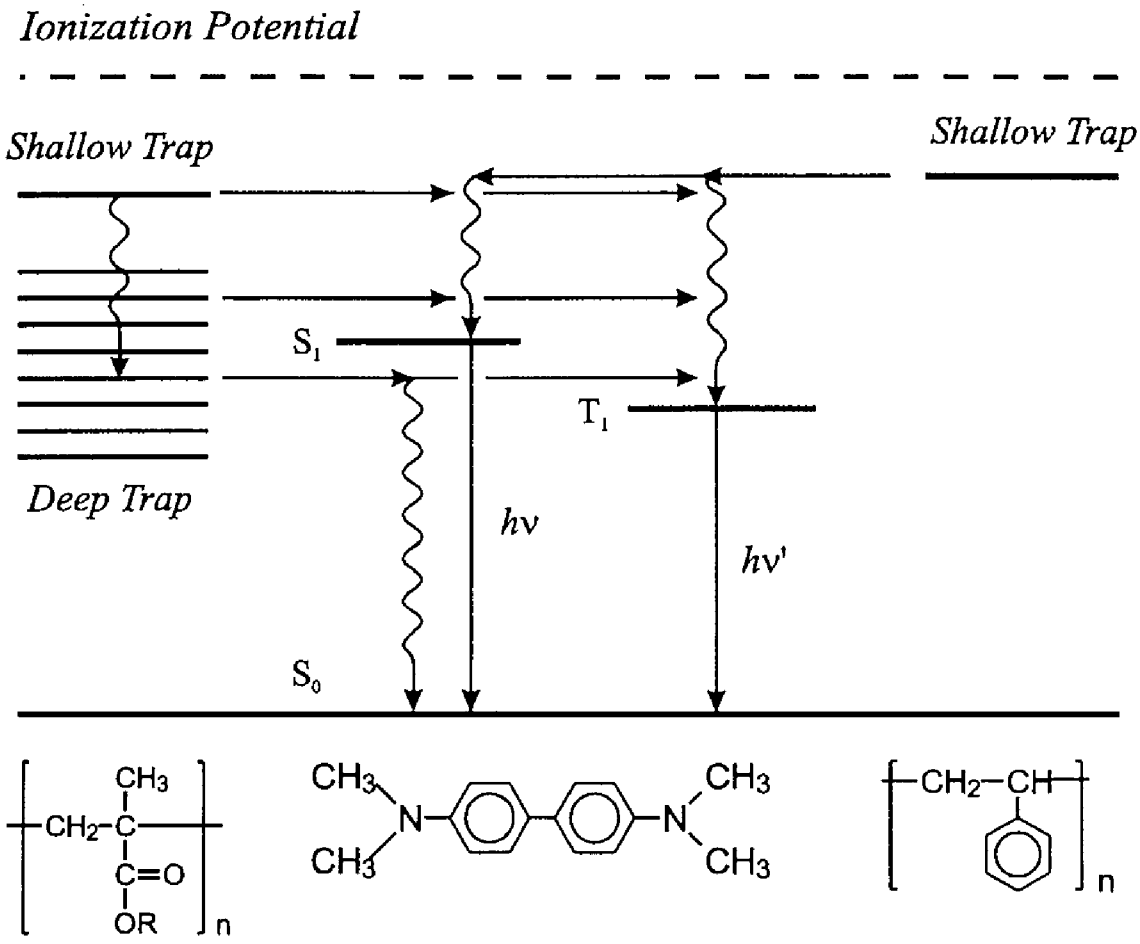

Figure 5–9. Reaction scheme for the charge recombination of a trapped electron with the parent cation in a polymer solid. As shown in the right hand, the charge recombination in a polystyrene solid occurs from a shallow trap to the parent cation both in ITL at 20 K and TL at temperatures from 20 to 300 K. On the other hand, the left hand in the figure shows the scheme for the charge recombination in poly(alkyl methacrylate)s; in the case of ITL at 20 K and the TL at low temperatures, the charge recombination mainly from a shallow electron trap results in the excited singlet state and triplet state of the parent-cation chromophore, whereas the TL at higher temperatures results from the charge recombination from a deeper trap leading to only the excited triplet state of the parent-cation chromophore.

As described above, the change in the intensity ratio I_P/I_F was observed for poly(alkyl methacrylate)s while no change was observed for polystyrene. This difference shows that the stabilization of trapped electrons results from a photoinduced chemical reaction in polymer solids because poly(alkyl methacrylate)s are classified as the scission type polymer to radiation whereas polystyrene is highly resistant to the radiation.[25,26] Furthermore, the increase in the intensity ratio I_P/I_F was closely related to the small scale motion of the main chain governed by the interchain potential. These findings indicate that the stabilization of trapped electrons requires such certain scale motions as local motions of the main chain. There have been various reports on the mechanism of the main-chain scission investigated in detail by ESR measurement in radiation chemistry.[38,39] Sakai *et al.* reported that two-photon ionization of the dopant chromophore also leads to the main-chain scission of poly(methyl methacrylate) (PMMA) which is initiated through the formation of ester radical anion.[64,65] They observed an ester radical anion of PMMA just after the photoirradiation at 77 K and it changed into a methyl radical even at 77 K; this is an elimination of ester alkyl group. However, the spectral glow curves in the previous section show that the intensity ratio I_P/I_F is almost constant even at temperatures where the rotation of ester alkyl group in the side chain of the polymer is released, and increases at temperatures where local motions of the main chain governed by interchain potential is released. These findings suggest that the increase in the intensity ratio I_P/I_F results from the stabilization of trapped electrons through the main-chain scission rather than the elimination of ester alkyl group. It is therefore concluded that the photoejected electron is mainly trapped in a shallow trap at 20 K where the motions in polymer matrix are almost frozen and that trapped electrons in poly(alkyl methacrylate) films change into more stable anion species through chemical reactions, *e.g.*, main-chain scission, at higher temperatures where the small scale motion of the main chain is released.

5.4. Conclusion

The spectral change in ITL or TL caused by the charge recombination of a trapped electron with the parent cation was studied. The energy level decreased with increasing temperature for poly(alkyl methacrylate)s, which are classified as the scission type to radiation, and that the change in the energy level is induced by the small scale motion of the main chain. In poly(alkyl methacrylate) films, photoejected electrons are mainly captured in a shallow trap site at a low temperature where most of the polymer motions are frozen and change into more stable anion species through chemical reactions with increasing temperature. Furthermore, the depth of the deeper trap was estimated to be more than 1.8 eV at 200 K where the phosphorescence component but not the fluorescence component was observed in the TL of a photoirradiated PnBMA film.

References and Notes

1) W. D. Gill, in *"Photoconductivity and Related Phenomena"*, eds. J. Mort and D. M. Pai, Elsevier, Amsterdam (1976).

2) K. C. Kao and W. Hwang, *"Electrical Transport in Solids"*, Pergamon, New York (1981).

3) W. E. Moerner and S. M. Silence, *Chem. Rev.*, **94**, 127 (1994).

4) R. Chen and Y. Kirsh, in *"Analysis of Thermally Stimulated Processes"*, ed. B. Pamplin, Pergamon Press, Oxford (1981).

5) P. Debye and J. O. Edwards, *J. Chem. Phys.*, **20**, 236 (1952).

6) Kh. S. Bagdasar'yan, R. I. Milyutinskaya, and Yu. V. Kovalev, *Khim. Vysok. Energii*, **1**, 127 (1967).

7) F. Kieffer, C. Meyer, and J. Rigaut, *Chem. Phys. Lett.*, **11**, 359 (1971).

8) F. Kieffer, C. Meyer, and J. Rigaut, *Int. J. Radiat. Phys. Chem.*, **6**, 79 (1974).

9) Y. Hama, Y. Kimura, M. Tsumura, and N. Omi, *Chem. Phys.*, **53**, 115 (1980).

10) Y. Hama and K. Gouda, *Radiat. Phys. Chem.*, **21**, 185 (1983).

11) A. I. Mikhailov, *Dokl. Akad. Nauk SSSR*, **197**, 136 (1970).

12) M. Tachiya and A. Mozumder, *Chem. Phys. Lett.*, **28**, 87 (1974).

13) F. S. Dainton, M. J. Pilling, and S. A. Rice, *J. Chem. Soc., Faraday Trans. 2*, **71**, 1311 (1975).

14) M. Tachiya and A. Mozumder, *Chem. Phys. Lett.*, **34**, 77 (1975).

15) J. T. Randall and M. H. F. Wilkins, *Proc. R. Soc. London, Ser. A*, **184**, 347 (1945).

16) V. G. Nikolskii and N. Ya. Buben, *Dokl. Akad. Nauk SSSR*, **134**, 134 (1960).

17) A. Charlesby and R. H. Partridge, *Proc. R. Soc. London, Ser. A*, **271**, 170 (1963).

18) A. Charlesby and R. H. Partridge, *Proc. R. Soc. London, Ser. A*, **283**, 312 (1963).

19) A. Tsuchida, M. Nakano, M. Yoshida, M. Yamamoto, and Y. Wada, *Polym. Bull.*, **20**, 297 (1988).

20) M. Yamamoto, A. Tsuchida, and M. Nakano, *MRS Int. Meeting Avd. Mater.*, **12**, 243 (1989).

21) A. Tsuchida, W. Sakai, M. Nakano, M. Yoshida, and M. Yamamoto, *Chem. Phys. Lett.*, **188**, 254 (1992).

22) A. Tsuchida, W. Sakai, M. Nakano, and M. Yamamoto, *J. Phys. Chem.*, **96**, 8855 (1992).

23) As a review, R. J. Fleming, *Radiat. Phys. Chem.*, **36**, 59 (1990).

24) In this chapter, the term "trapped electron" is used not in the general sense that an electron is bound weakly in a small cavity of the matrix before it is solvated but in a wide sense that electrons are captured in the matrix; this includes trapped electrons, solvated electrons, radical anions, and other anionic species.

25) K. Shinohara and H. Kashiwabara, *"Houshasen To Koubunshi"*, Makishoten, Tokyo (1968).

26) W. Schnabel, *"Polymer Degradation —Principles and Practical Applications—"*, Carl Hanser Verlag, Munich (1982).

27) P. Peyser, in *"Polymer Handbook"*, 3rd ed., eds. J. Brandrup and E. H. Immergut, John Wiley & Son, New York (1989).

28) B. Brocklehurst, *Nature*, **221**, 921 (1969).

29) T. Higashimura and K. Hirayama, *Ann. Rep. Res. Reactor Inst. Kyoto Univ.*, **5**, 11 (1972).

30) Strictly speaking, the slope of the log-log plots was less than unity. This deviation results from multi-shot photoirradiation; see Chapter 3.

31) The ITL decay can be simulated by the electron tunneling model with the assumption of only one kind of trap depth with no energetic distribution. Then, even if there are deeper trap sites, trap depth is so deep that the trapped electrons cannot be transferred to the parent cations. In other words, photoejected electrons captured in deeper trap sites cannot recombine with the parent cations at a temperature as low as 20 K.

32) J. Heijboer and M. Pineri, in *"Nonmetallic Materials and Composites at Low Temperatures 2"*, eds. G. Hartwig and D. Evans, Plenum Press, New York (1982).

33) K. Shimizu, O. Yano, and Y. Wada, *J. Polym. Sci., Polym. Phys. Ed.*, **13**, 1959 (1975).

34) M. Yamamoto, H. Ohkita, W. Sakai, and A. Tsuchida, *Synth. Metals*, **81**, 301 (1996).

35) N. Saito, K. Okano, S. Iwayanagi, and T. Hideshima, in *"Solid State Physics Vol. 14, Advances in Research and Applications"*, eds. F. Seitz and D. Turnbull, Academic Press, New York (1963).

36) K. Okano, *Rikagaku Kenkyu-sho Houkoku*, **40**, 273 (1964).

37) Y. Wada, *"Koubunshi No Kotai Bussei"*, Baihukan, Tokyo (1971).

38) M. Tanaka, H. Yoshida, and T. Ichikawa, *Polym. J.*, **22**, 835 (1990).

39) H. Yoshida and T. Ichikawa, in *"Recent Trends in Radiation Polymer Chemistry"*, Advances in Polymer Science, Vol. 105, ed. S. Okamura, Springer-Verlag, Berlin (1993), p. 3.

40) V. Frosini and A. E. Woodward, *J. Polym. Sci., Part A-2*, 7, 525 (1969).

41) K. M. Sinnott, *J. Polym. Sci.*, **35**, 273 (1959).

42) H. Sclein and M. C. Shen, *Rev. Sci. Instr.*, **40**, 587 (1969).

43) J. M. Crissman, J. A. Sauer, and A. E. Woodward, *J. Polym. Sci., Part A*, **2**, 5075 (1964).

44) K. Shimizu, O. Yano, Y. Wada, and Y. Kawamura, *J. Polym. Sci., Polym. Phys. Ed.*, **11**, 1641 (1973).

45) Y. Tanabe, J. Hirose, K. Okano, and Y. Wada, *Polym. J.*, **1**, 107 (1970).

46) J. Heijboer, in *"Physics of Non-Crystalline Solids"*, ed. J. A. Prins, North-Holland, Amsterdam (1965), p. 231.

47) Y. Kawamura, S. Nagai, J. Hirose, and Y. Wada, *J. Polym. Sci., Part A-2*, 7, 1559 (1969).

48) J. Kolarík, in *"Behavior of Macromolecules"*, Advances in Polymer Science, Vol. 46, ed. K. Dušek, Springer-Verlag, Berlin (1982), p. 119.

49) K. Schmidt-Rohr, A. S. Kulik, H. W. Beckham, A. Ohlemacher, U. Pawelzik, C. Boeffel, and H. W. Spiess, *Macromolecules*, **27**, 4733 (1994).

50) A. S. Kulik, H. W. Beckham, K. Schmidt-Rohr, D. Radloff, U. Pawelzik, C. Boeffel, and H. W. Spiess, *Macromolecules*, **27**, 4746 (1994).

51) M. Goldstein, *J. Chem. Phys.*, **51**, 3728 (1969).

52) G. P. Johari and M. Goldstein, *J. Phys. Chem.*, **74**, 2034 (1970).

53) G. P. Johari and M. Goldstein, *J. Chem. Phys.*, **53**, 2372 (1970).

54) G. P. Johari and M. Goldstein, *J. Chem. Phys.*, **55**, 4245 (1971).

55) K. Schmieder and K. Wolf, *Kolloid-Z.*, **134**, 149 (1953).

56) K. H. Illers and E. Jenckel, *J. Polym. Sci.*, **41**, 528 (1959).

57) K. H. Illers, *Z. Elektrochem.*, **65**, 679 (1961).

58) O. Yano and Y. Wada, *J. Polym. Sci., Part A-2*, **9**, 669 (1971).

59) A. Fulton and L. E. Lyons, *Aust. J. Chem.*, **21**, 873 (1968).

60) M. Born, *Z. Phys.*, **1**, 45 (1920).

61) R. Katoh, K. Lacmann, and W. F. Schmidt, *Z. Phys. Chem.*, **190**, 193 (1995).

62) J. T. Edward, *J. Chem. Educ.*, **47**, 261 (1970).

63) Y. Kawamura, S. Nagai, J. Hirose, and Y. Wada, *J. Polym. Sci., Part A-2*, 7, 1559 (1969).

64) W. Sakai, A. Tsuchida, M. Yamamoto, T. Matsuyama, H. Yamaoka, and J. Yamauchi, *Macromol. Rapid Commun.*, **15**, 551 (1994).

65) W. Sakai, A. Tsuchida, M. Yamamoto, and J. Yamauchi, *J. Polym. Sci., Polym. Chem. Ed.*, **33**, 1969 (1995).

Part II

Chapter 6

Direct Observation of Carbazole Hole Trap in Polymer Solid Films by Charge-Resonance Band

6.1. Introduction

Carbazole (Cz) is a historically important chromophore whose spectroscopic and photoconductive properties have been studied in detail.[1-3] The mechanism of the Cz carrier generation and transport is still of interest, and many reports have been published on the photoconductivity of Cz-containing polymers.[4,5] Recently, a few authors studied the hole transport in poly(*N*-vinylcarbazole) (PVCz) film by transient absorption spectroscopy. Miyasaka *et al.* showed that the time constant of the Cz hole migration is *ca.* 2 ns by picosecond transient absorption spectroscopy and dichroism measurements.[6] Masuhara *et al.* elucidated that the decay kinetics of the transient ionic species obeys a $t^{-1/2}$ dependence over the time range from microsecond to millisecond by transient absorption spectroscopy.[7,8]

Although the detailed mechanism of the Cz hole transport is not fully understood, it has been generally assumed that the presence of a structural hole trap is responsible for the decrease in the hole drift mobility. This structural trap is believed to have an excimer-like conformation of the Cz chromophores. Several reports have been published thus far to elucidate the relationship between the hole drift mobility and the structural hole trap. For example, Yokoyama *et al.* measured the hole drift mobilities of dimer model compounds for PVCz dispersed in polycarbonate.[9] They suggested that a "full-overlap" excimer-forming site acts as a hole trap. Most of these discussions were based on information on the excimer-forming site obtained by the excimer emission measurements; the excimer site is, however, an energy trap but not a hole trap. No attempts have ever been made for a direct measurement of the Cz hole trap in a polymer solid film by absorption.

Yamamoto *et al.* have studied the hole resonance and stabilization of PVCz in solution by the measurement of the charge-resonance (CR) absorption band.[10-12] This CR band is caused by a hole resonance among two or more Cz chromophores. Therefore, the Cz hole trap having an excimer-like conformation can be directly observed by the measurement of the CR band and the degree of hole resonance and stabilization can be determined from its peak position.[13-16] In this chapter, the Cz hole trap in polymer solid films was observed directly by the measurement of the CR band.

6.2. Experimental Section

6.2.1. Chemicals

Poly(*N*-vinylcarbazole) (PVCz, Tokyo Kasei Kogyo, Co., Ltd., $M_w > 1 \times 10^5$) and poly(methyl methacrylate) (PMMA, Wako Pure Chem. Ind., Ltd., $M_w = 1.2 \times 10^5$) were purified by precipitation from a benzene solution into methanol three times. *N*-Ethylcarbazole (EtCz) was synthesized by the reaction of sodium carbazole with ethyl bromide and purified by recrystallization. Copolymers of *N*-vinylcarbazole (VCz, Nacalai Tesque, Inc.) with methyl methacrylate (MMA, Wako) were prepared by a radical copolymerization initiated by AIBN in degassed benzene at 333 K. Copolymers (abbreviated as VCz(x)/MMA, where x is the mol% of VCz) were purified by precipitation and the mol% of VCz was determined by UV absorption and/or NMR spectra. The copolymerization of VCz (1) with MMA (2) indicates a tendency towards alternation of Cz chromophore, where the monomer reactivity ratios are $r_1 = 0.06$ and $r_2 = 1.80$.[17]

Spectroscopic grade of 1,2-dichloroethane (DCE, Nacalai) was used for the film cast without further purification.

6.2.2. Measurements

Sample films (*ca.* 60 μm thickness) of PVCz and VCz(x)/MMA were prepared by the solution cast method on a quartz plate. The remaining DCE solvent was removed by evacuation for more than 12 hours.

Sample polymer films were sandwiched by another quartz plate and were immersed

in liquid nitrogen on the sample holder of a quartz Dewar cell. The carbazole chromophore in sample films was selectively photoionized by intense 351-nm laser light pulses (*ca.* 60 mJ pulse energy, fwhm *ca.* 20 ns) from an excimer laser (Lambda Physik EMG101MSC, XeF gas), where the MMA unit has no absorption at this wavelength.[18,19] A few minutes after the photoirradiation, the absorption spectra of the Cz radical cation formed in the films were recorded with a Hitachi U-3400 spectrophotometer from 300 to 2500 nm in the Dewar cell at 77 K. Absorption of the ground-state Cz chromophore and the quartz plate in the near-IR region was corrected by subtracting the absorption spectra before photoirradiation. The control experiment where a PMMA film with no low molecular-weight dopant was photoirradiated in the same manner gave no appreciable new absorption.

6.3. Results and Discussion

As already reported, it is possible to produce a stable radical cation in a polymer solid by two-photon laser excitation.[18-20] Through the two-photon ionization of the copolymer of VCz with MMA, which acts as a shallow trap for an ejected electron as well as the diluent of the Cz chromophore, the visible and near-IR absorption of the Cz radical cation in the copolymer films at 77 K was obtained.

Figure 6–1 (top) shows the absorption spectrum of the VCz(1.5)/MMA film measured after the laser photoexcitation at 77 K. The visible absorption bands around 400 – 800 nm were ascribed to the monomeric radical cation of Cz produced through the two-photon ionization.[14] The Cz radical cation thus formed at a low temperature was stable enough to be observed without a large decay after several hours from the laser excitation. In the near-IR region, the VCz(1.5)/MMA gave no appreciable absorption band as shown in the figure; that is, this absorption spectrum is almost identical with that of EtCz doped in PMMA. This indicates that most Cz chromophores are isolated due to the low chromophore concentration.

Figure 6–1 (middle) shows the absorption spectrum of the Cz radical cation formed in the VCz(25)/MMA film by the laser photoexcitation at 77 K. In this figure, the absorption band around 1500 – 2200 nm is ascribed to the CR band caused by the charge

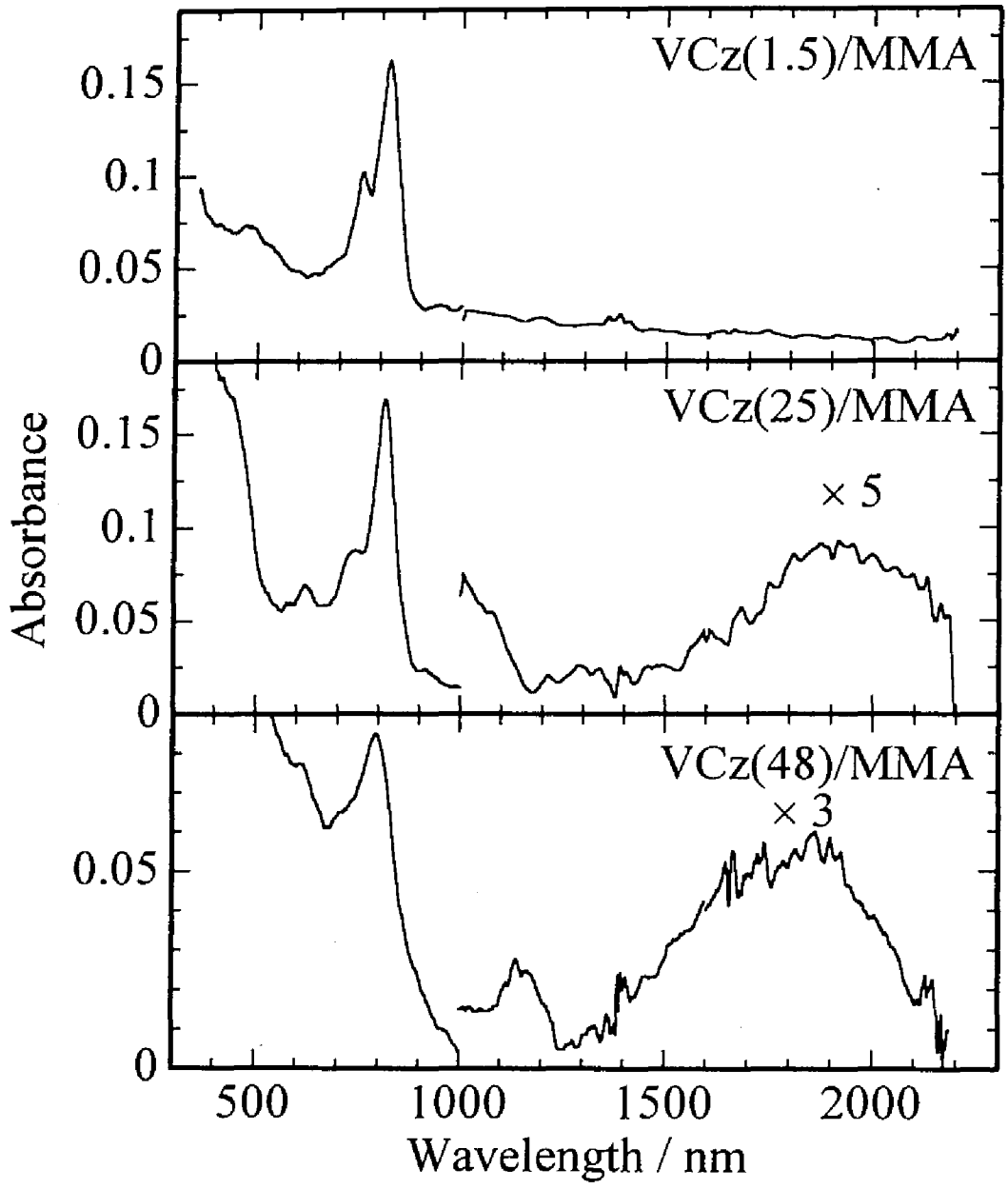

Figure 6–1. Absorption spectra of Cz radical cation produced by the two-photon laser excitation in the VCz(1.5)/MMA (top), the VCz(25)/MMA (middle), and the VCz(48)/MMA (bottom) copolymer films at 77 K. Discontinuities at *ca.* 1400, 1700, and 2100 nm were due to the correction of the quartz absorbance.

resonance between two Cz chromophores in a dimer radical cation. This CR band reflects the degree of the interaction among neighboring chromophores. For example, the energy diagram for a dimer radical cation can be schematized as shown in Figure 6–2. The orbital interaction between a neutral chromophore and a radical cation makes the orbitals split into two energy levels. The CR band is based on the transition between these split orbitals. The larger interaction makes the orbital split larger and the dimer radical cation more stable; the blue-shift of the band indicates the greater stabilization of the dimer radical cation.[13–16] Thus, the stabilization energy of a dimer radical cation can be estimated from the CR-band peak position; it is in correspondence with half of the energy between the two split orbitals. It is noteworthy that the CR-band peak of this VCz(25)/MMA film appeared at *ca.* 1900 nm as shown in the figure. The stabilization energy of the Cz hole resonance is *ca.* 0.33 eV estimated from the CR-band peak. Although this value is slightly smaller than that of the activation energy of the hole drift mobility for PVCz (0.36 – 0.65 eV),[21] it seems reasonable to conclude that the Cz hole trap site results from the Cz hole resonance.

Figure 6–1 (bottom) shows the absorption spectrum of the VCz(48)/MMA film, which is similar to that of the VCz(25)/MMA. However, the lower spectrum is different from the upper spectrum. First, the vibronic structure of the absorption band in the visible region is less clear: the band is assigned to the local excitation (LE) in a dimer radical cation.[22,23] Second, the peak absorbance ratio of the CR band to the visible 800-nm band is 0.24 and 0.11 for the VCz(48)/MMA and the VCz(25)/MMA, respectively. Third, the absorbance in the shorter wavelength of the CR band around 1400 – 1800 nm has a larger fraction. The first and the second show that the fraction of the isolated monomeric Cz radical cation formed in the VCz(48)/MMA is less than that formed in the VCz(25)/MMA. In other words, both of them indicate that the stabilization caused by charge delocalization (charge resonance) is greater in the VCz(48)/MMA than in the VCz(25)/MMA. On the other hand, the third shows that the charge is not delocalized among more than two Cz chromophores because the charge delocalization among more than two Cz chromophores leads to the red-shift of the CR band with an increase in the Cz fraction. It is therefore concluded that the hole observed in the present measurement is mainly delocalized between two Cz chromophores in solid films.

It is worthwhile to compare the result for this solid system with that for a solution system. In a solution, the CR-band peak position of the copolymers containing Cz

chromophores is almost constant at lower Cz fractions, although the red-shift of the CR band is observed at higher Cz fractions.[11,12] This result for the solution system shows that charge resonance will occur mainly at a dyad sequence of Cz at the low Cz fractions where the probability that a VCz unit is found in the sequence of more than two is not so high. The same is true of the result for the solid system; a positive charge in a solid film is mainly delocalized between two Cz chromophores at the low Cz fractions. Furthermore, in solid films, the increase in Cz concentration at the low Cz fractions is considered to favor the greater stabilization of the dimer radical cations. The most likely explanation for this stabilization is that the higher Cz concentration will result in efficient hole migration to more stable hole sites and/or an increase in the fraction of more stable Cz hole sites.

Although the laser photoionization of a larger Cz fraction film of the VCz(58)/MMA gave a larger absorbance ratio of the CR band to the visible 800-nm band,

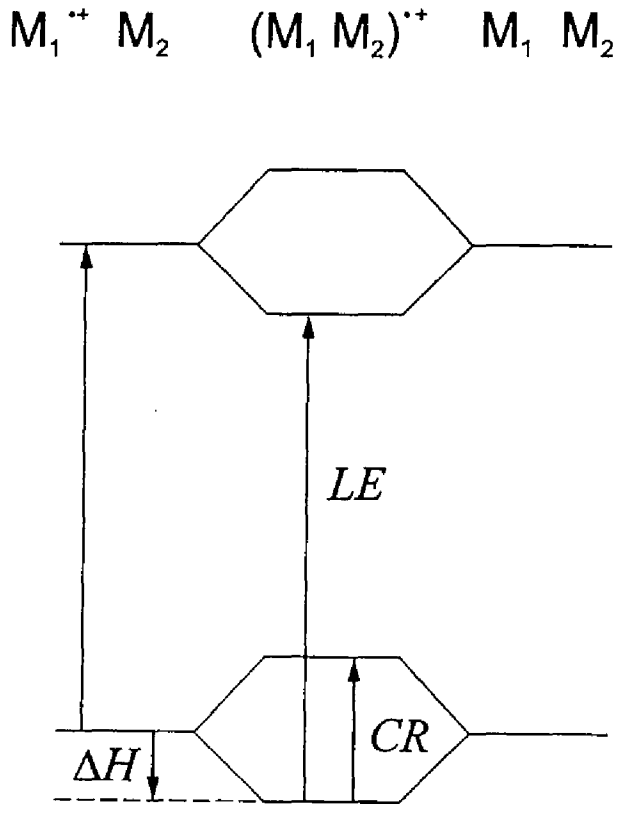

Figure 6–2. Schematic energy diagram of a dimer radical cation. M_1 and M_2 are the same kind of aromatic molecules. $M_1^{\bullet+}\ M_2$ represents an electronic configuration of the dimer; a positive charge is completely localized at the M_1 molecule. CR and LE represent the transition of the charge resonance and the local excitation in a dimer radical cation, respectively. ΔH denotes the enthalpy for the formation of a dimer radical cation.

the obtained absorbance was too weak to be quantitated. Then, no appreciable absorption was observed for the largest Cz fraction film, that is, a PVCz film photoirradiated at 77 K. This indicates that the photoionization quantum yield decreases at larger Cz fractions. The decrease in the photoionization quantum yield at larger Cz fractions is explained as follows. A higher Cz concentration corresponds to a shorter average mutual distance between Cz chromophores and a lower concentration of MMA unit which acts as a shallow electron trap. The former induces efficient hole migration as well as energy migration. The latter leads to the decrease in the ability of the polymer matrix to trap an electron. The fast energy migration causes efficient $S_1 - S_1$ annihilation,[24] which prevents stepwise two-photon ionization. The fast hole migration and the decrease in the ability of the polymer matrix to trap an electron cause efficient charge recombination between the Cz radical cation and an ejected electron. All these processes decrease the observed amount of ionized Cz chromophores at higher Cz concentrations. An accurate measurement of these small absorption spectra under various conditions is in progress to obtain more detailed information on the hole trap in a polymer solid film.

References

1) W. D. Gill, in *"Photoconductivity and Related Phenomena"*, eds. J. Mort and D. M. Pai, Elsevier, Amsterdam (1976), Chap. 8.
2) J. Mort and G. Pfister, in *"Electronic Properties of Polymers"*, eds. J. Mort and G. Pfister, Wiley Interscience, New York (1982), Chap. 6.
3) H. Masuhara and A. Itaya, in *"Dynamics and Mechanism of Photoinduced Electron Transfer and Its Related Phenomena"*, eds. N. Mataga, T. Okada, and H. Masuhara, Elsevier, Amsterdam (1992), p. 363.
4) H. Sakai, A. Itaya, and H. Masuhara, *J. Phys. Chem.*, **93**, 5351 (1989).
5) T. Sasakawa, T. Ikeda, and S. Tazuke, *Macromolecules*, **22**, 4253 (1989).
6) H. Miyasaka, T. Moriyama, S. Kotani, R. Muneyasu, and A. Itaya, *Chem. Phys. Lett.*, **225**, 315 (1994).
7) T. Ueda, R. Fujisawa, H. Fukumura, A. Itaya, and H. Masuhara, *J. Phys. Chem.*, **99**, 3629 (1995).
8) K. Watanabe, T. Asahi, and H. Masuhara, *Chem. Phys. Lett.*, **233**, 69 (1995).
9) M. Yokoyama, K. Akiyama, N. Yamamori, H. Mikawa, and S. Kusabayashi, *Polymer J.*, **17**, 545 (1985).
10) Y. Tsujii, A. Tsuchida, M. Yamamoto, and Y. Nishijima, *Macromolecules*, **21**, 665 (1988).
11) Y. Tsujii, A. Tsuchida, Y. Onogi, and M. Yamamoto, *Macromolecules*, **23**, 4019 (1990).
12) A. Tsuchida, A. Nagata, M. Yamamoto, H. Fukui, M. Sawamoto, and T. Higashimura, *Macromolecules*, **28**, 1285 (1995).
13) B. Badger, B. Brocklehurst, and R. D. Russel, *Chem. Phys. Lett.*, **1**, 122 (1967).
14) M. Yamamoto, Y. Tsujii, and A. Tsuchida, *Chem. Phys. Lett.*, **154**, 559 (1989).
15) Y. Tsujii, A. Tsuchida, M. Yamamoto, T. Momose, and T. Shida, *J. Phys. Chem.*, **95**, 8635 (1991).
16) T. Nagamura, A. Tanaka, H. Kawai, and H. Sakaguchi, *J. Chem. Soc., Chem. Commun.*, 559 (1993).
17) A. Ledwith, G. Galli, E. Chiellini, and R. Solaro, *Polym. Bull.*, **1**, 491 (1979).
18) A. Tsuchida, M. Nakano, M. Yoshida, M. Yamamoto, and Y. Wada, *Polym. Bull.*, **20**,

297 (1988).

19) A. Tsuchida, W. Sakai, M. Nakano, M. Yoshida, and M. Yamamoto, *Chem. Phys. Lett.*, **188**, 254 (1992).

20) A. Tsuchida, W. Sakai, M. Nakano, and M. Yamamoto, *J. Phys. Chem.*, **96**, 8855 (1992).

21) J. M. Pearson and M. Stolka, *"Poly(N-vinylcarbazole)"*, Gordon and Beach Science Publishers, New York (1981), p. 150.

22) H. Masuhara, N. Tamai, N. Mataga, F. C. De Schryver, and J. Vandendriessche, *J. Am. Chem. Soc.*, **105**, 7256 (1983).

23) H. Masuhara, K. Yamamoto, N. Tamai, K. Inoue, and N. Mataga, *J. Phys. Chem.*, **88**, 3971 (1984).

24) H. Fukumura, K. Hamano, and H. Masuhara, *J. Phys. Chem.*, **97**, 12110 (1993).

Chapter 7

Localization of Photoejected Electrons Produced through Two-Photon Ionization of Dopant Chromophores in Electron Accepting Polyester Film

7.1. Introduction

The behavior of charged species formed in polymer solids is of interest from the viewpoint of practical application as well as basic research, because they play important roles in an elementary process of charge transport in solid systems, *e.g.*, photoconduction,[1] electroluminescence,[2] and photorefractive effect.[3] There have been many investigations on the charged species in condensed phases produced by ionizing radiation mainly in the field of radiation chemistry. In condensed media, an ejected electron can travel to some extent and escape from the parent cation; the ejected electron changes into a trapped electron or solvated electron in various liquids, including alcohols, ethers, amines, and alkanes, and in rigid glasses of these liquids at 77 K.[4,5] For example, photoexcitation of the 3-methylpentane glass matrix doped with *N,N,N',N'*-tetramethyl-*p*-phenylenediamine (TMPD) at 77 K shows two main absorption peaks in the visible and near-IR region: one is due to the $TMPD^{\bullet+}$ around 600 nm and the other is a very broad one around 1600 nm ascribed to the trapped electron.[6]

Many studies have been reported on the effects of radiation on polymers, and on the behavior of the transient species: ionic species, excited state, and radicals, produced in irradiated polymers. However, there have been surprisingly few studies on the dynamics of ionic species in polymer solids by pulse radiolysis. This is because the assignment of transient species itself is difficult; in many cases the assignment is not clear, and the absorption is too small to discuss the dynamics.[7] Kira and Imamura reported a study on the dynamics of solute ions formed in a polymer solid by pulse radiolysis.[8] In their report,

solute ionic species were observed and the polymer was used just as a medium. From the viewpoint of charge transport in polymer solids, the high concentration of functional groups of polymers is one of the most important factors. For example, in poly(*N*-vinylcarbazole), which is widely known as a photoconductive polymer, the efficient hole migration results from large electronic interaction between neighboring chromophoric groups owing to the high concentration of carbazolyl groups in the polymer solids. At the same time, the high concentration makes the direct observation of transient ionic species difficult.[9] Recently, two groups revealed the dynamics of the short-lived ionic species formed in poly(*N*-vinylcarbazole) solids by laser photolysis.[10–12]

Although absorption spectroscopy is a powerful method for observing the transient species, not all of the charged species have a large absorption. For example, the photoejected electron captured in polymer solids such as poly(alkyl methacrylate)s and polystyrene has not been observed by absorption spectroscopy, whereas the dopant radical cations can be easily observed with a conventional spectrophotometer.[13–18] This is probably because the molar absorption coefficient of the ester radical anion is too small to be observed by absorption measurements.

In this chapter, aromatic chromophores with low ionization potential were doped in a polyester film having a weak electron accepting group, phthaloyl group. One component of the polyester is dimethylterephthalate (DMTP) or dimethylisophthalate (DMIP), which is often used as an electron acceptor. In such electron accepting polymer solids, photoejected electrons are expected to be captured by the electron accepting group, resulting in phthaloyl radical anions. Herein, the photoejected electron formed in an electron accepting polymer solid was examined by absorption spectroscopy.

7.2. Experimental Section

7.2.1. Chemicals

Polymer matrices used here were a linear polyester, as shown in Scheme 7–1, poly[(ethylene glycol ; neopentyl glycol)-*alt*-(terephthalic acid ; isophthalic acid)], (PENTI, $M_n = 1.5 \times 10^4$, $T_g = 340$ K, Toyobo Co., Ltd.)[19] and poly(methyl methacrylate) (PMMA, $M_w = 3.95 \times 10^5$, $T_g = 293$ K, Scientific Polym. Prod.). The polymers were purified by

reprecipitation from a benzene solution into methanol three times. Dopant chromophores used were *N*-ethylcarbazole (EtCz, Tokyo Chemical Industry Co., Ltd.) and pyrene (Py, Tokyo Chemical Industry Co., Ltd.). These chromophores were purified by recrystallization several times. Pyrene was purified further by silica-gel flash column chromatography eluted with benzene.

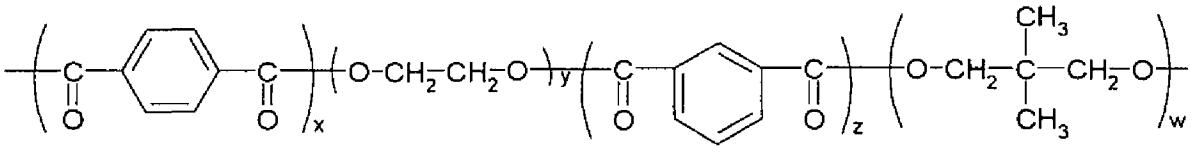

Scheme 7–1. Chemical structure of PENTI. The structure of the main chain contains a terephthaloyl (TP) and isophthaloyl (IP) group. The ratio of each components was evaluated by ^{1}H-NMR measurement: x ≈ 25%, y ≈ 22%, z ≈ 27%, w ≈ 26%.

The sample film was prepared by the solution cast method. A dopant chromophore was dissolved in a benzene solution of PMMA or in a dichloromethane solution of PENTI to make the concentration of the dopant chromophore in the final polymer film *ca.* 3×10^{-3} mol/L. The solution was cast on a glass plate in a dry box for two days at room temperature and then evacuated for a day at room temperature. The film on the glass plate was immersed in water for several hours and then peeled off from the glass plate. Finally, the polymer films were dried *in vacuo* above the T_g for more than 24 h to remove the remaining trace of the casting solvent. These prepared films have a thickness of about 100 μm.

7.2.2. Measurements

Several sheets of the polymer film doped with a chromophore were sandwiched with two quartz plates (15 × 15 × 0.5 mm) and then set tightly on a copper cold finger of a cryostat (Iwatani Plantech Corp., CRT510). The sample films were cooled down to 20 K and the sample temperature was kept constant using a PID temperature control unit (Iwatani Plantech Corp., TCU-4). The temperature was monitored with a calibrated Au + 0.07 % Fe / chromel thermocouple at the sample films position using an indium gasket.

A chromophore doped in polymer solids was selectively photoirradiated with 351-nm light pulses from a XeF excimer laser (Lambda Physik, EMG101MSC, *ca.* 20 ns, *ca.* 60 mJ/pulse) for 5 min. The photoirradiation conditions were as follows: the distance from the sample films to a cylindrical lens was 1.25 times as long as the focal length, which makes the laser pulse a 5 × 40 mm rectangle; the laser pulse interval was set at 0.05 Hz.

The steady-state absorption spectra of the photoirradiated sample films were measured 3 min after the photoirradiation at 20 K with a spectrophotometer (Hitachi, U-3500) using a 2-nm slit width in the UV-visible region and an automatic slit width in the near-IR region.

7.3. Results and Discussion

The absorption spectrum of a PMMA film doped with EtCz was measured 3 min after the photoirradiation at 20 K in the wide wavelength range 400 – 2000 nm. If the photoejected electrons changed into solvated electrons or trapped electrons, a broad absorption band would be observed in the visible or near-IR region, respectively. However, no absorption due to photoejected electrons was observed in the above wavelength range. According to the absorption and/or ESR measurements of irradiated PMMA at 77 K, some ejected electrons are captured as ester radical anions, not trapped electrons.[20-23] The ester radical anion has a very small absorption band at 440 nm.[20,24] Therefore, no absorption band of photoejected electrons was observed for the photoirradiated PMMA film doped with EtCz probably because the absorption band of the ester radical anion is too small to be observed with a spectrophotometer. Similar results were obtained for other poly(alkyl methacrylate)s and polystyrene films.

On the contrary, the matrix anion as well as the dopant cation was observed by absorption measurement when a PENTI film doped with a chromophore was photoirradiated at 20 K. These ionic species were so stable at 20 K that most of the ionic species survived even 25 h after the photoirradiation. Figures 7–1a and 7–1b show the absorption spectra of ionic species formed in a PENTI film observed 3 min after the photoirradiation at 20 K. The absorption peak common to these systems at about 535 nm is ascribable to the matrix anion, a terephthaloyl radical anion and/or an isophthaloyl radical

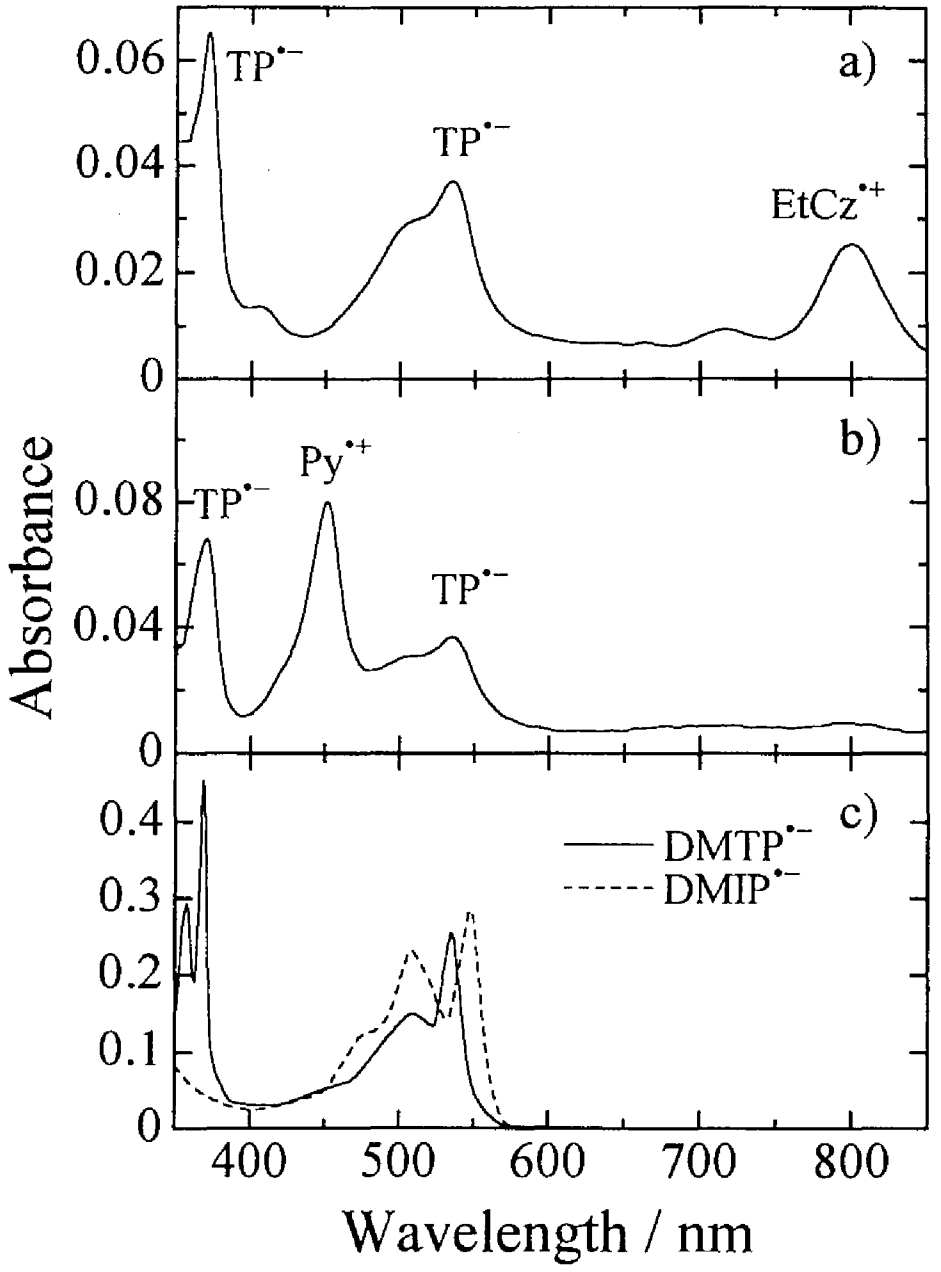

Figure 7–1. The absorption spectra of a PENTI film doped with dopant chromophores: a) EtCz/PENTI, b) Py/PENTI. The electron donor was selectively ionized at 20 K by intense 351-nm light from an excimer laser. Figure 7–1c is the absorption spectra of $DMTP^{\bullet-}$ (solid line) and $DMIP^{\bullet-}$ (broken line) formed by γ-irradiation in a 2-MTHF rigid solvent at 77 K. The absorbed dose was 1700 Gy for DMTP and 3400 Gy for DMIP. The concentration of DMTP and DMIP was 3×10^{-3} M and 5×10^{-2} M, respectively.

anion. Absorption bands observed around 800 nm and around 450 nm are ascribed to $EtCz^{\bullet+}$ and $Py^{\bullet+}$, respectively. Furthermore, no other absorption, *e.g.*, solvated electron, trapped electron, and charge-resonance band, was observed in either the visible or near-IR region. These results indicate that the photoejected electron is localized at a terephthaloyl and/or an isophthaloyl group in the main chain of PENTI.

According to ^{1}H-NMR measurement, the PENTI consists of terephthaloyl group (*ca.* 49%) and isophthaloyl group (*ca.* 51%) acid component. Thus, the possible assignment of the matrix anion is, as mentioned above, a terephthaloyl radical anion ($TP^{\bullet-}$) and/or an isophthaloyl radical anion ($IP^{\bullet-}$). Here the absorption spectra of the matrix anion are compared with that of the constituent radical anions. The two reference absorption spectra shown in Figure 7–1c were taken in a 2-methyltetrahydrofuran (2-MTHF) rigid matrix at 77 K by γ-irradiation. The absorption peak position of the matrix anion ($\lambda_{max} \approx 535$ nm) was in agreement with that of $DMTP^{\bullet-}$ ($\lambda_{max} \approx 535$ nm) rather than that of $DMIP^{\bullet-}$ ($\lambda_{max} \approx 548$ nm). Furthermore, it is noteworthy that the matrix anion and $DMTP^{\bullet-}$ have a sharp absorption peak at 370 nm but $DMIP^{\bullet-}$ dose not. Thus, the photoejected electron is mainly localized at the terephthaloyl group in the main chain of PENTI rather than isophthaloyl group.

The reduction potentials $E(A/A^{\bullet-})$ of DMTP and DMIP were 2.10 and 2.40 V (*vs.* SCE), respectively.[25] In other words, the electron accepting ability of DMTP is higher than that of DMIP. It is, therefore, reasonable to suppose that the photoejected electron captured by an isophthaloyl group transfers to a terephthaloyl group having larger electron accepting ability.

Here, let us evaluate quantitatively the amount of ionic species formed in the photoirradiated PENTI film doped with EtCz. If it is assumed that the molar absorption coefficients are as follows: $EtCz^{\bullet+}$ (ε = 9400 at 800 nm)[26] and $TP^{\bullet-}$ (ε = 13 000 at 535 nm),[27,28] the amount of $TP^{\bullet-}$ produced by the photoirradiation is almost equal to that of $EtCz^{\bullet+}$. It is, therefore, concluded that most of the photoejected electrons are captured by terephthaloyl groups in the matrix polymer.

In Chapter 6, it was shown that the positive charge of carbazole (Cz) radical cation formed in a copolymer of *N*-vinylcarbazole (VCz) with methyl methacrylate (MMA), *i.e.*, VCz(*x*)/MMA, is delocalized between two neighboring Cz chromophores, even when the VCz content *x* is no more than 25 mol%.[9] On the contrary, the negative charge in the

PENTI film is localized at a terephthaloyl group. The negative charge in the PENTI can be expected to be more easily delocalized over neighboring molecules than the positive charge in VCz(25)/MMA from the viewpoint of the concentration of chromophoric groups in polymer solids: The average distance[29] ρ between neighboring phthaloyl groups in PENTI ($\rho \approx 6.6$ Å in PENTI) is shorter than that of Cz in VCz(25)/MMA ($\rho \approx 8.8$ Å in VCz(25)/MMA).[30] However, as mentioned above, no absorption ascribable to the charge-resonance band was observed in either the visible or near-IR region. This indicates that the negative charge in PENTI is not delocalized over two or more neighboring phthaloyl groups. The charge resonance due to the dimer radical anion of aromatic molecules has not been reported except for the paracyclophane molecule.[31] This is probably because the sum of the destabilization energy of the electrostatic energy, exchange repulsion, and non-bonded repulsion overcomes that of the stabilization energy by the dispersion energy and charge resonance between $TP^{\bullet-}$ and TP / IP.[32]

In the case of polyethylene with low electron affinity and low polarity, ejected electrons are captured as trapped electrons in a small cavity of the matrix. The absorption due to the trapped electron with the oriented alkyl free radical has been reported to be observed at 77 K by ESR and absorption spectroscopy.[33] As mentioned above, some ejected electrons in PMMA are captured by the ester side chain resulting in ester radical anions,[20-23] since PMMA has a slightly larger electron affinity. In a polyester film having a weak electron accepting group in the main chain, most of the ejected electrons are captured by the electron accepting group and result in radical anions corresponding to the constituent electron accepting molecule. The negative charge is not delocalized over two or more neighboring chromophores. Therefore, it is concluded that the behavior of ejected electrons in condensed phases strongly depends on the electron affinity and polarity of the matrix.

Finally, concerning the photoionization mechanism, most of the long-lived ionic species observed in this system are generated through two-photon ionization because the amount of observed ionic species is proportional to the square of excitation light intensity; ionic species produced through the one-photon process probably recombine in a short time range. The steady-state emission spectrum of the PENTI film doped with EtCz was identical with that of the exciplex formed between EtCz and DMTP in solution.

Nevertheless, the two-photon process is probably dominant because of the laser intensity high enough to compete with the exciplex formation process.

7.4. Conclusion

The absorption spectra of ionic species formed through two-photon ionization of dopant chromophores in an electron accepting polymer (PENTI) film were measured at 20 K. The absorption spectrum of the matrix anion was similar to that of the constituent molecule radical anion $DMTP^{\bullet-}$ rather than that of $DMIP^{\bullet-}$ and the amount of matrix anions produced in the polymer solid was almost equal to that of the dopant cation. Therefore, it is concluded that most of the photoejected electrons are localized at a terephthaloyl group in the main chain of PENTI.

References and Notes

1) W. D. Gill, in *"Photoconductivity and Related Phenomena"*, eds. J. Mort and D. M. Pai, Elsevier, Amsterdam (1976).

2) K. C. Kao and W. Hwang, *"Electrical Transport in Solids"*, Pergamon, New York (1981).

3) W. E. Moerner and S. M. Silence, *Chem. Rev.*, **94**, 127 (1994).

4) T. Higashimura, *Annu. Rep. Res. Reactor Inst. Kyoto Univ.*, **6**, 38 (1973).

5) L. Kevan, *Acc. Chem. Res.*, **14**, 138 (1981).

6) J. B. Gallivan and W. H. Hamill, *J. Chem. Phys.*, **44**, 2378 (1966).

7) M. Ogasawara, in *"Recent Trend in Radiation Polymer Chemistry"*, Advances in Polymer Science, Vol. 105, ed. S. Okamura, Springer-Verlag, Berlin (1993).

8) A. Kira and M. Imamura, *J. Phys. Chem.*, **88**, 1865 (1984).

9) H. Ohkita, Y. Nomura, A. Tsuchida, and M. Yamamoto, *Chem. Phys. Lett.*, **263**, 602 (1996).

10) H. Miyasaka, T. Moriyama, S. Kotani, R. Muneyasu, and A. Itaya, *Chem. Phys. Lett.*, **225**, 315 (1994).

11) T. Ueda, R. Fujisawa, H. Fukumura, A. Itaya, and H. Masuhara, *J. Phys. Chem.*, **99**, 3629 (1995).

12) K. Watanabe, T. Asahi, and H. Masuhara, *Chem. Phys. Lett.*, **233**, 69 (1995).

13) A. Tsuchida, M. Nakano, M. Yoshida, M. Yamamoto, and Y. Wada, *Polym. Bull.*, **20**, 297 (1988).

14) M. Yamamoto, A. Tsuchida, and M. Nakano, *MRS Int. Meeting Adv. Mater.*, **12**, 243 (1989).

15) A. Tsuchida, W. Sakai, M. Nakano, M. Yoshida, and M. Yamamoto, *Chem. Phys. Lett.*, **188**, 254 (1992).

16) A. Tsuchida, W. Sakai, M. Nakano, and M. Yamamoto, *J. Phys. Chem.*, **96**, 8855 (1992).

17) A. Tsuchida, M. Nakano, and M. Yamamoto, in *"Polymers for Microelectronics — Science and Technology—"*, eds. Y. Tabata, I. Mita, S. Nonogaki, K. Horie, and S. Tagawa, Kodansha, Tokyo (1990).

18) M. Yamamoto, H. Ohkita, W. Sakai, and A. Tsuchida, *Synth. Metals*, **81**, 301 (1996).

19) The polymer structure in the main chain consists of ethylene glycol component (*ca.* 22 %), neopentyl glycol component (*ca.* 26 %), terephthalic acid component (*ca.* 25 %) and isophthalic acid component (*ca.* 27 %) evaluated by ^{1}H-NMR measurement.

20) A. Torikai, H. Kato, and Z. Kuri, *J. Polym. Sci., Polym. Chem. Ed.*, **14**, 1065 (1976).

21) A. Torikai and S. Okamoto, *J. Polym. Sci., Polym. Chem. Ed.*, **16**, 2689 (1978).

22) W. Sakai, A. Tsuchida, M. Yamamoto, T. Matsuyama, H. Yamaoka, and J. Yamauchi, *Macromol. Rapid Commun.*, **15**, 551 (1994).

23) W. Sakai, A. Tsuchida, M. Yamamoto, and J. Yamauchi, *J. Polym. Sci., Polym. Chem. Ed.*, **33**, 1969 (1995).

24) M. Ogasawara, M. Tanaka, and H. Yoshida, *J. Phys. Chem.*, **91**, 937 (1987).

25) The reduction potentials of DMTP and DMIP were measured by polarography in acetonitrile solvent containing 0.1 N tetrabutylammonium perchlorate (*vs.* SCE).

26) A. Tsuchida, M. Yamamoto, and Y. Nishijima, *J. Phys. Chem.*, **88**, 5062 (1984).

27) Y. Tsujii, A. Tsuchida, M. Yamamoto, Y. Nishijima, and Y. Wada, *Polym. J.*, **20**, 837 (1988).

28) Molar absorption coefficient of terephthaloyl radical anion $TP^{\bullet-}$ in PENTI is assumed to be equal to that of the terephthaloyl radical anion formed in a copolymer of vinyl methyl terephthalate with vinyl acetate; see Ref. 27.

29) The average distance ρ is estimated from the cube root of the inverse of the number density: $\rho = (d\ N_A\ /\ MW)^{-1/3}$; d is the density of the polymer, N_A is the Avogadro constant, MW is the molecular weight of a chromophoric group.

30) In unpublished data, the charge delocalization of Cz radical cation was also observed in VCz(13)/MMA, where the average distance of neighboring Cz is $\rho \approx 10.6$ Å.

31) A. Ishitani and S. Nagakura, *Mol. Phys.*, **12**, 1 (1967).

32) B. T. Lim, S. Okajima, A. K. Chandra, and E. C. Lim, *J. Chem. Phys.*, **77**, 3902 (1982).

33) R. M. Keyser, K. Tsuji, and F. Williams, in "*The Radiation Chemistry of Macromolecules*", Vol. I, ed. M. Dole, Academic Press, New York (1972), Chap. 9, p. 145.

Part III

Chapter 8

Photocleavage Mechanism of Polyimides Having Cyclobutane Rings

8.1. Introduction

Owing to their excellent material properties such as thermal stability, high glass transition temperature (T_g), mechanical toughness, and insensitivity to organic solvents, aromatic polyimides are already used for many important industrial applications, such as matrix resins in high-temperature composites and as interlayer dielectrics in multilevel integrated circuits (IC).[1] In the fabrication of IC, photosensitive polyimides have a large advantage as photoresists because the etching process is greatly simplified. Several photosensitive polyimides have been prepared as photoresists, and most of them use a photo-induced crosslinking reaction (negative type).[2,3] Few positive-type photosensitive polyimides have been reported in spite of practical advantages in its fabrication.[4-6]

Polyimides having cyclobutane rings in the main chain have been already reported.[7,8] Moore *et al.* have reported that such polyimides act as a positive-type photoresist.[9-13] There are many practical advantages for the positive-type photosensitive polyimide when it is compared to the negative working type, but most of the current positive-type polyimides still suffer a disadvantage that the remainder, photo-acid generator used for the photochemical reaction will damage the final products.

In this chapter, the photocleavage mechanism of the photosensitive polyimides containing cyclobutane rings in their main chain was examined. The photochemistry was studied using the dimer model unit of the photosensitive polyimides by the measurement of absolute cleavage quantum yield of the cyclobutane rings as well as the transient absorption measurements with laser photolysis.

8.2. Experimental Section

8.2.1. Chemicals

Photosensitive polyimides containing cyclobutane rings in their main chain were synthesized from the photodimers of maleic anhydride derivatives. Photodimers as model compounds of photosensitive polyimide containing cyclobutane rings in the main chain were examined. These dimers were purified by repeated recrystallization. The details of the synthetic procedure have already been published.[9-13]

Spectroscopic grade solvents (Dotite Spectrosol), 1,4-dioxane, chloroform, dichloromethane, and acetonitrile, were used without further purification.

8.2.2. Measurements

The absolute cycloreversion quantum yields of the dimer models were determined as follows. Sample solution (~ 10^{-5} mol/L) in a 1-cm quartz cuvette was freed from oxygen by argon bubbling for 15 min. The solution was irradiated under the 254-nm monochromatic light of a spectrofluorophotometer (Shimadzu, RF-501) at 298 K. Immediately after the photoirradiation, the amounts of the product monomer and the remaining dimer were determined by liquid chromatography (JASCO, TRI ROTAR-V, a silica-gel column) eluted with the mixed solvent of dichloromethane / hexane or ethyl acetate using a UV absorption detector (JASCO, UVIDEC-100-VI). By potassium ferrioxalate actinometry, it was determined that the photon number of the 254-nm exciting light was 1.80×10^{-10} E s^{-1}. The absorption of light by the product monomer (inner-filter effect) was corrected. The quantum yield of photocleavage was obtained by the corrected absorbance ratio of the product monomer to the reactant dimer at 254 nm. The control experiment where the monomer model was photoexcited in the same manner gave no appreciable photoproduct. The details of the methods described above have already been reported.[14-17]

Transient absorption spectra and their decays were measured by nanosecond laser photolysis.[18,19] A light pulse from a Lambda Physik EMG101MSC excimer laser was used for sample excitation (KrF gas, 248 nm, *ca.* 20 ns fwhm). A pulsed 450-W (Ushio) or a steady-state 150-W (Hamamatsu Photonics) xenon lamp was used as a monitor light source. In the measurements of transient absorption decay, a 50 Ω resistor was used as the signal terminator of

an R1477 photomultiplier (Hamamatsu Photonics), whereas in the long time-scale measurements a 500 Ω resistor with an R928 photomultiplier (Hamamatsu Photonics) was used to enhance the sensitivity. The transient absorption spectra were measured by an Optical Multichannel Analyzer (Unisoku USP-500), the details of which have been described elsewhere.[18,19]

Steady-state absorption and emission spectra were measured with a Shimadzu UV-200S spectrophotometer and a Hitachi 850 spectrofluorophotometer, respectively. All the spectroscopic measurements were done for the argon bubbled samples at 298 K. For the quenching experiments on the excited triplet state, the solution was bubbled with oxygen gas.

8.3. Results and Discussion

8.3.1. Photosensitive Polyimides Having Cyclobutane Rings in the Main Chain

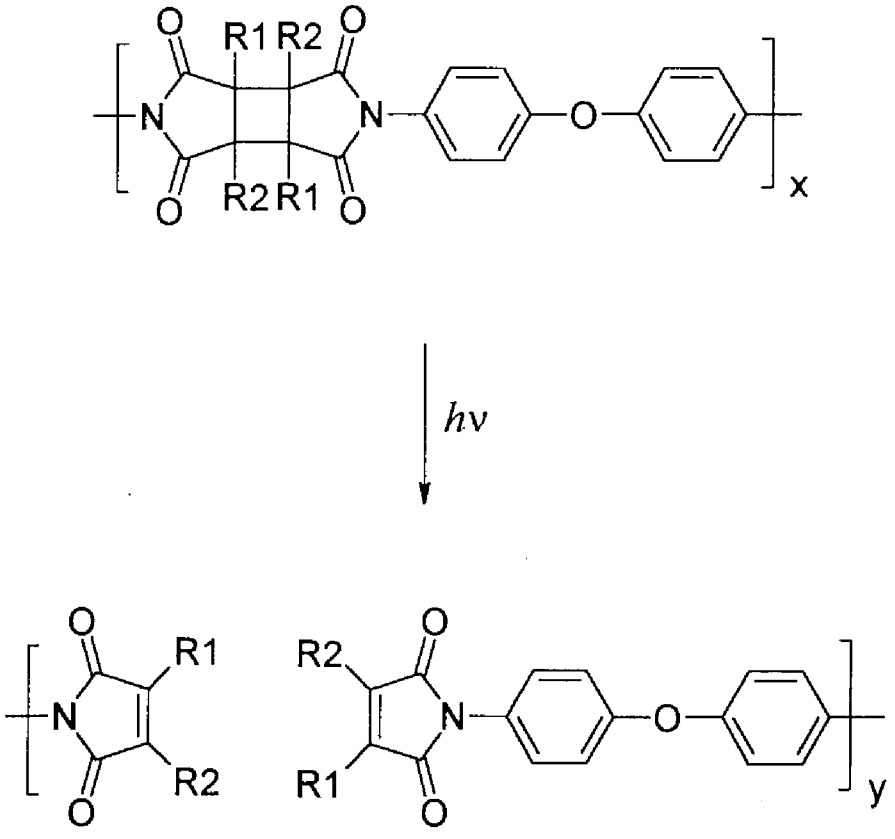

Scheme 8–1. Photocleavage reaction scheme for the photosensitive polyimides containing cyclobutane rings in the main chain.

Dimer Model

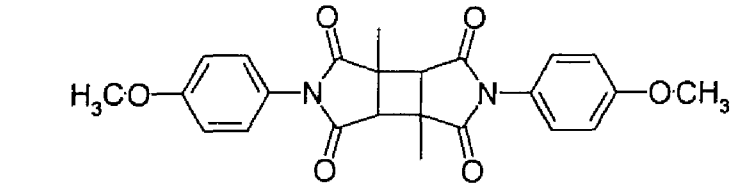

CBAM2

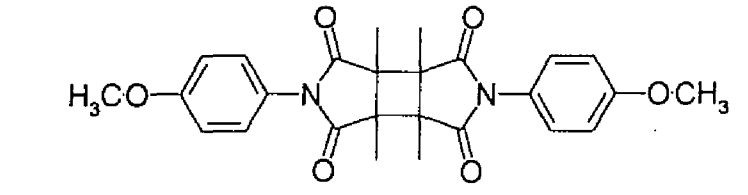

CBAM4

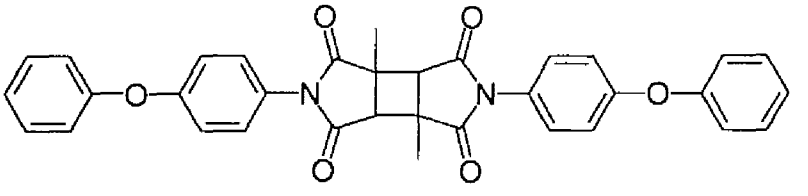

CMPM2

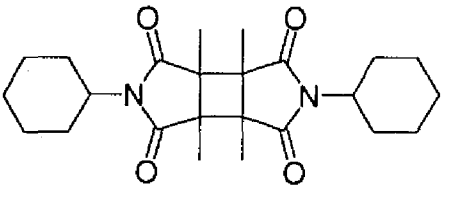

CBCM2

Monomer Model

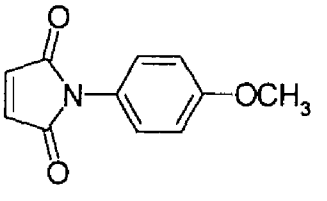

MAM0

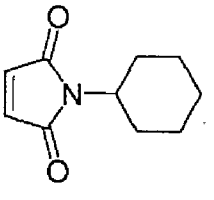

MCM0

Scheme 8–2. Dimer and monomer model compounds used in this work with their abbreviations.

Moore *et al.* prepared a photosensitive polyimide,[9-13] which had cyclobutane rings in the main chain, that underwent photodegradation by the cycloreversion reaction of the rings. Therefore, this photosensitive polyimide is a positive working type and has an advantage of not being contaminated by either inorganic ions or acid-forming groups.

Scheme 8–1 shows the reaction path for the cyclobutane-containing photosensitive polyimide.[7,11] The cyclobutane rings in the main chain are cleaved by photoirradiation with UV-light. Here, the photochemistry of the cyclobutane-type polyimide was studied using dimer models. Scheme 8–2 shows the molecular structures of the compounds used in this work with their abbreviations.

8.3.2. Solvent Effects on Photocleavage Quantum Yield of Cyclobutane Dimers

To elucidate the photoreactivity of the cyclobutane ring in the photosensitive polyimide chain, the effects of solvent polarity on the cycloreversion reaction were examined using dimer models. The solvents used were 1,4-dioxane, chloroform, dichloromethane, and acetonitrile, with dielectric constants (ε_r) of 2.10 (293 K), 4.86 (293 K), 7.77 (283 K), and 37.5 (293 K), respectively. The absolute quantum yields for the photocleavage of the dimers were measured in these solvents.

Table 8–1. Photocleavage Quantum Yield of Cyclobutane Dimers

Solvent	Dielectric constant	CBAM2[a]	CBAM4[a]	CBPM2[a]	CBCM2[b]
1,4-Dioxane[c]	2.10	0.30	0.36	0.41	—
Chloroform[c]	4.86	0.72	0.73	0.63	—
Dichloromethane[c]	7.77	0.54	0.53	0.59	< 0.001
Dichloromethane[d]	7.77	0.56	0.53	0.60	< 0.001
Acetonitrile[c]	37.5	0.25	0.33	0.58	—

a) Molar absorption coefficient (ε) of MAM0 was used for the calibration.
b) Molar absorption coefficient (ε) of MCM0 was used for the calibration. Because of the poor solubility, measurement was done only for dichloromethane solvent.
c) Argon bubbling for 15 min.
d) Oxygen bubbling for 15 min.

Table 8–1 summarizes the solvent effects on the cycloreversion quantum yield. This table shows two significant characteristics of this photocleavage reaction. First, the photocleavage quantum yields were considerably large for CBAM2, CBAM4, and CBPM2 dimers which have aromatic substituents at the imide groups, whereas it was close to zero for the CBCM2 dimer which has no aromatic ring but cyclohexane rings. The large reaction quantum yield of dimers with aromatic substituents is consistent with the already reported high reactivity of the corresponding polymers as a photoresist.[9–13] The emission quantum yield of these dimer compounds was less than 10^{-3}, which is due to the high cycloreversion efficiency of the dimers. Considering the molecular structures of CBAM2, CBAM4, and CBPM2, they may form an intramolecular excited charge-transfer (CT) state since these compounds have electron-donating aromatic rings and electron-accepting imide groups in the main chain. On the contrary, CBCM2 has probably weaker intramolecular excited CT nature than those with aromatic substituents. These findings suggest that the intramolecular excited CT state plays an important role to the reactivity of cycloreversion of the dimer compounds.

Secondly, Table 8–1 shows that the photocleavage quantum yields for CBAM2, CBAM4, and CBPM2 were higher in moderately polar solvents. For example, the photocleavage quantum yield of CBAM2 was 0.30 in 1,4-dioxane (non-polar solvent) and 0.25 in acetonitrile (polar solvent), whereas it was 0.72 in chloroform (medium-polar solvent). The following mechanism is proposed. In moderately polar solvents the excited intramolecular CT state of $(D^{\delta+} - A^{\delta-})^*$ is stable enough to have a long lifetime for the cycloreversion reaction. On the other hand, the polar excited intramolecular CT state of $(D^{\delta+} - A^{\delta-})^*$ is not so stable in non-polar solvents and it is deactivated immediately. In polar solvents this $(D^{\delta+} - A^{\delta-})^*$ state is stabilized by forming the intramolecular ion-pair state of $(D^+ - A^-)^*$, whose lifetime is not long enough to cause the cleavage reaction. This tendency is very similar to the solvent polarity effect on quantum yields of exciplex emission for many systems so far reported.[14,20–22] In many cases the exciplex is more emissive in medium-polar solvents; in non-polar solvents the polar exciplex state is not so stable, and in polar solvents the exciplex changes into a more stable ion-pair state. This effect of solvent polarity also suggests that the dimer model compounds are photocleaved *via* their excited intramolecular CT state.

8.3.3. Excited Triplet State Quenching by Oxygen

Figure 8–1 shows the transient absorption spectra of CBPM2 measured by laser

photolysis in dichloromethane as a solvent at 298 K. Transient absorption spectra were measured also in an oxygen atmosphere to examine the participation of an excited triplet state in the photocleavage reaction.

Recently Hoyle *et al.* measured the transient absorption spectra of aromatic polyimide by laser photolysis.[23] They found that the transient absorption bands of *N*-phenylphthalimide appear around 300, 330, and 500 nm with a single lifetime of *ca.* 11.5 μs and that they are all effectively quenched by oxygen. To identify the transient species, they examined the Stern-Volmer plot, *i.e.*, the relationship between the ratio of the transient lifetimes before and after adding cyclohexadiene as a quencher and the cyclohexadiene concentration. The slope of the Stern-Volmer plot was linear and provided an essentially diffusion-controlled quenching rate constant of 6.0×10^9 L mol^{-1} s^{-1}. They concluded from these results that the transient bands are ascribed to the excited triplet state of *N*-phenylphthalimide. In the present experiment, a transient absorption band appeared around 330 nm as shown in Figure 8–1a (argon bubbled CBPM2). For the oxygen-bubbled CBPM2 sample, the transient absorption peak was completely quenched and no absorption was observed; see Figure 8–1b. This means that the transient absorption can be ascribed to the excited triplet state of CBPM2 and it is effectively quenched by oxygen. This assignment seems to be reasonable in comparison with the absorption spectra obtained by Hoyle *et al.*

As for the photocleavage quantum yields, the oxygen-bubbled dimer samples had almost the same quantum yields as the argon bubbled samples in the dichloromethane solvent, as shown in the fourth row in Table 8–1. These findings indicate that the photocleavage reaction of the cyclobutane ring does not occur in the excited triplet state but in the excited singlet state. Along with the discussion in the previous section, it is suggested that the excited singlet state is immediately relaxed to the intramolecular excited CT state before intersystem crossing to the excited triplet state, and from this intramolecular excited CT state the cyclobutane ring is cleaved efficiently.[24]

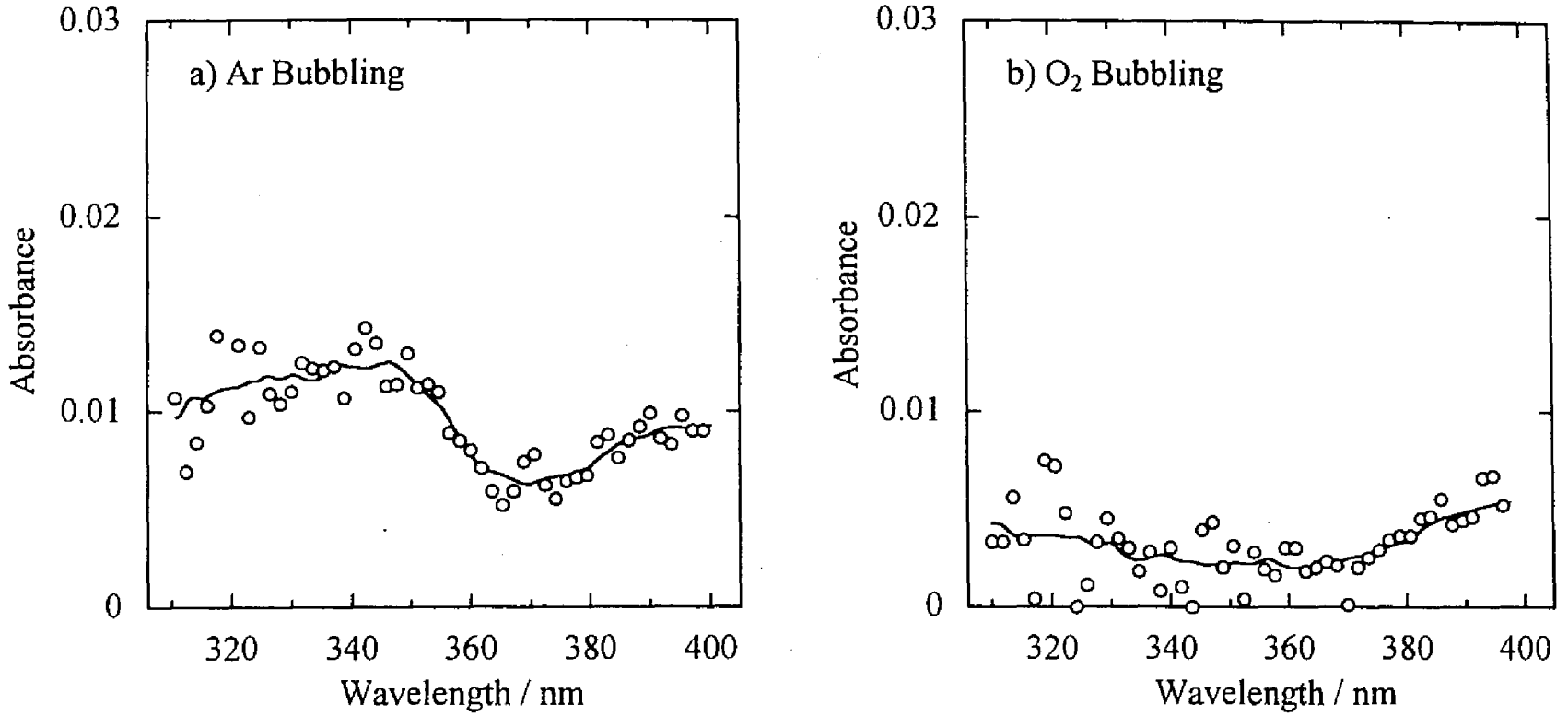

Figure 8–1. Transient absorption spectra of CBPM2 measured in dichloromethane at 298 K: a) argon bubbling; b) oxygen bubbling. Gate time = 170 ns, delay time = 150 ns, number of accumulations = 100.

8.4. Conclusion

The photocleavage mechanism of photosensitive polyimide having cyclobutane rings in the main chain was studied using dimer model compounds. The absolute quantum yield of photocleavage for the dimers with different substituents at the imide group was measured in various solvents with different polarity. Judging from the solvent effect on the photocleavage quantum yield and the excited triplet behavior, it was concluded that the photocleavage of the cyclobutane ring occurs *via* the intramolecular excited singlet CT state.

References

1) M. Kato, T. Yamaoka, R. Hurditch, and H. Honda, *Polym. Adv. Technol.*, **4**, 215 (1993).

2) R. Rubner, W. Bartel, and G. Bald, *Siemens Forsch. Entwickl. Ber.*, **5**, 92 (1976).

3) N. Yoda and H. Hiramoto, *J. Macromol. Sci., Chem.*, **A21**, 1641 (1984).

4) S. Kubota, T. Moriwaki, T. Ando, and A. Fukami, *J. Macromol. Sci., Chem.*, **A24**, 1407 (1987).

5) J. V. Crivello, J. L. Lee, and D. A. Conlon, *J. Polym. Sci., Polym. Chem. Ed.*, **25**, 3293 (1987).

6) T. Omote, K. Koseki, and T. Yamaoka, *Macromolecules*, **23**, 4788 (1990).

7) F. Nakanishi, M. Hasegawa, and H. Takahashi, *Polymer*, **14**, 440 (1973).

8) F. C. De Schryver, N. Boens, and G. Smets, *J. Am. Chem. Soc.*, **96**, 6463 (1974).

9) J. A. Moore and A. N. Dasheff, *Polym. Mater. Sci. Eng.*, **59**, 999 (1988).

10) J. A. Moore and A. N. Dasheff, in *"Polyimides: Materials, Chemistry and Characterization"*, eds. C. Feger, M. M. Khojasteh, and J. E. McGrath, Elsevier, Amsterdam (1989), p. 115.

11) J. A. Moore and A. N. Dasheff, *Chem. Mater.*, **1**, 163 (1989).

12) J. A. Moore and A. N. Dasheff, *Abstr. 3rd Int. SAMPE Electron. Conf. (Electron. Mater. Processes)* 1989, p. 861.

13) J. A. Moore and D. R. Gamble, *Polym. Eng. Sci.*, **32**, 1642 (1992).

14) A. Tsuchida, M. Yamamoto, and Y. Nishijima, *J. Chem. Soc., Perkin Trans. 2*, 239 (1986).

15) A. Tsuchida, M. Yamamoto, and Y. Nishijima, *Bull. Chem. Soc. Jpn.*, **60**, 2899 (1987).

16) A. Tsuchida, M. Yamamoto, and Y. Nishijima, *J. Chem. Soc., Perkin Trans. 2*, 507 (1987).

17) A. Tsuchida, M. Yamamoto, and Y. Nishijima, *Bull. Chem. Soc. Jpn.*, **64**, 3402 (1991).

18) G. W. Haggquist, K. Hisada, A. Tsuchida, M. Yamamoto, and K. R. Naqvi, *J. Phys. Chem.*, **98**, 10756 (1994).

19) A. Tsuchida, A. Nagata, M. Yamamoto, H. Fukui, M. Sawamoto, and T. Higashimura, *Macromolecules*, **28**, 1285 (1995).

20) T. Okada, T. Fujita, M. Kubota, S. Masaki, and N. Mataga, *Chem. Phys. Lett.*, **14**, 563 (1972).

21) T. Okada, T. Fujita, and N. Mataga, *Z. Phys. Chem. NF*, **101**, 57 (1976).

22) T. Okada, T. Saito, N. Mataga, Y. Sakata, and S. Misumi, *Bull. Chem. Soc. Jpn.*, **50**, 331 (1977).

23) C. E. Hoyle, E. T. Anzures, P. Subramanian, R. Nagarajan, and D. Creed, *Macromolecules*, **25**, 6651 (1992).

24) M. Hasegawa, Y. Shindo, T. Sugimura, S. Ohshima, K. Horie, M. Kochi, R. Yokota, and I. Mita, *J. Polym. Sci., Polym. Phys. Ed.*, **31**, 1617 (1993).

Summary

In Chapter 1, historical backgrounds of this thesis were described to clarify the location and significance of this study. First, two-photon ionization in condensed media, one of the primary processes induced by photoexcitation, was reviewed to elucidate its feature and a future application as a new kind of photochromism was briefly mentioned. Next, the following charge recombination in condensed media was described from the viewpoint of the charge recombination luminescence, *i.e.*, isothermal luminescence (ITL) and thermoluminescence (TL), and then several reports on the initial distribution function of ejected electrons were introduced: Exponential type, Gaussian type distribution. Subsequently, the chemical reactions initiated through the formation of charged species were surveyed from the viewpoint of degradation of irradiated polymers: the mechanism of main-chain scission in irradiated PMMA solids. Finally, the behavior of a radical cation formed in PVCz was described as an example of charged species formed in polymer solids. Furthermore, the relationship among each chapter was displayed and the outline of this thesis was described.

In Chapter 2, the photochromism induced by two-photon ionization of a dopant chromophore in polymer films was demonstrated. The coloration of polymer films results from two-photon ionization of the dopant chromophore and can be recognized even after a one-year storage at room temperature. This can be a writing and storage of information, and furthermore an input threshold enables one to read out signals without erasing the signal by absorption measurement of radical cations. The backward charge recombination was also observed through ITL and TL. The application of electric field and heating procedure promote the charge recombination resulting in the enhancement of ITL and TL intensity. These perturbations can be utilized to read-out by emissive way as well as to erase the stored signal.

In Chapter 3, the mechanism of the charge recombination of electron-cation pairs formed in a polymer solid at 20 K through two-photon ionization of a dopant chromophore was examined by emission as well as absorption spectroscopy. Both the decay of ITL intensity $I(t)$ and the absorbance decay of the dopant radical cation obeyed the same

kinetics at 20 K: the t^{-m} law, $I(t) \propto t^{-m}$ with $m \approx 1$. The temperature dependence of the ITL decay kinetics remained the same from 20 to 200 K far below the glass transition temperature of the polymer matrix (PnBMA, 293 K). These findings show that the ITL decay at low temperatures can be explained in terms of long-range electron transfer process by electron tunneling. Multi-shot photoirradiation was found to cause the deviation of the ITL decay from the t^{-m} law. Multi-shot photoirradiation probably induces larger separation of a photoejected electron from the parent cation and/or the deepening of the trap depth.

In the following Chapter 4, the charge recombination of a photoejected electron with the parent dopant cation formed in polymer solids at 20 K through two-photon ionization was considered in terms of long-range electron transfer by electron tunneling. The decay kinetics of the ITL was quantitatively compared with that of the dopant radical cation observed directly by absorption spectroscopy. The comparison shows good agreement for polystyrene, but not for poly(alkyl methacrylate)s classified as scission type polymers to high energy radiation. In the latter case, the decrease in radical cations observed by absorption measurement was less than that expected from the ITL decay. This disagreement suggests that photoejected electrons in poly(alkyl methacrylate)s are captured in a chemical trap as well as in a physical trap even at 20 K; an electron in a physical trap participates in the charge recombination and emits ITL, but that in a chemical trap does not.

In Chapter 5, the behavior of a photoejected electron with the parent cation formed through two-photon ionization of a dopant chromophore in poly(alkyl methacrylate)s and polystyrene was studied by measurement of the emission spectra of the charge recombination luminescence, *i.e.*, ITL at 20 K and TL at temperatures from 20 to 300 K. The ITL spectral shape remained the same between 10 min and 10 h after the photoirradiation. On the other hand, the intensity ratio of phosphorescence (I_P) to fluorescence (I_F), I_P/I_F in the TL spectra increased for poly(alkyl methacrylate)s above a temperature where small scale motions of the main chain are released, but was almost constant for polystyrene in the temperature range examined. These findings show that, for poly(alkyl methacrylate)s, the photoejected electrons change into more stable anion species with a motional relaxation of the polymer. From the TL spectral change, the depth of the deeper trap at higher temperatures was estimated to be more than 1.8 eV.

In Chapter 6, the behavior of the ionic species formed in the copolymer of electron-donating *N*-vinylcarbazole (VCz) with methyl methacrylate was examined at 77 K by the measurement of the charge-resonance (CR) band. In the case where the mole fraction of VCz is less than 50 %, it was found that the Cz hole in solid films is mainly stabilized by charge resonance between two Cz chromophores and that the fraction of more stable Cz hole traps increases with the Cz concentration.

In Chapter 7, anionic as well as cationic species formed through photoionization of dopant chromophores in a polyester film having a weak electron-accepting group, phthaloyl group, were observed at 20 K by absorption measurement. The amount of the anionic species was almost equal to that of the dopant cations, and the absorption spectrum of the anionic species was similar to that of the isolated phthaloyl radical anion. These findings indicate that photoejected electrons are localized at a phthaloyl group in the main chain of the polyester.

In Chapter 8, the photocleavage reaction of dimer model compounds of photosensitive polyimides having cyclobutane rings in the main chain was studied. Efficient photocleavage was observed for the dimer models (CBAM2, CBAM4, and CBPM2) having an electron-donating aromatic substituent with the electron-accepting imide group. On the other hand, the cleavage quantum yield was nearly zero for a dimer (CBCM2) having a cyclohexane substituent instead of the aromatic ring. Solvent polarity effects on the cleavage quantum yield revealed that these dimers give the largest photocleavage efficiency in medium-polar solvents. The transient absorption band of the excited triplet CBPM2 was effectively quenched by oxygen, whereas no oxygen quenching was observed for the cleavage quantum yield. These findings lead to the conclusion that the cyclobutane ring in the polyimide is photocleaved *via* the excited singlet intramolecular CT state.

List of Publications

Chapter 2.

"Photoionization and Thermoluminescence in Poly(alkyl methacrylate) Films",
M. Yamamoto, H. Ohkita, W. Sakai, and A. Tsuchida,
Synthetic Metals, **81**, 301 (1996).

Chapter 3.

"Charge Recombination via Electron Tunneling after Two-Photon Ionization of Dopant Chromophore in Poly(n-butyl methacrylate) Film at 20 K",
H. Ohkita, W. Sakai, A. Tsuchida, and M. Yamamoto,
Bull. Chem. Soc. Jpn., in press.

Chapter 4.

"Charge Recombination of Electron-Cation Pairs Formed in Polymer Solids at 20 K through Two-Photon Ionization",
H. Ohkita, W. Sakai, A. Tsuchida, and M. Yamamoto,
J. Phys. Chem. A, in press.

Chapter 5.

"Charge Recombination Luminescence via the Photoionization of a Dopant Chromophore in Polymer Solids",
H. Ohkita, W. Sakai, A. Tsuchida, and M. Yamamoto,
Macromolecules, **30**, 5376 (1997).

Chapter 6.

"Direct Observation of the Carbazole Hole Trap in Polymer Solid Films by the Charge-Resonance Band",
H. Ohkita, Y. Nomura, A. Tsuchida, and M. Yamamoto,
Chem. Phys. Lett., **263**, 602 (1996).

Chapter 7.

"Stabilization of Photoejected Electrons Produced through Two-Photon Ionization of Dopant Chromophores in Electron Accepting Polyester Film",
H. Ohkita, T. Koizumi, W. Sakai, T. Osako, M. Ohoka, and M. Yamamoto,
Chem. Phys. Lett., in press.

Chapter 8.

"Photocleavage Mechanism of Polyimides Having Cyclobutane Rings.",
H. Ohkita, A. Tsuchida, M. Yamamoto, J. A. Moore, and D. R. Gamble,
Macromol. Chem. Phys., **197**, 2493 (1996).

Acknowledgments

The present thesis is based on the studies that the author has carried out at the Department of Polymer Chemistry, Graduate School of Engineering, Kyoto University, from 1992 to 1997, under the guidance of Professor Masahide Yamamoto. The author wishes to express his sincere gratitude to Professor Masahide Yamamoto for his continuous guidance from a point of wide view and heartful encouragement throughout the course of this work.

The author is sincerely indebted to Assistant Professor Akira Tsuchida, Department of Applied Chemistry, Gifu University, for his invaluable guidance and discussions.

The author is sincerely grateful to Assistant Professor Shinzaburo Ito for his pointed suggestions and discussions. The author is grateful to Mr. Masataka Ohoka for his helpful suggestions and kind supports.

The author wishes to express his sincere thanks to Professor Yoshimasa Hama, Science and Engineering Research Laboratory, Waseda University, for his invaluable discussions on thermoluminescence of γ-irradiated polymer solids. The author would like to thank Professor Hitoshi Yamaoka, Department of Polymer Chemistry, Graduate School of Engineering, Kyoto University, for permitting the use of a spectrophotometer (Hitachi U-3400). The author is grateful to Mr. Tadahiko Osako, Toyobo Co., Ltd., for permitting the use of poly[(ethylene glycol ; neopentyl glycol)-*alt*-(terephthalic acid ; isophthalic acid)] (Vylon 200®). The author is indebted to Professor James A. Moore and Mr. Donald R. Gamble, Department of Chemistry, Polymer Science and Engineering Program, Rensselaer Polytechnic Institute, for the preparation of the dimer model compounds of photosensitive polyimides having cyclobutane rings in the main chain.

The author wishes to thank Dr. Wataru Sakai, Department of Polymer Science and Engineering, Kyoto Institute of Technology, for his useful discussions.

The author deeply wishes to thank Messrs. Yasuyuki Nomura and Takeshi Koizumi for their active collaborations. The author also thanks the nice members of Yamamoto Laboratory for carrying a cryostat used in thermoluminescence measurements and for their encouragement and kind help.

Finally, the author would like to express his sincere gratitude to his parents Naoharu Ohkita and Tamiko Ohkita, and his sister Kyoko Ohkita for their continuous supports.

May, 1997

Hideo Ohkita